SPATIALLY AND TEMPORALLY RESOLVED MEASUREMENTS FROM SINGLE NEUROENDOCRINE CELLS

BY

CHARINA D. PARAS

A DISSERTATION PRESENTED TO THE GRADUATE SCHOOL
OF THE UNIVERSITY OF FLORIDA IN PARTIAL FULFILLMENT
OF THE REQUIREMENTS FOR THE DEGREE OF
DOCTOR OF PHILOSOPHY

UNIVERSITY OF FLORIDA

1998

To Noel

ACKNOWLEDGMENTS

I would like to thank my advisor, Dr. Robert T. Kennedy, for his support, help and guidance during my stay at the University of Florida.

I would like to thank all the members of the Kennedy group (esp. Lan, Sunday, Hong, Li, Mark, Craig, Brendan, Steve, Karen, Danielle and Lisa) for their assistance, helpful discussions and most of all the camaraderie that helped me get through graduate school. Also, I would like to thank Dr. Waldemar Gorski for helpful discussions in electrochemistry.

I would like to thank Dr. Weihong Tan for allowing me to use the fluorescence setup in his laboratory and for all the helpful discussions.

I would like to thank the UF Department of Chemistry Machine Shop staff for all their help.

I would like to thank my parents for their understanding, encouragement and love. I would like to thank my brother and sister for believing in me.

I would like to thank Noel for his support, understanding, patience and love during all these years.

Finally, I would like to thank God for all his blessings and all the wonderful and learning experiences in graduate school.

TABLE OF CONTENTS

		page
ACKNOWLEDGMENTS		iii
ABSTRACT		vi
CHAPTERS		
1	INTRODUCTION	1
	Electroanalysis as a Tool in Neurochemical Studies	2
	Electrochemical Methods	4
	Monitoring Secretion from Single Cells	6
	Thesis Overview	9
2	ELECTROCHEMICAL DETECTION OF EXOCYTOSIS AT SINGLE RAT MELANOTROPHS	12
	Introduction	12
	Experimental	14
	Results and Discussion	18
	Conclusion	24
3	AMPEROMETRY AND CYCLIC VOLTAMMETRY OF TYROSINE AND TRYPTOPHAN-CONTAINING OLIGOPEPTIDES AT CARBON FIBER MICROELECTRODES APPLIED TO SINGLE CELLS	33
	Introduction	33
	Experimental	36
	Results and Discussion	38
	Conclusion	45
4	CATECHOLAMINE DEPLETION BY RESERPINE AND TYRAMINE	57
	Introduction	57
	Experimental Section	59
	Results and Discussion	61

Conclusion 68

5 SPATIALLY-RESOLVED AMPEROMETRIC MEASUREMENTS OF 5-HYDROXYTRYPTAMINE SECRETION AT SINGLE PANCREATIC β-CELLS..... 78

Introduction 78
Experimental 79
Results and Discussion 85
Conclusion 96

6 SUMMARY AND FUTURE WORK 120

REFERENCES 125

BIOGRAPHICAL SKETCH 132

Abstract of Dissertation Presented to the Graduate School
of the University of Florida in Partial Fulfillment of the
Requirements for the Degree of Doctor of Philosophy

SPATIALLY AND TEMPORALLY RESOLVED MEASUREMENTS FROM SINGLE NEUROENDOCRINE CELLS

By

Charina D. Paras

May, 1998

Chairman: Robert T. Kennedy
Major Department: Chemistry

Electrochemical techniques were used to monitor secretion from single neuroendocrine cells. In the amperometric mode, stimulation of a cell resulted in a series of current spikes observed at the electrode. The shape, area, frequency and number of spikes were analyzed to provide unique information on exocytosis. Cyclic voltammetry was used to identify the compunds detected at the electrode.

The detection of pro-opiocortin (POC) peptides secreted from melanotrophs is based on the electrochemical oxidation of tryptophan and tyrosine residues. In amperometry, current spikes were observed when cells were stimulated by application of 64 mM K^+ and by mechanical stimulation. It was concluded that the current spikes represent detection of concentration pulses that are expected following exocytosis events. In amperometry, fouling of electrodes was reversed by an electrochemical treatment. By exploring the effects of scan rate, scan interval and potential window, the conditions for cyclic

voltammetry were optimized. Using cyclic voltammetry at 800 V/s in the potential window of 0 to 1.2 V, it was possible to distinguish MSH from other POC peptides based on the peak-shaped voltammogram for MSH.

Carbon fiber microelectrodes were used to investigate the mechanisms of depletion of reserpine and tyramine in PC12 (pheochromocytoma) cells. Reserpine depleted a large number of catecholamine containing granules which resulted in a decrease in the number of current spikes during nicotine (in high K^+ balanced salt solution) stimulation. Tyramine caused quantal release of catecholamines. Results suggest the presence of two pools of catecholamine containing vesicles in PC12 cells which respond differently to tyramine and nicotine.

Flame-etched electrodes (~2 μm diameter) were used to probe exocytosis release sites on the surface of pancreatic β-cells. When single pancreatic β-cells were stimulated with high K^+ buffer or tolbutamide, current spikes were observed at specific regions or hotspots on the cell membrane. Occurrence of abnormally large spikes was attributed to multigranular exocytosis. The number of spikes detected at these small electrodes was used as a direct evidence for compound exocytosis. Fluorescent monitoring of FM1-43, a membrane dye, confirmed the presence of active and inactive sites of release on the surface of the cell.

CHAPTER 1
INTRODUCTION

Secretion and regulation of hormones and neurotransmitters have been associated with a wide variety of biological functions including memory, learning, growth and metabolism. Abnormalities in the regulation and secretion of these compounds have far-reaching implications for both the pathophysiology and treatment of associated diseases (e.g. Parkinson's disease and diabetes mellitus) (Cooper and Martin, 1980). Hormones and neurotransmitters are frequently stored in intracellular vesicles and in the presence of an appropriate stimulus secretion occurs through a process called exocytosis. Exocytosis is a calcium dependent process by which vesicles move towards the plasma membrane, fuse with the inner surface of membrane and then subsequently release their contents to the extracellular space (Schweizer et al., 1995). Previous studies on exocytotic secretion have been performed on population of cultured cells by protein assay, fluorimetric analysis and chromatography. However, these techniques suffer from inadequate sensitivity and are not capable of monitoring the dynamics of secretion in "real time". The overall objective of this work is to develop and apply analytical techniques for monitoring peptides and neurotransmitters secreted from single cells with high temporal and spatial resolution. We developed electrochemical techniques useful for monitoring peptides secreted from melanotrophs. In addition, we explored various applications of

electrochemical techniques in understanding the dynamics of secretion in pheochromocytoma (PC12) cells and pancreatic β-cells.

Electroanalysis as a Tool in Neurochemical Studies

The use of electrochemical methods in the study of neurobiological systems was introduced by Ralph Adams in the early 1970s (Adams, 1976; Wightman, 1991). This pioneering study involved on line monitoring of dopamine and norepinephrine in the rat brain by implanting graphite electrodes in the brain tissue of an anesthetized rat. The results provided a new approach on studying chemical changes in the brain since earlier methods were very tedious required long analysis time and did not allow measurements at the site of action (Adams, 1976). This spawned a widespread interest in electroanalysis for studies in complex biological matrices.

Electrochemical methods can provide both quantitative and qualitative information while providing selectivity to electroactive species (Chen and Ewing, 1997). Interferences are minimized since only easily oxidizable and reducible substances are detected. Selectivity of electrodes can be further improved by developing appropriate voltammetric techniques (e.g., differential pulse voltammetry and fast scan cyclic voltammetry) and by modifying the surface of electrodes. In brain studies, perfluorinated ion exchange membranes improved the selectivity of the carbon electrode to dopamine (Wightman, 1988). Chemical modifications are also employed to detect nonelectroactive substances. For instance, enzymes are attached to the electrode surface through entrapment in a polymer matrix like Nafion (Harrison et al., 1988) and by covalently linking with carbodiimide (Sasso et al., 1990). Enzyme-modified electrodes are used to indirectly detect substrates (e.g. glucose, glutamate and choline) with electroactive enzymatic

products. In some cases, the electrode's surface is modified with an inorganic catalyst that can catalyze oxidation. Deposition of a thin film of mixed-valent ruthenium (III,II) cyanide on the surface of the electrode has been reported to catalyze the oxidation of insulin (Cox and Kulesza, 1984; Kennedy et al., 1993).

Carbon electrodes are very suitable for in vivo monitoring in the brain since most of the neurotransmitters (e.g. dopamine, norepinephrine and serotonin) can be oxidized at the carbon surface (Wightman, 1981). In this type of analysis, microelectrodes have greater advantage over conventional electrodes because they can provide sensitive measurements in smaller sample matrices. But this is not the only advantage for using microelectrodes. Many of the limitations associated with conventional electrodes are minimized or removed by using microelectrodes ($\leq$ 25 μm radius disc) (Bond, 1994). A major advantage of microelectrodes is that the electrochemical data is less distorted by ohmic drop than when recorded with electrodes of conventional size. Steady state currents are obtained because the electrolysis rate is approximately equal to the rate of diffusion of molecules at the surface of the electrode (Wightman, 1981). Double layer charging currents are also minimized due to the small surface area, allowing for faster measurements (Wightman, 1981). Due to the extremely small current produced at the electrode, these electrodes can be used in solutions of very high resistance (Wightman, 1981). In addition, a simple two electrode configuration can be used for the analysis (Bond, 1994).

Recently, microelectrode techniques have made major contributions in the study of the dynamics of secretion from single cells (Leszczyszyn et al., 1990, Chow et al., 1992, Alvarez de Toledo et al., 1993, Kennedy et al., 1993, Chen et al., 1994 and Paras and Kennedy, 1995). This was made possible with the use of carbon fiber microelectrodes that

were about the size of a single cell (See Figure 1.1). Secretion of peptides and neurotransmitters was monitored by positioning the electrode adjacent to the cell. Stimulant was applied by pressure ejection from a micropipette positioned about 30-40 μm away from the cell. Cyclic voltammetry is used to identify the compounds secreted while amperometry is used to increase the temporal resolution. This method brought about a simple and direct way of monitoring secretion at single exocytosis events.

Electrochemical Methods

Ponchon and coworkers first introduced the use of carbon fibers in making microelectrodes in 1979. The broad potential range of carbon fiber microelectrodes allows the detection of most of the neurotransmitters in the central nervous system including their metabolites (Ponchon et al., 1979). The small size of the carbon fiber microelectrode makes it ideal for monitoring release of neurotransmitters and hormones from single cells. The following voltammetric techniques have been used for monitoring secretion at single cells: cyclic voltammetry, amperometry and differential pulse voltammetry. This discussion will focus on cyclic voltammetry and amperometry since these are the most widely used electrochemical techniques for single cell detection.

Cyclic voltammetry. In cyclic voltammetry, the voltage is linearly scanned from an initial potential (E_i) to a switching potential (E_λ) then back to the initial potential. The resulting current is plotted as a function of the potential. In measuring secretion from single cells fast scan rates are employed and the resulting peak-shaped voltammograms are used to identify electroactive species. At the starting potential, Ei, usually there is no electrochemistry occurring. The current starts to increase at a potential sufficient to oxidize the analyte until it reaches a maximum value. The current then decreases to the

baseline as the concentration of analyte around the electrode decreases. The decrease in concentration is due to the faster electrolysis rate as compared to the rate of diffusion of molecules towards the electrode (Wightman, 1981). During the cathodic (reduction) scan, a peak shaped voltammogram is also obtained due to the decrease in concentration of reductive specie. The anodic (Ep,a) and the cathodic (Ep,c) peaks are useful for the identification of the analyte (Kawagoe, 1993). The shape of the current voltage curve is greatly affected by the rate of electron transfer at the electrode. So for slow electrochemical reactions, a drawn out current-voltage curve is obtained.

At high scan rates, the limit of detection in cyclic voltammetry is limited by the residual current due to double layer capacitance and redox reactions of surface-bound species. The residual current increases linearly with scan rate whereas the faradaic current (from redox reactions of solution species) increases with the square root. Thus, at very high scan rates, faradaic current is masked by the presence of very high residual current. To obtain analytically useful cyclic voltammogram, background subtraction is employed.

Amperometry. In amperometry, a constant potential is applied at the electrode and current is continuously monitored. Usually, the potential at the working electrode is applied at a value such that complete electrolysis of the desired analyte occurs. However, in complex matrices, the magnitude of the applied potential is minimized to avoid undesirable signal due to the electrolysis of other species in the media. The magnitude of the current is directly proportional to the concentration of analyte as described by the equation for limiting current at a microelectrode at steady state conditions:

$$i_{lim} = 4rnFDC$$

where r is the radius of the electrode, n is the number of electrons transferred in the electrode reaction, F is the Faraday constant (96,485 C/equivalent), D is the diffusion coefficient and C is the concentration of the analyte. And by Faraday's law, the amount of analyte oxidized or reduced at the electrode can be calculated.

Faraday's Law:

$$N = \frac{Q}{nF}$$

where N is the number of moles of substance detected, Q is the total charge passed, n is the number of electrons transferred per molecule, and F is the Faraday's constant (96,485 C/eq) (Kissinger, P.T., et al, 1996).

Monitoring Secretion from Single Cells

The small size and rapid response time of microelectrodes make them very suitable for studying the dynamics of release from single cells. Previous studies indicate that this technique can measure secretion of a few thousand molecules with millisecond time resolution. Analytes detected range from easily oxidizable neurotransmitters like dopamine and norepinephrine to less oxidizable peptides like melanocyte stimulating hormone and insulin. In addition, microelectrodes have been employed to measure intracellular oxygen and glucose levels (Chien et al., 1990; Lau at al., 1992; Abe et al., 1992). This section will discuss briefly some of the research done with the use of microelectrode techniques.

An alternative way of monitoring exocytosis is by measuring the capacitance change as the vesicles fuse with the cell membrane. Like electrochemical techniques, cell membrane capacitance measurements can detect exocytosis with a few millisecond time

resolution (Neher and Marty, 1982). However, capacitance measurements can be distorted by changes in cell membrane area (Zorec and Tester, 1993) and changes in the electrical circuit of the cell (e.g. changes in dielectric constant caused by membrane proteins) that are unrelated to secretion (Fernandez et al., 1982; Horrigan and Bookman, 1994; Oberhauser et al., 1996).

Electrochemical methods have been used to study exocytosis at various cell types including adrenal chromaffin cells, PC12 cells, mast cells, melanotrophs and β-cells. In amperometry, current spikes are obtained that correspond to single exocytotic event. The area of the current spikes is used to determine the amount of substance release while the spike shape is used to study the dynamics of vesicular release (Aspinwall et al, 1997). As an example, the spike width is associated with the kinetics of the extrusion of the vesicular contents (Wightman et al., 1995; Aspinwall et al., 1997). Occurrence of a foot at the onset of a single spike can represent slow leakage of molecules coming from a narrow opening of the fusion pore during the initiation of exocytosis (Chow et al., 1992).

Depending on the stimulus, current spikes may be observed within a second or may be delayed for several seconds. By measuring the time between the application of stimulus to the detection of release, it has been observed that cells respond differently to various drugs or stimulus. The latency of exocytosis depends on the cascades of events following stimulus application and leading to exocytosis (Ewing and Chen, 1997). In PC12 cells, application of 105 mM K^+ triggered release of dopamine in a few seconds while the secretion due to 1 mM muscarine occured after ~ 100 ms (Zerby and Ewing, 1996). In β-cells, current spikes were observed a few milliseconds (0-2 ms) after exposure to 60 mM

K^+ but for glucose (16 mM) induced secretion, spikes were observed after 60 to 240 s (Huang et al., 1995).

Studies on chromaffin cells, mast cells, PC12 cells and β-cells have demonstrated the dependence of spike areas to the volume of the vesicle and concentration of molecules in each vesicle. The distribution of the cube root of spike areas can fit a gaussian curve with a standard deviation (SD) similar to that for the vesicular radii. The mean vesicular radii from ultrastructural studies and the mean vesicular quantal from the gaussian fit can be used to calculate the concentration of molecules inside the vesicles (Finnegan et al., 1996).

Cyclic voltammetry provide additional information that can not be obtained by amperometry. For example, adrenal chromaffin cells are known to secrete both epinephrine and norepinephrine. These two compounds have similar structures and are both electroactive at carbon fiber microelectrodes. However, by fast scan cyclic voltammetry, different voltammograms can be obtained due to the differences in the rates of intracyclization for the oxidized forms (Ciolkowski et al., 1992). In another study, the co-released of histamine and 5-hydroxytyptamine was observed at single mast cells by fast scan cyclic voltammetry. To enhance the sensitivity of the carbon fiber microelectrode to these two compounds, an electrochemical pretreatment was employed. The use of cyclic voltammetry for the identification of compounds released from single cells will be further discussed in Chapter 2 and 3 of this study.

Electrochemical detection can be coupled with other methods to further explore the dynamics of secretion. In the study of single rat chromaffin cells, the coupling of action potential activity to quantal release of cathecolamines in chromaffin cells was investigated by combining perforated patch current-clamp recording with amperometric detection at

carbon fiber microelectrodes. The results showed that secretion is highly dependent on action potential frequency and that certain drugs like acetylcholine triggers exocytosis even in the absence of electrical activity (Zhuan Zhou, 1995). In another experiment, by combining capacitance measurements and electrochemical techniques, it was confirmed that a single amperometric spike correspond to the fusion of a single vesicle (Alvarez de Toledo et al., 1993). Recently, the correlation of catecholamine release and intracellular Ca^{2+} at single bovine chromaffin cells was determined by coupling fluorescence techniques to microelectrode techniques. By using Fura-2 as a probe for cytosolic free Ca^{2+} and carbon fiber microelectrode to detect the released catecholamines, it was demonstrated that exocytosis of catecholamines can be induced by different pathways that leads to cytosolic Ca^{2+} elevation (Finnegan and Wightman, 1995).

Thesis Overview

Chapter 2 describes the electrochemical detection of peptides secreted from single melanotrophs of the pituitary intermediate lobe at carbon fiber microelectrodes. The electrochemical activity of each peptide was determined by flow injection analysis. In the amperometric mode we monitored secretion after application of 64 mM K^+ and after inducing mechanical stimulation. The Ca^{2+} dependency of the occurrence of current spikes in K^+ stimulation was determined. Cyclic voltammetric recordings from mechanical stimulation at a single melanotroph were also obtained.

In Chapter 3 the amperometric and cyclic voltammetric detection of MSH, β-endorphin and corticotropin-like intermediate lobe peptide was further explored. In amperometry, the extent of fouling was determined and various electrochemical treatment were tested to reverse its effects. For cyclic voltammetry, the effects of scan rate, scan

interval and potential window on the detection of pro-opiocortin (POC) peptides were investigated. The optimized conditions for cyclic voltammetry were applied for the selective detection of MSH from single melanotrophs.

Chapter 4 compares the mechanism of cathecolamine depletion of reserpine to that of tyramine. Experiments were performed using PC12 cells, a tumor cell line derived from the adrenal medulla. Secretion of dopamine and norepinephrine was monitored by amperometry at 0.65 V. The effect of reserpine on the number of spikes and spike areas upon Nicotine(1mM)/K^+(105 mM) stimulation was determined. The mechanism of release of tyramine was compared to that of Nicotine/K^+ stimulation.

Chapter 5 is a study on the organization of β-cell secretion machinery. Flame etched electrodes with ~ 2 μm tips were used to monitor secretion on different zones on the cell surface. Measurements of discrete secretion events were interpreted in terms of the different modes of exocytosis. To further explore the dynamics of exocytosis, imaging techniques were also used. Quinacrine dye was used to locate insulin-containing granules and FM1-43 dye was used as a marker for vesicular membranes that fused with the cell membrane during exocytosis. Fluorescence measurements were performed in the laboratory of Dr. Weihong Tan (Chemistry Department, University of Florida).

Chapter 6 is a summary of all the studies discussed in previous chapters.

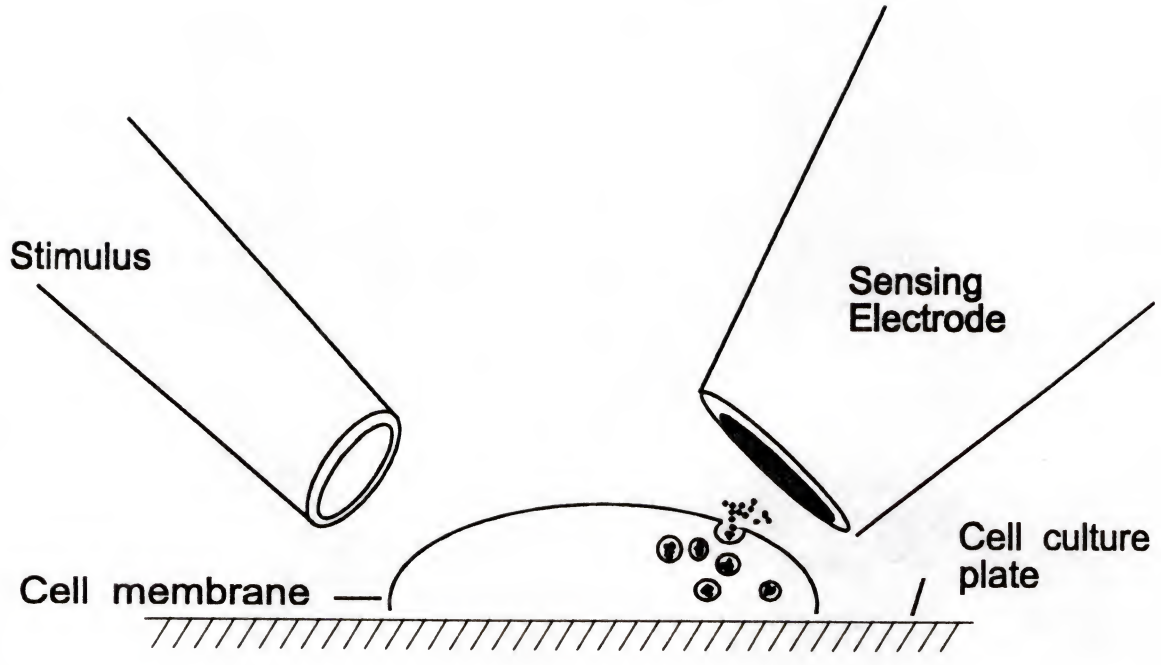

Figure 1-1. Setup for monitoring secretion from single cells. To perform secretion measurements, the electrode is positioned to within 1 μM of the cell surface using a piezoelectric micropositioner as shown above. Stimulus is applied from a glass micropipette which is also positioned near the cell. Substances release by the cell diffuse from the cell to the electrode for detection.

CHAPTER 2
DETECTION OF EXOCYTOSIS AT SINGLE RAT MELANOTROPHS

Introduction

Peptide hormones secreted from pituitary cells control a wide variety of biological functions. In addition, these cells serve as useful models for the study of neurons. Understanding the regulation and mechanism of secretion of these peptides is therefore of considerable interest. A significant limitation in the study of pituitary cells has been the lack of methods to monitor peptide release on the same time scale that cells regulate secretion. For example, although it is generally agreed that pituitary cells release peptide by exocytosis, the direct measurement of peptide secretion with temporal and spatial resolution to detect single exocytosis events has not been accomplished. The most commonly used method for monitoring secretion is to assay fractions collected from perfusion of large collection of cells (Munemura et al., 1980; Raymond et al., 1981; Tsuruta et al., 1982; Jackson and Lowry, 1983; Kongsamut et al., 1993). This method provides temporal resolution on the minute time scale and is not compatible with single cells. Cell capacitance measurements have allowed secretory activity at single cells to be measured; however, for pituitary cells the sensitivity has not been sufficient to detect single exocytosis events (Thomas et al., 1990).

Several recent reports have focused on the use of microelectrodes for detection of exocytosis at single cells. In this technique, an electrode, typically a carbon fiber

microelectrode of about the same size as the cell, is positioned adjacent to a single cell. Substances secreted from the cell are detected after they diffuse the short distance between the cell and electrode. Exocytosis of epinephrine and norepinephrine from adrenal cells (Leszczyszyn et al., 1990; Wightman et al., 1991), dopamine from PC12 cells (Chen et al., 1994), serotonin from mast cells (Alvarez de Toledo, et al., 1993), and insulin from pancreatic β-cells (Kennedy et al., 1993) has been detected using electrochemical methods. Both amperometry and voltammetry have been used for detection. For both methods, high temporal resolution and mass sensitivity results from the close proximity of the cell and electrode and fast response time of the electrodes. When used to measure exocytotic release, stimulation of a cell results in a series of current spikes observed at the electrode. It has been demonstrated that the current spikes correspond to direct detection of multimolecular packets released from vesicles. In many cases, it is found that isolated current spikes correspond to single exocytosis events.

In this chapter, this technique was used to monitor the release of α-melanocyte stimulating hormone (α-MSH) and related peptides from single melanotrophs of the pars intermedia of the rat pituitary gland. Current spikes were obtained at carbon fiber microelectrodes following stimulation of melanotrophs, which correspond to detection of concentration pulses resulting from exocytosis. The observations are the highest resolution yet obtained for detection of α-MSH secretion and demonstrate the first direct detection of peptide secreted from pituitary cells at the level of single exocytosis events. Since the exocytosed material is detected directly, this method should allow the kinetics of release separate from kinetics of pore openings and endocytosis to be studied. Thus, the

method provides information complementary to the cell capacitance method of monitoring secretion in these cells.

Experimental

Cell Isolation and Culture

Melanotrophs were isolated and dispersed using a procedure similar to that described elsewhere (Thomas and Almers, 1990). Pituitaries were obtained from three adult male Sprague-Dawley rats weighing 200-300 g. The pituitaries were washed with a Ca^{2+}-free balanced salt solution (137 mM NaCl, 5 mM KCl, 0.7 mM Na_2HPO_4, 25 mM HEPES, 10 mM glucose, adjusted to pH 7.25). The neurointermediate (NI) lobe was separated from the anterior lobe under a dissecting microscope. The isolated NI lobes were rinsed twice with the Ca^{2+}-free balanced salt solution at 37 °C for 30 min. They were then digested in 0.5 mL trypsin (0.5 mg/mL in Ca^{2+}-free balanced salt solution) at 37 °C for 15 min. During digests the cells were triturated three times using a fire polished siliconized Pasteur pipette. After each digest, the cells were centrifuged at 550 g for 4 min at room temperature. After dispersion the cells were washed with Dullbecco's modified Eagle's medium (DMEM, GIBCO cat. No. 11885) and plated in small spots on 7 polylysine coated Petri dishes. The cells were incubated at 37 °C, 100% humidity, and 5% CO_2 in DMEM containing 10% fetal calf serum, 100 mM glutamine, 0.081 g/L non essential amino acid supplement (Sigma Chemical Co., catalog number 2025), 100,000 U/L penicillin and 100 mg/L streptomycin. Cells were used on days 2-6 of culture.

Electrode Preparation

Glass encased carbon fiber microelectrodes were prepared using previously described techniques (Kelly and Wightman, 1986). A single, carbon fiber of 9 μm diameter (P-55S

from Amoco Performance Products) was inserted into a microfilament glass capillary (0.68 mm i.d., 1.2 mm o.d., 4" long AM systems). The capillary containing the carbon fiber was then pulled to a fine tip on a commercial pipette puller (Narishige PE-2). The carbon fiber was cut in the middle to yield two electrodes. The tip of the electrode was trimmed using a small scalpel to produce a small gap between the capillary and the carbon fiber. The carbon fiber was sealed at the glass tip of the electrode by dipping it in epoxy. The epoxy was prepared by heating up 3 mg of Shell EPON Resin 828 (Miller-Stephenson Chemical Company, Inc.) to approximately 80 °C. At this temperature, the resin was as viscous as water and 0.5 mg metaphenylenediamine (MPDA) was added. The electrode was dipped in epoxy for about 10-15 s to allow the epoxy to enter the capillary. The epoxy was allowed to gel overnight at room temperature. Then, the electrodes were cured in an oven at 100 °C for 2 h or more followed by 150 °C for 2 h. Proper curing process is important to avoid the formation of gaps between the carbon fiber and epoxy. Presence of gaps will result in high residual currents. Once the epoxy was cured, the electrodes were polished at 30 to 45° angle on a micropipet beveler (Sutter Instruments). Immediately after polishing, electrodes were dipped in isopropanol for 10-15 min and then ultrasonicated in H_2O for 5 min. The capillaries were filled with mercury and a nicrome wire was inserted for electrical connection.

Electrode Testing

Calibration and other electrode tests were performed using a flow injection apparatus (as shown in Figure 2-1). This system consisted of a syringe pump (Harvard Apparatus 11) connected to a two position, six port valve (Valco AC6UHC) equipped with a 1 ml sample loop. The outlet of the valve emptied into a glass cell via 0.25 mm inner diameter

tubing. The working electrode was positioned in the outlet of the tubing using a micromanipulator. The entire flow injection system was housed in a Faraday cage. Data were collected using an EI-400 potentiostat (Ensman Instrumentation, Bloomington, IN). For amperometric recordings, the electrode was poised at 0.80 V (all potentials are versus sodium-saturated calomel electrode). Amperometric data were collected at 300 Hz and low pass filtered with a cutoff frequency of 100 Hz. The data were collected by an IBM-compatible personal computer (Gateway 2000 486-66 MHz) via a National Instruments multifunction board. The data collection program used for testing electrode was provided by Prof. Mark Wightman (University of North Carolina, Chapel Hill).

Fast scan cyclic voltammetry was performed as described elsewhere (Bauer et al., 1991). Briefly, the potential on the electrode was linearly scanned from 500 mV to 1100 mV and back to 500 mV at a rate of 300 V/s. Each scan took 3.3 ms and scans were obtained at a rate of 10 Hz. All voltammograms shown are background subtracted. The background was obtained prior to application of substances to the electrode or, in the case of the single cell measurements, prior to the stimulation. The cyclic voltammograms were filtered at 2 kHz.

The number of electrons transferred per mole (n) were determined using chronoamperometry at a microelectrode according to a previously described method (Heinze, 1993). For this experiment, the background subtracted steady state current (Δi) was measured following a potential step from +0.40 V to +0.80V. Values for n were calculated according to the following equation: $n = \Delta i/4rCDF$ where r is the radius of the electrode (disk carbon electrodes were used for these experiments, C is the concentration of α-MSH, D is the diffusion coefficient, and F is the Faraday constant.

The diffusion coefficient for α-MSH used for these calculations was 3.75×10^{-6} cm^2/s. This value was calculated by measuring the dispersion of an α-MSH concentration pulse as it flowed through a capillary tube. Calculation was based on the Golay equation which predicts dispersion in open tubular chromatography columns. At sufficiently high flow rates, the Golay equation (Golay, 1959) simplifies to: $D = d^2v/(96H)$ where d is the inner diameter of the capillary, v is the flow velocity in the capillary and H is plate height. Details of using this method are given elsewhere (St. Claire III, 1986).

Single Cell Measurements

Single cell measurements were performed in a manner similar to that described elsewhere (Leszczyszyn et al., 1990; Wightman et al., 1991). Petri dishes containing the cells were rinsed 3 times with balanced solution (same composition as the solution used for cell isolation except 2.0 mM $CaCl_2$ was also added). The dish was filled with the balanced salt solution and placed in a microincubator (Medical Systems, Inc.) on the stage of an inverted microscope (Zeiss axiovert 35). The microincubator maintained the temperature at 34 °C. To perform measurements (see Figure 1-1), a cell was located with the microscope and a working microelectrode brought to within 1 μm of a cell using a micropositioner (Burleigh PC-1000).

Substances were applied to individual cells by pressure ejecting solutions from the tips of micropipettes which were positioned approximately 30 μm from the cell. Flow rates through the pipette tips were approximately 1 nL/s. Stimulants were dissolved in balanced salt solution with an equivalent amount of NaCl removed. For mechanical stimulation, the electrode was pressed against the cell, usually until current spikes were observed, and then retracted until the electrode was approximately 1 mm away from the cell.

All cell data are reported as the mean ±1 standard deviation. Spikes were counted and measured only if their peak height was five times the peak to peak noise.

Chemicals. Unless stated otherwise, all chemicals used for standards and buffers were obtained from Sigma Chemical Co. (St. Louis, MO) and cell culture chemicals and media were obtained from GIBCO (Grand Island, NY).

Results and Discussion

Electrochemical Detection of α-MSH

Melanotrophs secrete a collection of peptides derived from the cleavage of pro-opiocortin. Primary secretory products are α-MSH, corticotropin-like intermediate lobe peptide (CLIP), lipotropin (γ-LPH), and β-endorphin or variants of these peptides with post-translational modifications (Mains and Eipper, 1979; Glembotski, 1981; Smelik et al., 1983). In addition, a 16 KD fragment (16K) of pro-opiocortin is also a major vesicle component (Mains and Eipper, 1979; Glembotski, 1981; Smelik et al., 1983). It is well known that small peptides containing tryptophan and tyrosine can be detected by oxidation at carbon electrodes (Bennet at al., 1981; Sauter and Frick, 1984; Drumheller at al., 1985). Since many of the secretory products of melanotrophs contain these amino acids, it seemed reasonable that it would be possible to detect secretory activity at a carbon microelectrode through detection of one or more of these products.

Figure 2-2 illustrates flow injection analysis for α-MSH, CLIP, and β-endorphin. In this experiment, the electrode potential was fixed at +0.80 V and 1 μM of each peptide was injected. At this potential, α-MSH gave a signal 9 times higher than β-endorphin and 10 times higher than CLIP. (γ-LPH produced no signal under these conditions). This selectivity is partially attributed to the presence of tryptophan in α-MSH. Of the two

electroactive residues, tryptophan gives 5 times the current at carbon-fiber microelectrodes for a given concentration as illustrated in the cyclic voltammograms in Figure 2-3. α-MSH contains a single tryptophan while the other electroactive peptides contain no tryptophan and just single tyrosine residues. The selectivity for tryptophan is useful in this case, but surprising since other types of carbon electrodes have much less selectivity for tryptophan over tyrosine (Bennet at al., 1981). The other factor which contributes to selectivity for α-MSH is its relatively small size, 13 amino acids, compared to β-endorphin (30 amino acids), CLIP (21 amino acids), and γ-LPH (58 amino acids). The likelihood of electroactivity being observed in a peptide decreases with increasing size since in larger peptides the electroactive residues may be sterically hindered from interacting with the electrode surface.

Cyclic voltammetry. Figure 2-4 illustrates a background subtracted fast scan cyclic voltammogram of 100 μM α-MSH obtained by flow injection analysis. The voltammogram is compared to that obtained for tryptophan at 100 μM. The similarity in the shape of the voltammograms supports the idea that the electroactivity observed is due to the tryptophan residue. α-MSH, which has the structure of N-acetyl adrenocortropin hormone 1-13, is actually one of three peptides with the same amino acid sequence released from melanotrophs. In addition, N,O-diacetyl α-MSH and desacetyl α-MSH are found (Goldman et al., 1983). Approximately 86% of the α-MSH-like material released is N,O-diacetyl α-MSH (Goldman et al., 1983). Only about 9% of the α-MSH-like substances is α-MSH which is the form used for calibrations. However, all forms of α-

MSH are detected equally because the modifications do not affect the tryptophan or its access to the electrode surface.

Amperometry. For amperometry, linear calibration curves were obtained for α-MSH over the range of 10 nM to 1 μM. A typical line had a slope of 10.9 pA/μM, a y-intercept of 0.71 pA, and a correlation coefficient of 0.994. Negative deviations from linearity were observed above 0.6 mM which were apparently due to adsorption of the peptide or its oxidized product on the electrode surface. When measuring the current at +0.9 V for cyclic voltammetry, the relative standard deviation was less than 2% at all concentrations and the detection limit was 10 nM. Although 10 nM was the detection limit when just measuring the current at +0.9 V, recognizable voltammograms could only be obtained at concentrations greater than 50 nM if at least 10 scans were averaged together. For single scans, approximately 150 nM was required to obtain a useful voltammogram.

Fouling of electrodes. In both amperometry and cyclic voltammetry, it was found that exposures of the electrode to concentrations over 10 mM would decrease the response of the electrode indicating fouling of the electrode surface. The mechanism of fouling is presumably adsorption of oxidized tryptophan on the electrode surface (Brabec and Mornstein, 1980).

Detection of Secretion at Single Cells

High K^+ stimulation. Figure 2-5 illustrates amperometric current recordings observed after application of 64 mM K^+ to a cell. As shown, currents spikes in the range of 0.5 to 2 pA height are observed following stimulation. Current spikes were rarely observed without stimulation of the cell. Also, current spikes were not observed if the electrode potential was insufficient to oxidize α-MSH. The occurrence of current spikes was

strongly dependent on the presence of Ca^{2+} in the extracellular fluid. Figure 2-6 illustrates a series of K^+ stimulations performed in Ca^{2+} free media. Application of 64 mM K^+ without Ca^{2+} produced a series of spikes of varying number. The average number of spikes observed with Ca^{2+} was 15 ± 3.8 while that observed without Ca^{2+} was 1.4 ± 0.81 (n=7).

Mechanical stimulation. An example of an amperometric recording following mechanical stimulation is shown in Figure 2-5. Mechanical stimulation, although not well characterized physiologically, has proven useful in adrenal medullary chromaffin cells as a method of eliciting exocytosis for electrochemical detection (Wightman et al., 1991). Using mechanical stimulation at melanotrophs, it was found that after an initial series of spikes, a low frequency of spikes continued for over 60 s (Figure 2-5B). This time course of spike activity is in marked contrast to that with K^+ stimulation which only occured during the stimulation and for a short time after the cessation of K^+ application. In spite of the different time course, the spikes had similar shapes and sizes. For example, the average width at half height for spikes elicited by mechanical stimulation was 36 ± 6 ms (n=20) and for spikes elicited by K^+ stimulation it was 36 ± 6 ms (n=4). The average areas under spikes elicited by mechanical stimulation was 38 ± 5 fC (n=19) and by K^+ stimulation the average spike area was 34 ± 6 fC (n = 35)

Cyclic voltammetry at single cells. Attempts made to monitor secretion following K^+ stimulation by cyclic voltammetry were unsuccessful. The difficulty was that voltammograms were obtained every 100 ms, which was too infrequent to detect spikes. In addition, the spikes were so narrow that it was impossible to signal average multiple cyclic voltammograms obtained during a single spike. Thus, the sensitivity by cyclic

voltammetry is likely to be low enough to prevent observing a voltammogram on a single spike. Using mechanical stimulation however, it was often possible to generate large, broad spikes that were apparently due to the overlap of many spikes (Wightman et al., 1991). This is illustrated in Figure 2-7A which shows the current at +1.0 V in a series of cyclic voltammograms obtained after mechanical stimulation. Figure 2-7B shows a cyclic voltammogram that was obtained at the peak of the spike shown in Figure 2-7A. The voltammogram is overlaid with that obtained for authentic α-MSH at the same electrode at the end of the experiment. The change in shape for the voltammogram shown in Figure 5B relative to those shown in Figure 2 for α-MSH was usually observed after the electrode had been exposed to the cells.

It is difficult to establish unequivocally the identity of the substances contributing to the current signals observed; however, the data strongly support the conclusion that the main source of current spikes is detection of α-MSH and its derivatives. Cyclic voltammograms obtained from the single cell releasates match that for a-MSH and are indicative of a small peptide containing tryptophan or tyrosine. From the amperometric experiments, we know that of the five peptides present in greatest abundance in rat melanotroph vesicles (α-MSH, CLIP, β-endorphin, γ-LPH, and 16 K), the electrode can detect α-MSH, CLIP, and β-endorphin; however, the electrode is 9 to 10 times more sensitive to α-MSH than to the other two detectable peptides. Given that the peptides are secreted in an equimolar ratio (Mains and Eipper, 1979; Jackson and Lowry, 1983), we can estimate that about 86% of the signal is due to α-MSH (and its derivatives) and the remaining percentage split is almost equally between the other two peptides.

Detection of exocytosis. The current spikes observed by amperometry have many of the characteristics that are expected for detection of exocytosis events. Their occurrence is closely related to stimulation and is strongly dependent on external Ca^{2+}. In addition, their shape is the same as that expected qualitatively based on diffusion of detected material from the cell to the electrode. The fact that the area of the spikes is independent of stimulation method also supports the idea that the spikes are detection of exocytosis events. The area under the current spikes corresponds to the amount detected according to Faraday's Law. Thus, if the current spikes are due to exocytosis, then the spike area should reflect vesicular content which should not change with different acute stimulations. Therefore, the spike area should be independent of stimulation method for detection of exocytosis events, as observed.

The average area of the current spikes that we measured was 36 fC. This value can be used to provide an estimate of the amount of α-MSH-like peptide in melanotroph vesicle as follows. From the discussion above, approximately 86% of this area , or 31 fC is due to detection of α-MSH and its derivatives. *n* for α-MSH was measured as $0.96 \pm .04$ at +0.80 V (n = 4); therefore, 31 fC from Faraday's Law corresponds to detection of 0.32 amole of a-MSH. Assuming that a spike corresponds to the detection of all vesicle content (Leszczyszyn et al., 1990; Wightman et al., 1991), this leads to a conclusion that the vesicles contain 0.32 amol of α-MSH-like peptide.

The amount expected per vesicle from previous studies was estimated as follows. Previous measurements of the basal secretion rate of dispersed melanotrophs have been reported and are consistent if the values are normalized to time of incubation and numbers of cells (Munemura at al., 1980; Tsuruta et al., 1982). A typical value is 1.31 ng/2 x 10^4

cells•20 min (Tsuruta at al., 1982). Assuming the rate of basal release is constant, and using a molecular weight of 1665 g/mol for α-MSH, this secretion rate corresponds to 118 amol/cell•hour (Tsuruta et al., 1982). Basal secretion in dispersed melanotrophs corresponds to approximately 0.9% of total hormone content per hour (Mains and Eipper, 1979; Thomas and Almers, 1990). Thus, if 118 amol/cell•hour corresponds to 0.9% of α-MSH content released per hour, then the cell content is 13 fmol. Based on electron micrographs of rat melanotrophs (Chronwall et al.,1988), it has been estimated that rat melanotrophs contain 80,000 vesicles (Thomas and Almers, 1990). Assuming that all of the hormone is found in the vesicle, this corresponds to a vesicular content of of 0.16 amol. Taking into account the limitations of the calculations, this value is in reasonable agreement with the value of 0.32 amol that we obtained. The value that we measured could be high for two reasons. One is that part of the spike could be due to detection of substances that we have not accounted for in calculations. In addition, the average spike area we obtained may be skewed to higher values because smaller spikes, which could result from smaller vesicles, may not be detected because of a poor signal to noise ratio. Nevertheless, the good agreement between the two estimates of vesicle content supports the idea that the spikes are of the appropriate size to correspond to detection of the exocytosis of single vesicles in rat melanotrophs.

Conclusion

It has been demonstrated that exocytosis can be detected at single melanotrophs using amperometry at carbon fiber microelectrode. The resolution and sti,ulation conditions allow single events to be observed. Cyclic voltammetry indicates that the detected substances are small tryptophan- or tyrosine-containing peptides. Based on previous

studies of melanotroph vesicle content and amperometry, the chemical origin of the signal is primarily α-MSH-like peptide with much smaller contribitions from CLIP and β-endorphin.

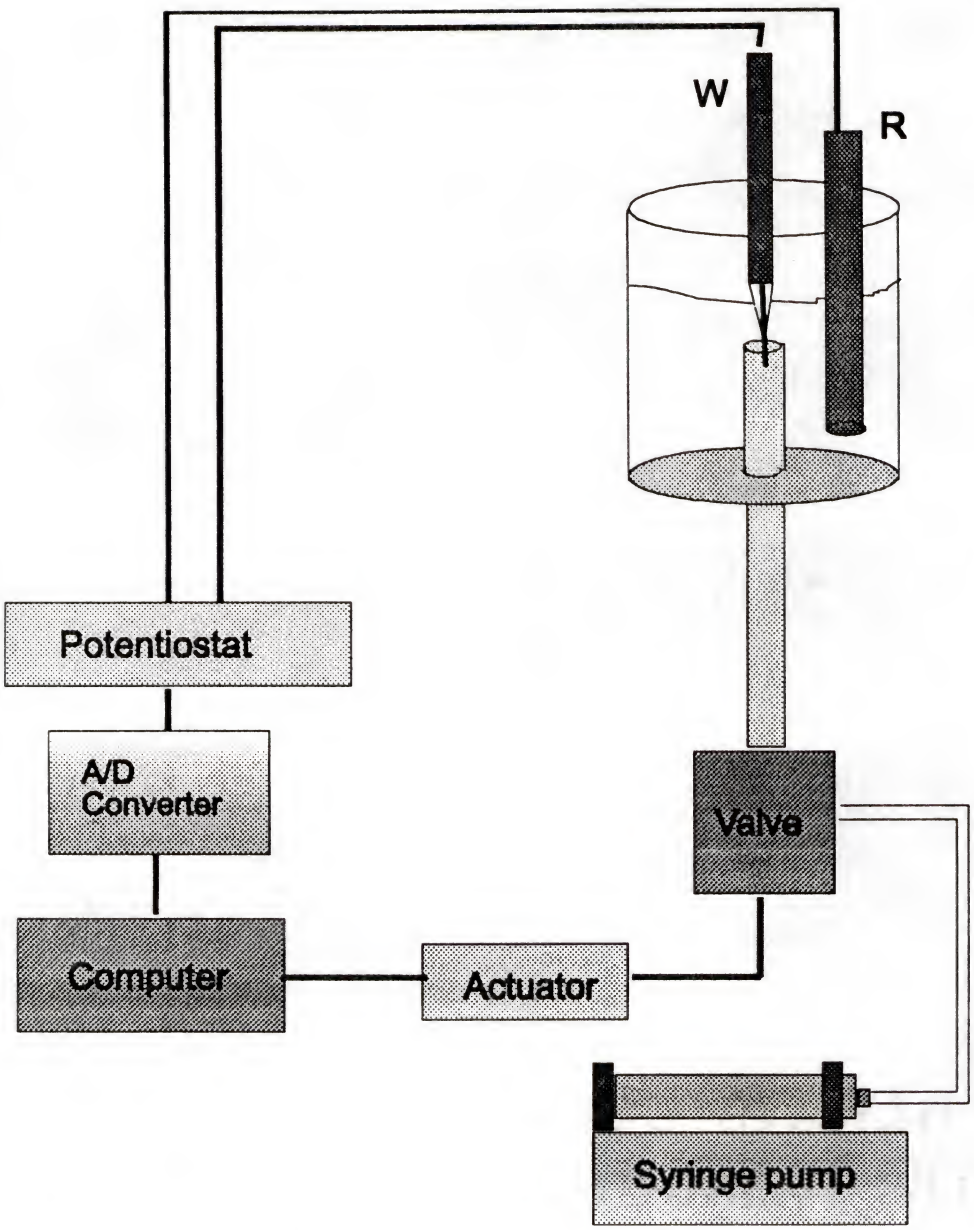

Figure 2-1. Schematic diagram of flow injection setup. R indicates reference electrode (SSCE) and W indicates working electrode (carbon fiber microelectrode).

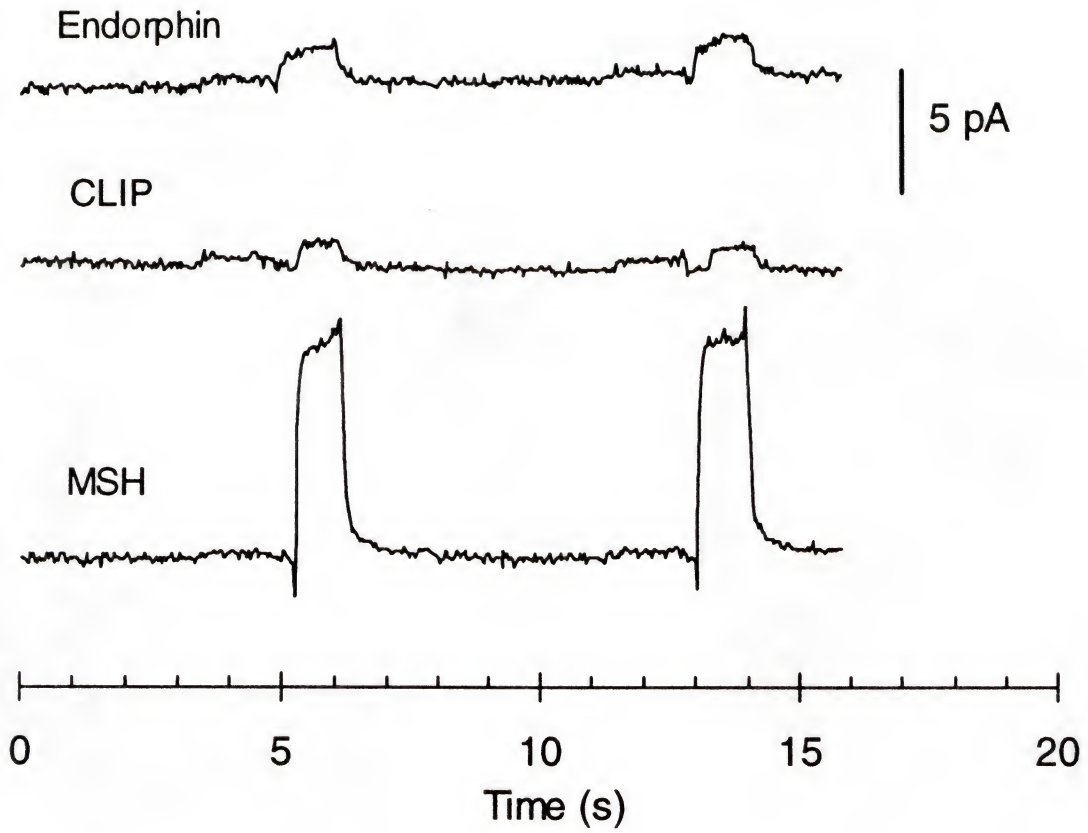

Figure 2-2. Flow injection analysis of pro-opiocortin peptides. Substances were injected at 1 μM each. Duplicate injections were performed approximately 8 s apart. Substances injected are β-Endorphin, CLIP and α-MSH.

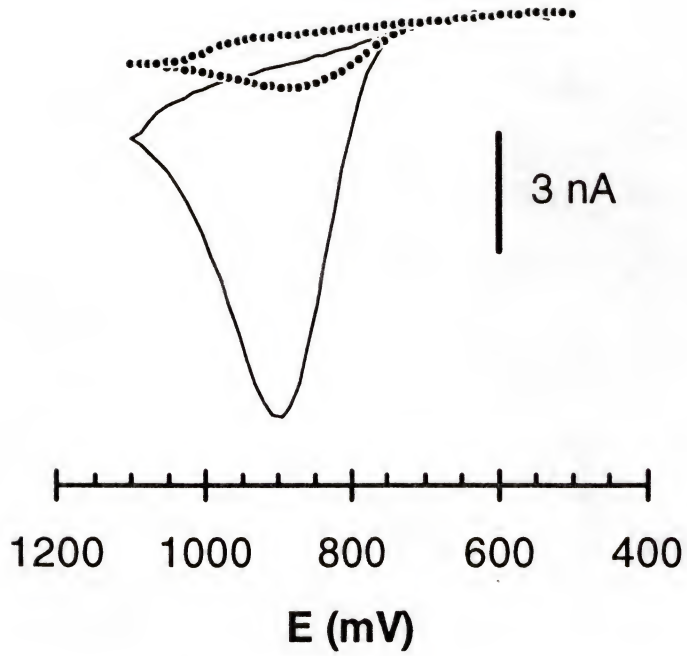

Figure 2-3. Background subtracted fast scan cyclic voltammograms for 0.1 mM tyrosine (solid circles) and 0.1 mM tryptophan (solid line). Each voltammogram is the average of 10 scans.

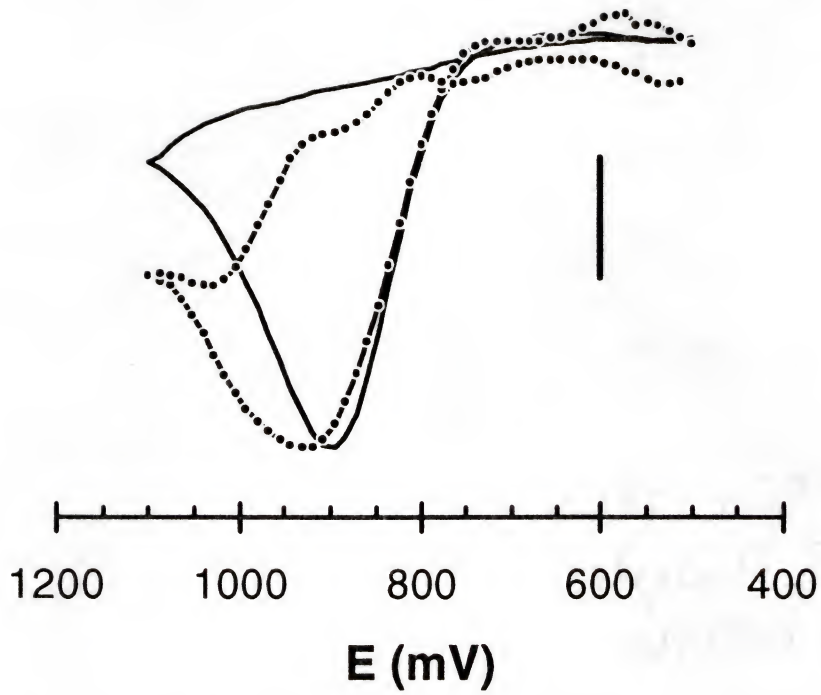

Figure 2-4. Background subtracted fast scan cyclic voltammograms for 0.1 mM α-MSH (solid circles) and 0.1 mM tryptophan (solid line). The current bar is 3 nA for tryptophan and 0.1 nA for α-MSH. Each voltammogram is the average of 10 scans.

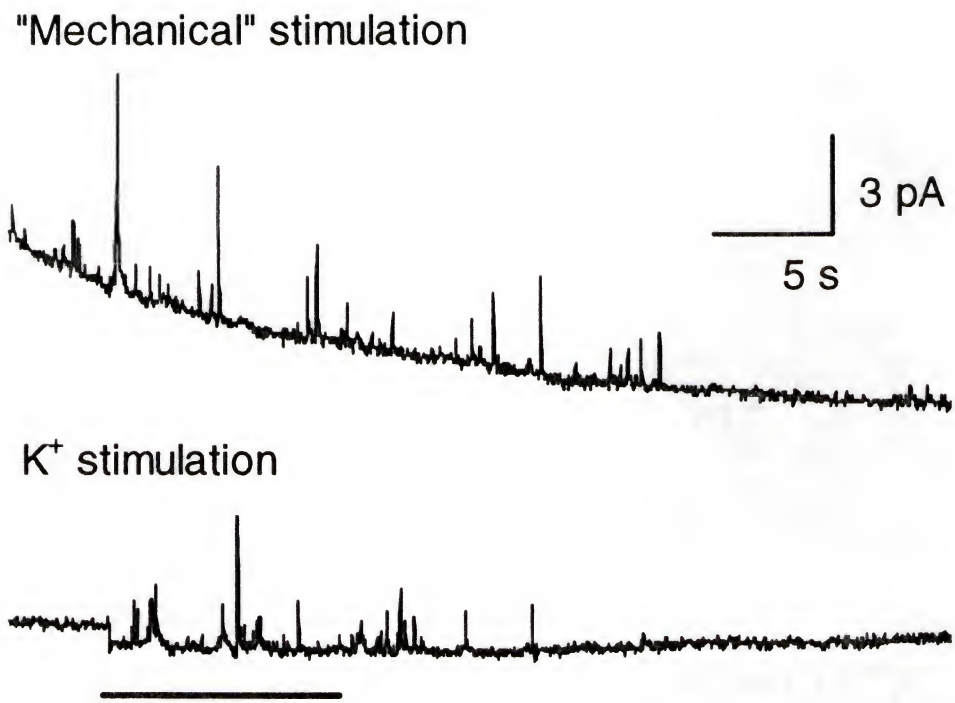

Figure 2-5. Amperometric current recordings made at single melanotrophs with electrode at +0.80 volts. Upper trace shows current recording from mechanical stimulation which was initiated approximately 30 s prior to the current recording. Lower trace was obtained upon application of 64 mM K^+ in balanced salt solution. Stimulation indicated by the solid line.

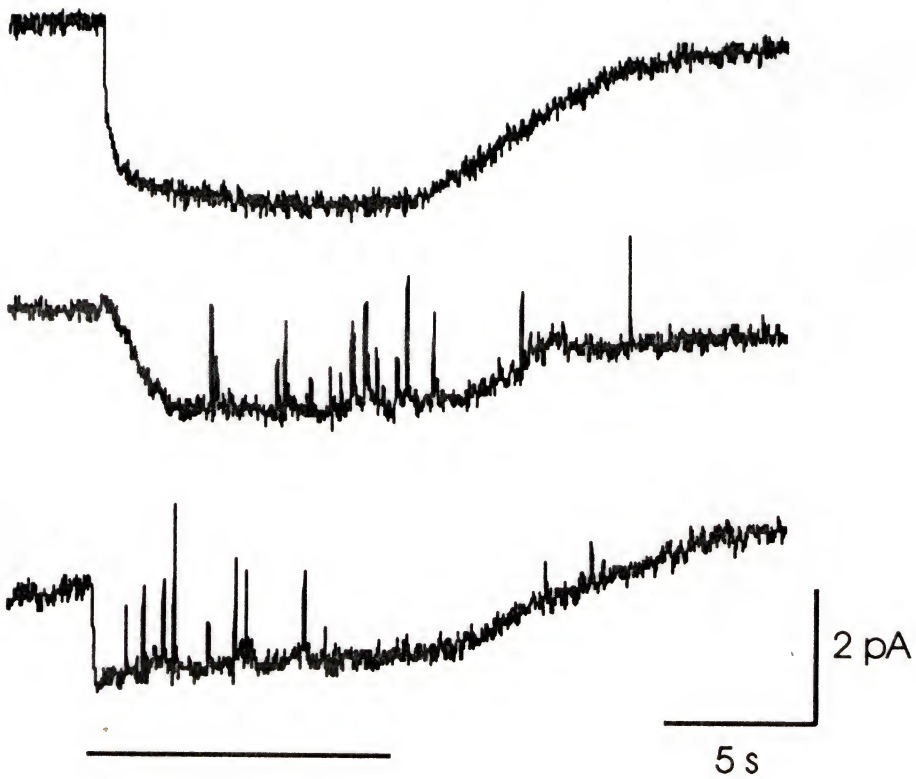

Figure 2-6. Current recordings made at a single melanotroph during stimulation with 64 mM K^+ in Ca^{2+}-free media. All recordings were made at the same cell. The recordings were made in order from top to bottom with 5 min between each stimulation. The first stimulation was 64 mM K^+ with no Ca^{2+}, the next two recordings were with 64 mM K^+ with 2.4 mM Ca^{2+} in the stimulation medium. The bar indicates the time of stimulation.

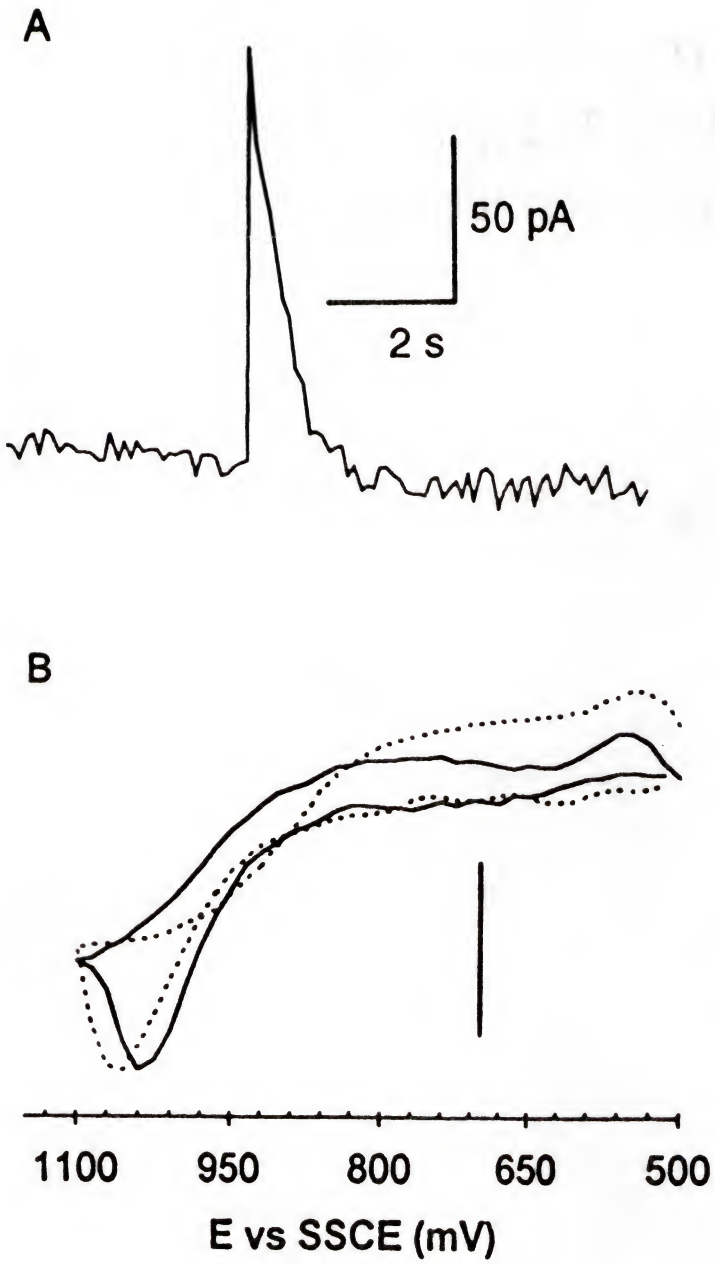

Figure 5-7. Cyclic voltammetric recordings from mechanical stimulation at single melanotroph. (A) Cyclic voltammograms were obtained every 100 ms and the current at +0.9V (the peak voltage for a-MSH) from each voltammogram was plotted. (B) Comparison of background subtracted cyclic voltammograms obtained during single cell stimulation (dashed line) and for authentic α-MSH (solid line). The background voltammograms were obtained from 1 s prior to the increase in current in (A). The voltammogram for the authentic α-MSH was obtained by applying 10 μM α-MSH. The current bar is 1 nA for the standard α-MSH and 0.2 nA for the cell recording.

CHAPTER 3
AMPEROMETRY AND CYCLIC VOLTAMMETRY OF TYROSINE AND TRYPTOPHAN-CONTAINING OLIGOPEPTIDES

Introduction

Peptides and proteins may contain a variety of electroactive moieties including disulfides, thiols, and metal ions. For analytical measurements, most interest has centered on anodic detection of small peptides that contain tyrosine and tryptophan residues (Tucker et al., 1989; Brabec and Mornstein, 1980a; Bennet and Brazell, 1981). The voltammetry of these amino acids is similar in that they are irreversible and yield similar peak potentials even though for tyrosine oxidation occurs at an indole (Brabec and Mornstein, 1980b). Both of these amino acids can be detected by amperometry with carbon electrodes at potential $\leq$ 1.0 V (Drumheller et al., 1985). Peptides containing tryptophan and/or tyrosine in positions that are accessible to an electrode surface can therefore be detected based on oxidation of these electroactive side chains (Brabec and Mornstein, 1980a). Since many neuropeptides and hormones, including enkephalins, endorphins, melanocyte stimulating hormone (MSH), and cholecystokinin, are small peptides that contain tyrosine or tryptophan, improved electrochemical methods could be of benefit in the study of these important compounds.

The most common analytical use of anodic detection of tyrosine and tryptophan-containing oligopeptides is for electrochemical detection in HPLC (Drumheller et al., 1985; Spatola and Benovitz, 1985; Sauter and Frick, 1984; Kissinger et al., 1981).

Another potentially interesting application of the electrochemical detection of such peptides is monitoring their secretion from single cells (Paras and Kennedy, 1995). In this application, a microelectrode is positioned next to a single cell in culture and concentration changes monitored by amperometry or fast scan cyclic voltammetry (CV). The high time resolution possible with electrochemical methods allows the kinetic aspects of secretion to be characterized (Kennedy et al., 1996; Leszczyszyn et al., 1990; Jankowski et al., 1994; Finnegan et al., 1996; Chow et al., 1992; de Toledo et al., 1993; Chen et al., 1994). For example, many neurotransmitters and hormones are stored in vesicles (50-350 nm diameter is typical) and released by exocytosis, a process in which vesicles fuse with the plasma membrane and extrude their contents to the extracellular space in a matter of milliseconds. Exocytosis results in pulses or "spikes" of concentration that can be resolved and detected using microelectrodes. The shape, area, frequency, and number of spikes can all be analyzed to provide unprecedented information on secretion. This technique has primarily been used for the detection of easily oxidized substances such as indoleamines (de Toledo et al., 1993) and catecholamines (Leszczyszyn et al., 1990; Jankowski et al., 1994; Finnegan et al., 1996; Chow et al., 1992; Chen et al., 1994; Wightman et al., 1991); however more recent work has extended this approach to more difficult compounds such as insulin (Kennedy et al., 1993) and histamine (Pihel et al., 1995).

In Chapter 2 carbon fiber microelectrodes were used to detect secretion of MSH and related peptides from single melanocytes (Paras and Kennedy, 1995). Melanocytes synthesize and secrete a collection of peptides derived from pro-opiocortin (POC). Previous reports have shown that although many peptide hormones can be produced from

the cleavage of POC, mammalian melanocytes produce primarily corticotropin-like intermediate lobe peptide (CLIP), β-endorphin, MSH, lipotropin (LPH), and a 16 kD fragment (Smelik et al., 1983; Glembotski, 1981; Mains and Eipper, 1979). As demonstrated in the previous chapter among these peptides, only CLIP, β-endorphin and MSH are electroactive at carbon fiber microelectrodes. (In melanocytes, some of these peptides may be acetylated; however, because of the similar electrochemical behavior of the acetylated and non-acetylated forms, they will not be distinguished here.) MSH is a 13-amino acid peptide with 1 tryptophan and 1 tyrosine residue. CLIP (22 amino acids) and β-endorphin (31 amino acids) each contain a single tyrosine residue. For amperometry, it was found that if the electrodes were exposed to the peptides at low concentrations (<1 μM) for brief periods (< 2s) then reproducible currents were obtained during calibration and electrode testing. At higher concentrations and longer exposures, electrode fouling was observable as decreases in current on subsequent injections. By amperometry, it was possible to detect isolated exocytosis events at melanocytes. Cyclic voltammetry at 300 V/s with a potential window from 0.5 to 1.1 V was also used to detect POC peptides. By applying this waveform every 100 ms, it was possible to measure secretion from single melanocytes; however, in that previous work no attempt was made to systematically investigate the effect of voltammetric conditions on the detection of the peptides. As a result, the CV conditions used had several deficiencies including the inability to distinguish among the different peptides and temporal resolution that was insufficient to detect concentration fluctuations due to exocytosis.

In this chapter, the amperometric and cyclic voltammetric detection of MSH and POC peptides at carbon microelectrodes was further explored. For amperometry, the main

concern is to determine the extent of electrode fouling and methods to reverse its effects. An electrochemical treatment is found that reversed the effect of fouling on the amperometric response for all of the electroactive POC peptides. For CV, the effects of scan rate, scan interval, and potential window on selectivity and temporal resolution for monitoring was investigated. As a result of these investigations, voltammetric conditions were developed that allow selective detection of MSH in the presence of other POC peptides as they are secreted from single melanocytes. The selectivity is based on the ability to distinguish between tryptophan and tyrosine at high scan rates. Although these improvements in the electrochemical detection of oligopeptides will have the most immediate impact for monitoring secretion at melanocytes, they may be readily applied to measurement of peptides at other cells and to electrochemical detection in HPLC and capillary electrophoresis (CE).

Experimental

Electrode preparation. Glass encased carbon fiber microelectrodes were prepared using previously described techniques(Kelly and Wightman, 1986). The details of the procedure are presented in Chapter 2. Briefly, a glass capillary containing a single, carbon fiber of 9 μm was pulled to a fine tip on a commercial pipettte puller. The electrodes were polished at 45° angle on a micropipette beveler. Immediately after polishing, electrodes were dipped in 2-propanol for 10-15 minutes and then ultrasonicated in H_2O for 5 minutes.

Electrode testing. Electrode tests were performed using by flow injection analysis (FIA) using apparatus similar to that described in Figure 2-1. The entire flow injection system was housed in a Faraday cage. Data were collected using an EI-400 potentiostat

(Ensman Instrumentation, Bloomington, IN) controlled by an IBM-compatible personal computer (Gateway 2000 486-66) equipped with a National Instruments multifunction board. For FIA, background electrolyte (0.060 M phosphate buffer, pH 7.4) was pumped at 1.5 mL/min and analytes dissolved in the background electrolyte were applied to the electrode by switching the valve to the inject position for 5 s.

For amperometry, the electrode was poised at 0.80 V (all potentials are versus sodium-saturated calomel electrode). Electrochemical treatments were applied while the electrodes were in the flow stream (FIA) or in balanced salt solution (single cell analysis). Data for single cell measurements were collected at 170 Hz and low pass filtered with a cut-off frequency of 20 Hz. Fast scan CV utilizing a variety of waveforms, scan rates, and scan interval was performed as described elsewhere (Bauer et al., 1991). All voltammograms shown are background subtracted with background scans acquired prior to injection (FIA) or prior to stimulation (single cell measurements). The cyclic voltammograms were filtered at 2-4 kHz. For dopamine and ascorbic acid, cyclic voltammetry was employed at 800 V/s with potential window set from -0.3 to 0.9V and -0.4 to 0.8V, respectively.

Cell isolation and culture. Melanocytes were isolated and dispersed using a procedure similar to that described in chapter 2.

Single-cell measurements. Single-cell measurements were performed in a manner similar to that described elsewhere (Leszczyszyn et al., 1990; Wightman et al., 1991). Petri dishes containing cells were rinsed twice with balanced salt solution (same composition as the solution used for cell isolation except 2.0 mM $CaCl_2$ was also added). The dish was filled with balanced salt solution and placed in a microincubator (Medical

Systems, Inc.) on the stage of an inverted microscope (Zeiss Axiovert 35 microscope. The microincubator maintained the temperature at 34 °C. To perform measurements, a cell was located with the microscope and a working electrode positioned so that it lightly touched the cell using a Burleigh PC-1000 micropositioner.

Substances were applied to individual cells by pressure ejecting solutions from the tips of micropipettes which were positioned ~30 μm from the cell. Flow rates through the pipette tips were ~1 nL/s. Stimulants were dissolved in balanced salt solution. For K^+ stimulation, 64 mM KCl was added to the balanced salt solution with an equivalent amount of NaCl removed. For digitonin stimulations, a 10 μM digitonin solution in balanced salt solution was applied to the cells.

Results and Discussion

Amperometry

Electrode fouling. A potential problem in amperometric detection of small peptides is fouling caused by detected species and their oxidation products adsorbing to the electrode and blocking active sites. This problem is illustrated by the FIA results summarized in Figure 3-1 which is a plot of the peak current from sequential injections of different peptides, tryptophan, and tyrosine. The data show that the current response for the peptides tends to decrease with subsequent exposures to the analyte during FIA. The signal for tyrosine decreases in a fashion similar to that for the peptides while the signal for tryptophan was relatively stable with a relative standard deviation (RSD) for 10 injections of 4.6%. These results suggest that oxidation of tyrosine in oligopeptides contributes to electrode fouling at carbon-fiber microelectrodes whereas tryptophan is of little consequence in causing fouling.

Electrochemical treatments. A variety of electrochemical treatments have been reported to improve the selectivity sensitivity and stability of carbon-fiber microelectrodes (Gonon et al., 1981; Feng et al., 1987; Edmonds and Guoliang, 1983; Suaud-Chagny, 1993). We investigated several of these procedures in an effort to lessen the effect fouling and improve the stability of the response of carbon-fiber microelectrodes to tyrosine and tyrosine-containing oligopeptydes. Figure 3-2 illustrates the effect of three of the treatments on the peak current from FIA of MSH. Method I, in which a triangular waveform was applied from 0.0 to 2.0 V for 20 s at 300 V/s (Gonon et al., 1981), completely abolished the amperometric signal for MSH. In general, we found that any electrochemical procedure that utilized potentials greater than 1.7 V significantly reduced or eliminated the signal for the POC peptides. Apparently, oxides formed at high positive potentials on carbon fiber surfaces (Kawagoe et al., 1993) hinders oxidation of these compounds. Electrochemical treatments which utilized negative potentials were considerably better for detection of MSH as illustrate by the results for Methods II and III in Figure 3-2. In method II, the electrode was linearly cycled between -0.5 V and +1.5 V at 300 V/s for 2 minutes (Edmonds and Guoliang, 1983). Method III had the same scan rate and duration but the potential window was -1.0 V to 1.0 V (Edmonds and Guoliang, 1983). Based on these results, it appears that although both methods are better than the Method I, Method III is the most useful analytically. As shown by the FIA results in Figure 2-3, Method III also improved the amperometric detection of CLIP, β-endorphin, and tyrosine. These results illustrate that the electroactive POC peptides can be reproducibly detected by amperometry if a cleaning procedure utilizing reductive potentials is used after exposure to the peptides. Since the electrochemical treatment also

benefited tyrosine detection, it seems likely that this is generally applicable to tyrosine-containing oligopeptides.

The particular application that we have been interested in is measurement of the POC peptides secreted from single cells. To determine the extent of fouling in this application, single melanocytes were stimulated repetitively as illustrated in Figure 3-4. The current spikes represent detection of concentration pulses caused by exocytosis event (Wightman et al., 1991). For the example shown in Figure 4, the average area of current spikes on the first stimulation was $0.047 \pm .026$ pC. For all cells tested (n=4), we found that when a given cell was stimulated two or more times, the average area and standard deviation were not significantly different even without electrochemical cleaning between stimulations. These results suggest that for detection of exocytosis, fouling is of little consequence. This is probably due to the fact that electrodes are exposed to such small amounts of peptides (the areas correspond to less than 0.5 amol for a 1 electron oxidation) for brief times as indicated by the short duration and small magnitude of current spikes. Thus, electrochemical cleaning is not of benefit for these particular measurements.

Although the use of electrochemical cleaning did not improve single cell data per se, it did facilitate measurements in other ways. For example, by using electrochemical cleaning after application of standard peptide solutions, it was possible to test an electrode in situ during an experiment with a cell without degradation of signals as a result of the testing. We also found that the use of electrochemical cleaning improved the success rate of using the same electrode to measure secretion from two cells; however, since cells and cell debris frequently adhere to the electrode surface after experiments at a given cell, it is not recommended that the same electrode be used on different cells. The cleaning

procedure may be of greater interest in electrochemical detection with HPLC and CE where higher concentrations and longer exposures to the peptides may be expected.

Cyclic Voltammetry

As mentioned in the introduction, in our previous report on the detection of POC peptides from single cells, no attempt was made to investigate and optimize voltammetric conditions. Thus, although voltammograms were obtained from single cells confirming the release of tyrosine and tryptophan-containing peptides, significant improvements are possible. Therefore, we investigated the effect of scan rate, potential window, and scan interval, on the voltammetric behavior of MSH and the other POC peptides.

Effect of scan rate. In order to improve temporal resolution for detection of peptide secretion, it is beneficial to use higher scan rates. Figure 3-5 illustrates voltammograms for the electroactive peptides at 800 V/s in the potential of 0 to 1.2 V. The voltammetric behavior of the peptides, especially b-endorphin and CLIP, which show anodic peaks while scanning in the cathodic direction, is clearly complex making interpretation difficult. However, with these conditions, the MSH voltammetry is quite different from that obtained for the other peptides. As shown by the comparison of the forward scans in Figure 3-5D, the distinct peak shape only for MSH allows confirmation of MSH in the presence of the other peptides. As shown by the comparison of the forward scans in Figure 3-5D, the distinct peak shape observed only for MSH allows confirmation of MSH in the presence of the other peptides. If the current at the peak for MSH is plotted as a function of time during FIA, the selectivity is further illustrated as shown in Figure 3-6. When plotted in this fashion, it is apparent that CV allows MSH to be detected 7.3-fold more sensitively than CLIP and 5.5-fold more sensitively than β-endorphin.

The selectivity of MSH over CLIP and β-endorphin observed in the CV's appears to be due to the presence of tryptophan in MSH. Figure 3-7 illustrates that tryptophan yields a peak shaped voltammogram under these conditions which is similar to that observed for MSH while tyrosine yields a flat voltammogram that more closely resembles that of CLIP and β-endorphin. Previous work has indicated nearly identical shapes for cyclic voltammograms for these amino acids at lower scan rates (Brabec and Mornstein, 1980b; Paras and Kennedy, 1995). Thus, at high scan rates it is possible to distinguish between tyrosine and tryptophan and this is true of peptides that contain these amino acids as well. The selectivity for tryptophan and MSH could be explained by several factors including faster electron transfer kinetics for indoles on carbon-fiber; however, the poorly defined voltammograms obtained for tyrosine, CLIP, and β-endorphin makes it difficult to perform a formal study to determine the cause of the selectivity.

A plot of peak current versus scan rate for MSH and tryptophan is illustrated in Figure 3-8. The data appear linear and a log-log plot reveals a slope of 0.87 for MSH and 0.69 for tryptophan. For purely adsorptive behavior a slope of 1.0 would be expected while for diffusion-controlled voltammograms the expected slope is 0.5 (Bard and Faukner, 1980). Thus, scan rate dependence of peak current and symmetric peak shape of the voltammogram support the idea that at least some of the current is due to adsorbed species. The lack of a peak for tyrosine, CLIP and β-endorphin in the same scan rate range made such an analysis impossible for these compounds.

Effect of scan interval. If fast scan cyclic voltammograms are collected at fixed intervals, then it is possible to monitor the concentration of a substance by monitoring the current around the voltammetric peak. The time between scans, or scan interval,

determines the frequency of sampling for monitoring concentration. Figure 3-9 illustrates the effect of scan interval on peak current for MSH compared to that for tryptophan, dopamine, and ascorbic acid. Since the CV's are obtained repetitively, a possible explanation for strong dependence of MSH peak current on scan interval is that not enough time was allowed to reestablish the diffusion layer between scans at shorter intervals resulting in the smaller signals. We eliminated this possibility based on two considerations. First, it has previously suggested that the diffusion layer for microelectrodes of similar size is established within a time frame of 10 times the scan period (time required for the voltammogram) (Kawagoe et al., 1993). In our case, the scan period is 3 ms, therefore the diffusion layer should be established in ~30 ms, yet we see a dependency well beyond this time. Second, both dopamine, which is chemically reversible, and ascorbic acid, which is chemically irreversible like MSH, have peak currents that are virtually independent of scan interval. However, tryptophan, which has some adsorptive character as noted above, has a dependence on scan interval similar to MSH. We conclude that the dependency of peak current on scan interval is due to the adsorption of MSH. As the time between scans is increased, more time is allowed for MSH to accumulate on the surface. Larger amounts on the surface are then stripped off during the scan resulting in larger currents. As a result of this effect, monitoring MSH by fast scan CV requires a compromise between temporal resolution and sensitivity. Smaller scan intervals will allow better temporal resolution at the expense of detection limit.

Optimization of potential window. Temporal resolution is further affected by the response time of the electrodes which is in turn can be affected by the potential window used. This is illustrated in Figure 3-10 which depicts the peak oxidation current obtained

from fast scan CV's as a function of time during FIA of MSH with different potential windows. At a starting potential of 0.5 V, a fast response of 0.5V, a fast response is observed; however, the baseline signal does not recover to its original level (Figure 3-10 A). This may be due to adsorption of peptide (or oxidation product) on the electrode which can decrease the capacitance of the electrode thus reducing the background current. With negative starting potentials, the response time (time to 90% of peak) increased to 1.2 s (Figure 3-10 C and D). Negative starting potentials, also generated larger signals; however this higher "signal" can be attributed to the increase in baseline current after exposure to the peptide. The elevated baseline is consistent with idea that an electroactive species that adheres to the electrodes is formed during voltammetry in this potential range. Indeed, voltammograms recorded after the removal of MSH under these conditions reveal highly symmetrical peaks further supporting this idea. Fast response times and stable baselines were obtained when using a starting potential of 0.0 V as illustrated by Figure 3-10 B.

The improved CV conditions (0 to 1.2 V potential window, 800 V/s scan rate, 16.7 ms scan interval) were used to measure secretion from single melanocytes following digitonin secretion. Digitonin acts by permeabilizing the cell membrane which allows Ca^{2+} in the extracellular medium to enter the cell and initiate exocytosis. Figure 3-11 shows that a similar time course of current spikes is recorded by amperometry (3-11 A) or by fast scan CV at melanocytes stimulated by digitonin. This is the first use of CV to detect concentration fluctuations caused by exocytosis of a peptide. A voltammogram taken from the point indicated in Figure 3-11 B is shown overlaid with a voltammogram obtained from application of standard peptide solutions to the same electrode in Figure

3-11 C. The peak-shaped voltammogram, unique to MSH among the POC peptides, confirms detection of MSH during exocytosis.

Conclusion

In this study, we examined the electrochemical detection of MSH and related POC peptides. The effect of fouling of carbon fiber microelectrode in amperometric detection of the peptides is apparently due to oxidation of tyrosine and can be reversed by a simple electrochemical treatment. The electrochemical treatment is not of benefit during monitoring of peptide release from single cells, possibly because of the brief exposure to low concentrations; however, it may be of use in other analytical situations such as electrochemical detection in HPLC. By CV at 800 V/s in the potential window of 0 to 1.2 V, it is possible to distinguish MSH from other POC peptides based on the peak-shaped voltammogram for MSH. The selectivity is based on the presence of tryptophan in this peptide. In addition, it was found that the potential window affects the temporal response while scan interval affects sensitivity of carbon fiber microelectrodes to MSH. Using the optimized waveform, it was possible to monitor MSH secretion from single melanocytes during exocytosis.

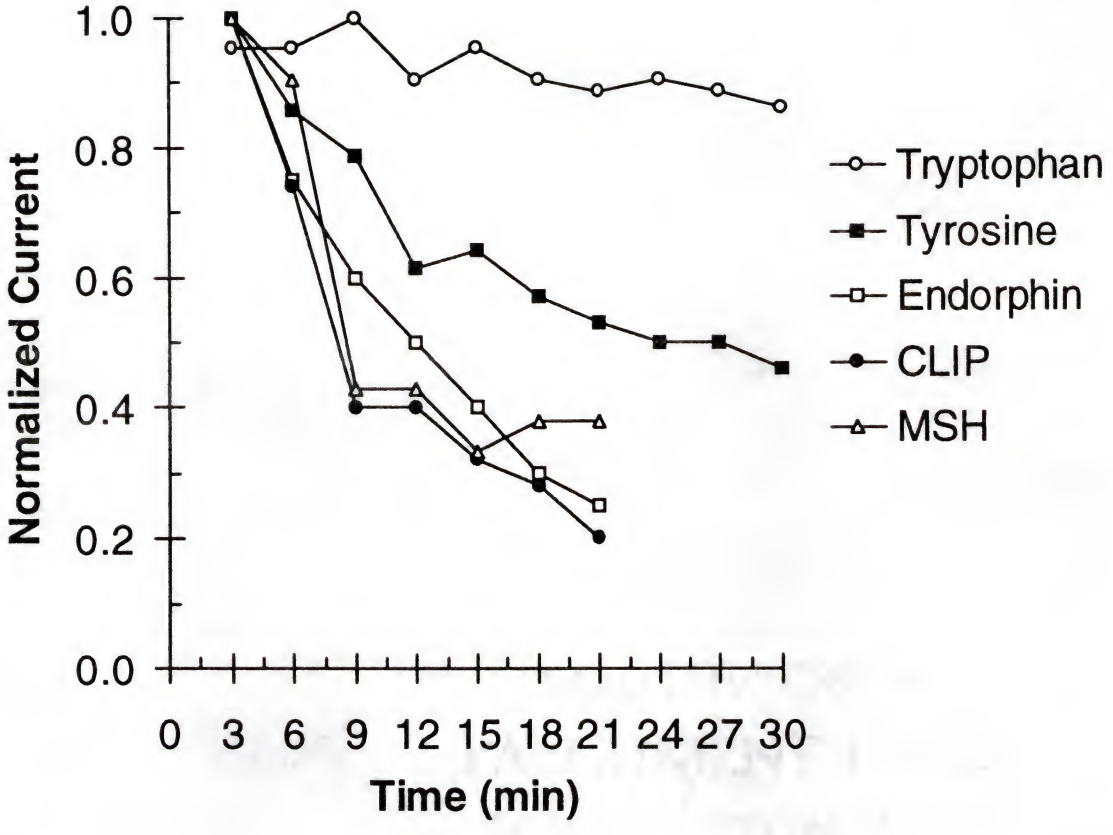

Figure 3-1. Current maxima for amperometric detection of 1 μM POC peptides, tyrosine, and tryptophan during FIA performed as described in the Experimental section. Each point is plotted relative to the time the detection potential was initially applied to the electrode and injections were performed at the times indicated (~3 min intervals). The current maxima were normalized with the highest current recorded for each compound scaled to 1.0. All points for a given compound were collected with the same electrode but different electrodes were used for each compound.

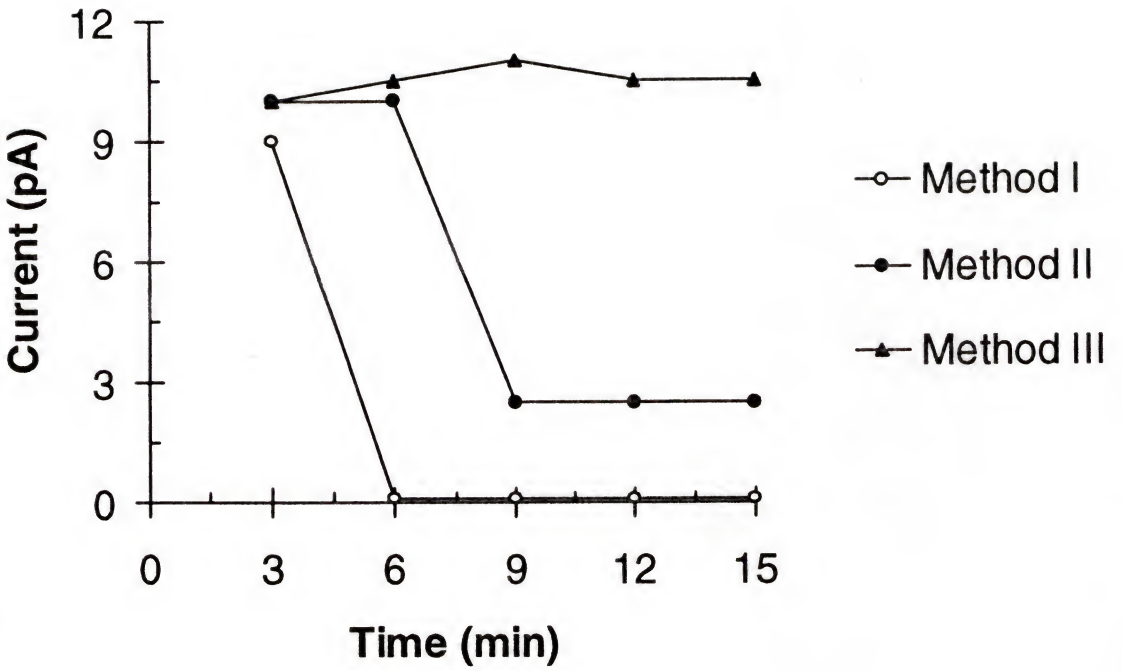

Figure 3-2. Effect of electrochemical cleaning on current maxima for amperometric detection of 1 μM MSH during FIA performed as described in the Exerimental section. Data treatment and experimental conditions are similar to Figure 3-1 except actual current is plotted. Between each injection electrochemical treatment was used. Details of the different methods are given in the text.

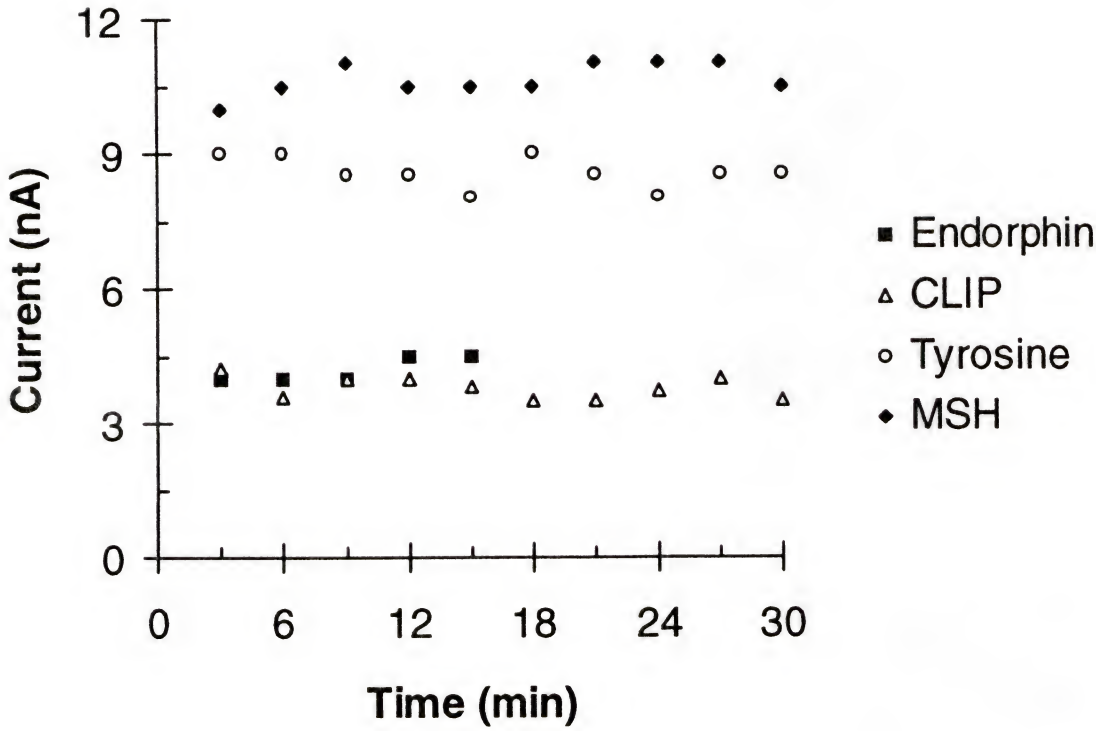

Figure 3-3. Effect of electrochemical cleaning (Method III) on amperometric detection of POC peptides and tyrosine. Experiment of Figure 3-1 was repeated except electrodes were cleaned using Method III between each injection on the FIA. Each point is the average current maxima from a sequence of 3 injections (5 s apart) collected at the time indicated.

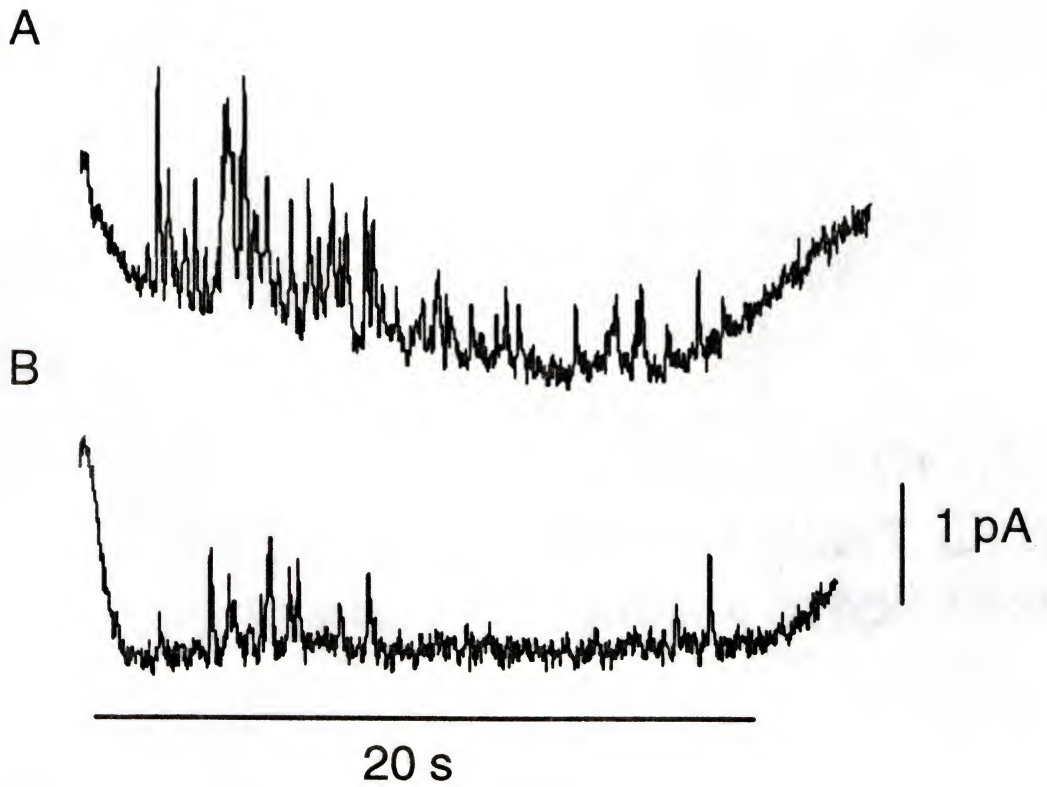

Figure 3-4. Current recordings made at a single melanocyte in Ca^{2+} -free media with the electrode at +0.80 V. Stimulation was by application of 64 mM K^+ with 4 mM Ca^{2+} in the stimulation buffer as described in the Experiment section. The bar indicates the time of stimulation. Recordings A and B were taken from the same cell 5 min apart.

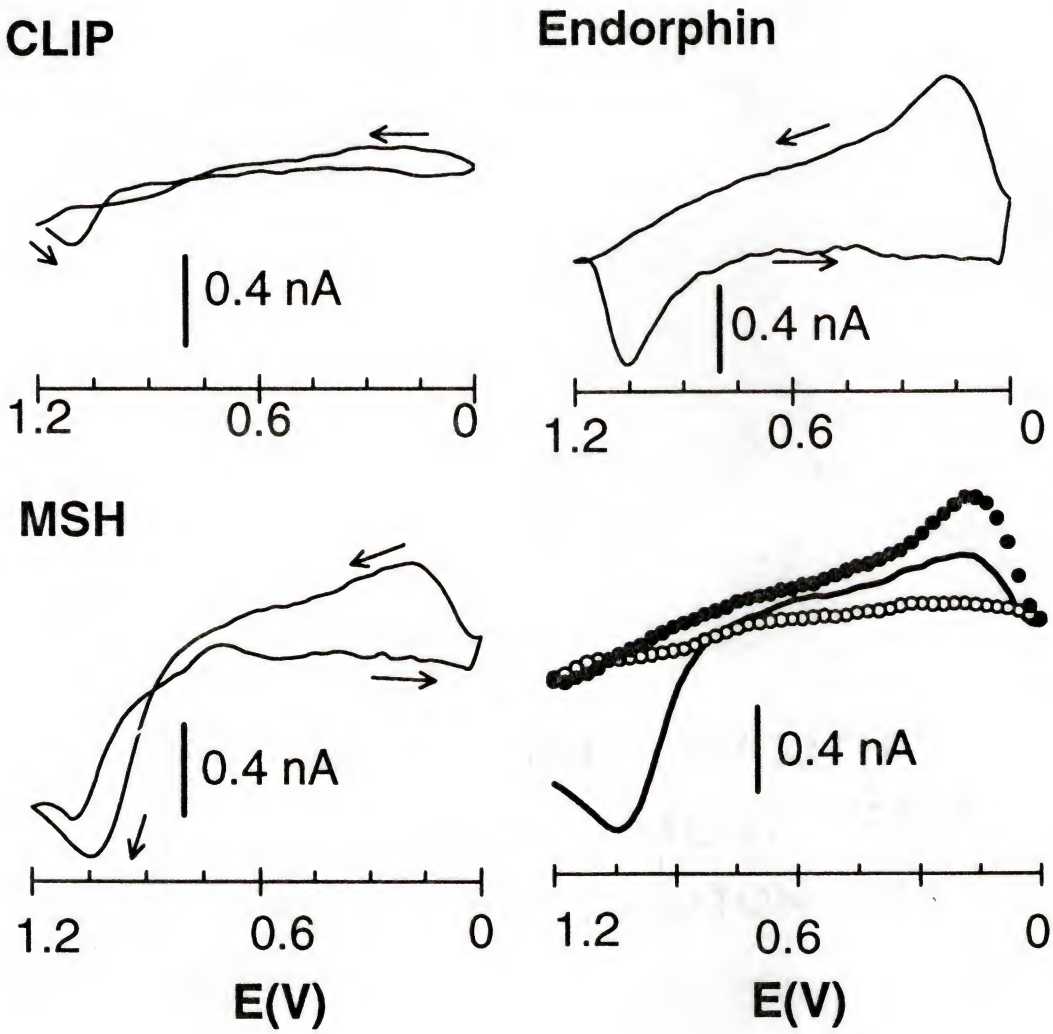

Figure 3-5. Background-subtracted fast-scan cyclic voltammograms for (A) 1.0 μM CLIP, (B) 1 mM β-Endorphin and (C) 1 μM MSH. Arrows indicate the direction of the voltage scan. Voltammetric conditions are given in the text. The current recorded during the forward (positive-going) scan are overlaid in (D) CLIP (open circles), β-Endorphin (solid circles) and MSH (solid line). Each trace is the average of 5 voltammograms.

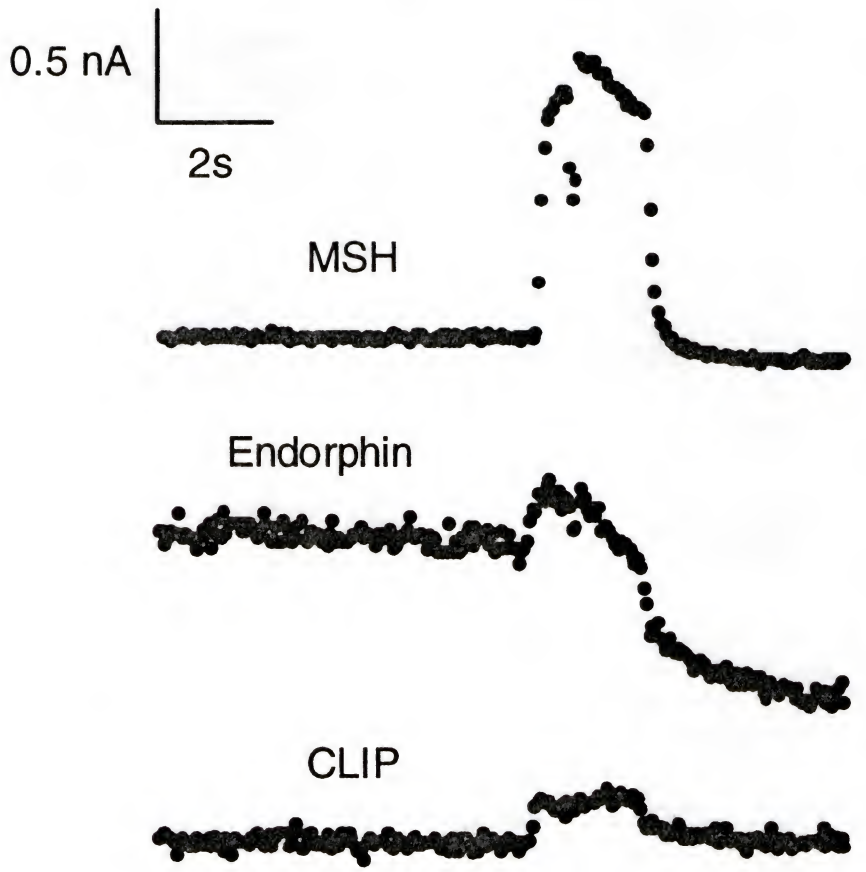

Figure 3-6. FIA using cyclic voltammetry for 1 μM MSH, β-Endorphin and CLIP. Each point is the average of current recorded between 1.0 and 1.1 V during the positive-going scan for a single cyclic voltammogram. Cyclic voltammograms were obtained every 100 ms and the integrated current was plotted against time. Peptides were injected for 2 s.

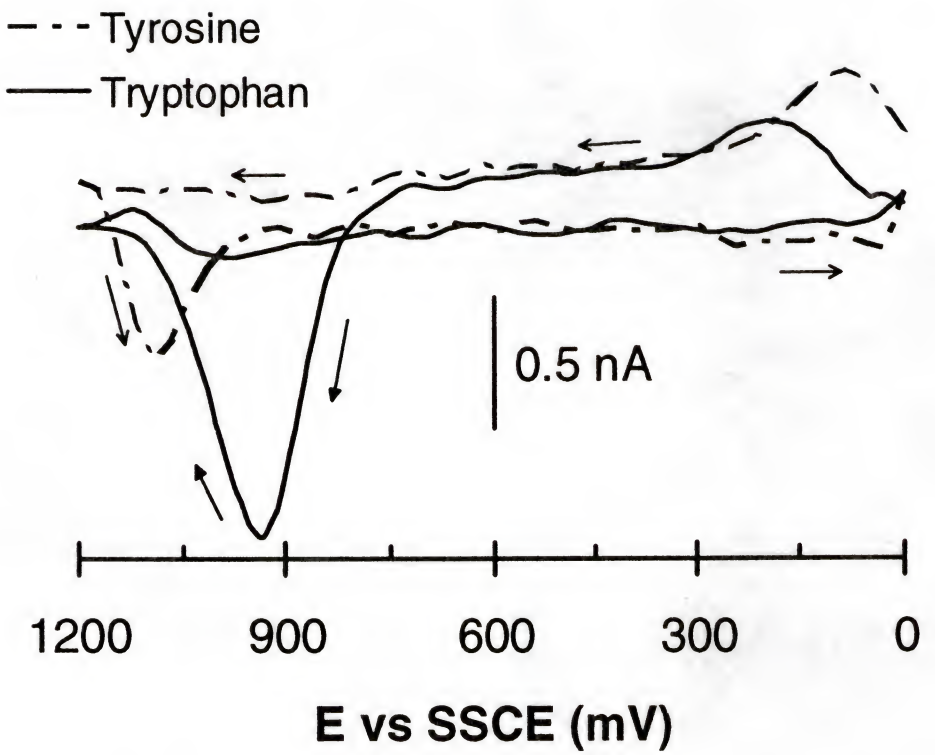

Figure 3-7. Comparison of cyclic voltammograms for 1 μM tryptophan and tyrosine. Conditions were the same as those for figure 3-5.

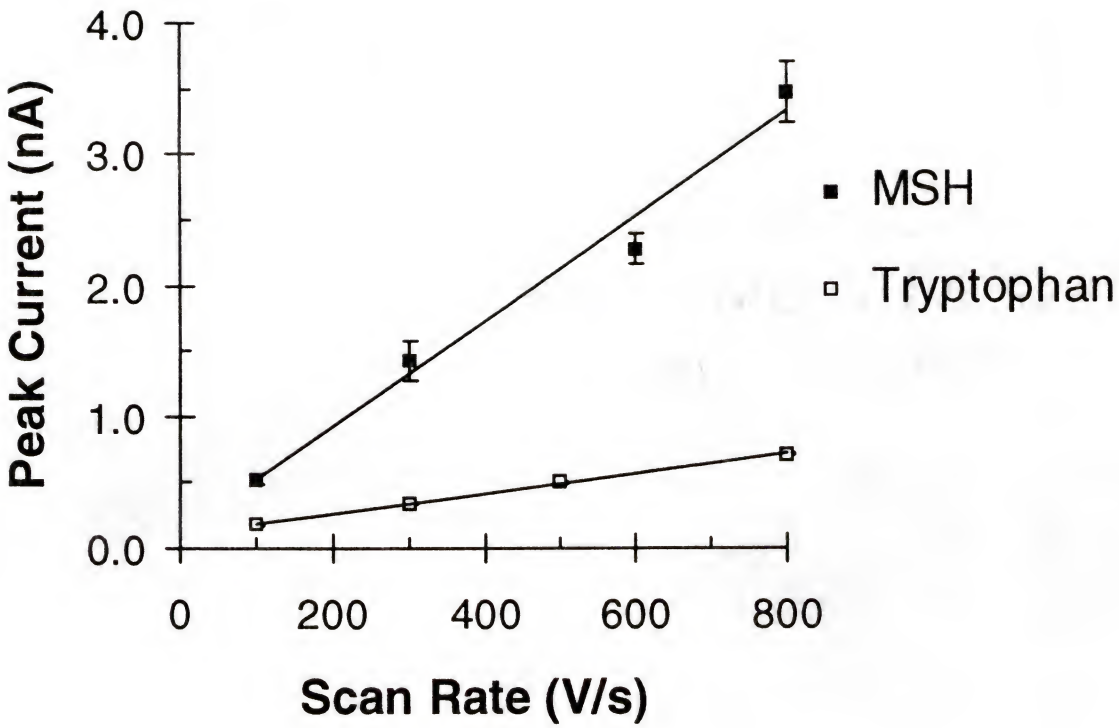

Figure 3-8. Effect of scan rate on the oxidation peak current of 1 μM tryptophan and MSH. The potential was linearly cycled between 0 and 1.2 V at the scan rate indicated every 400 ms. Electrochemical cleaning (Method III) was employed after every trial. Each point is the average of 3 trials and the error bars are ±1 standard deviation.

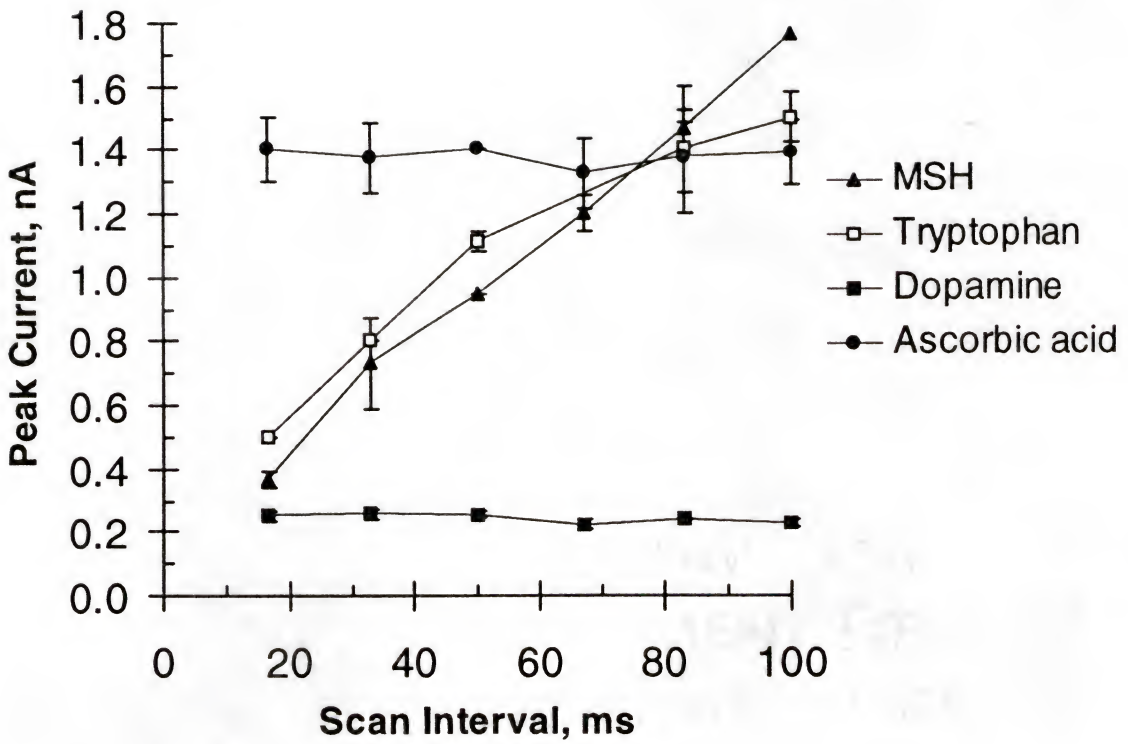

Figure 3-9. Effect of scan interval on peak oxidation current for MSH, tryptophan and dopamine at 1 μM and ascorbic acid at 1 mM. For ascorbic acid, current values were scaled down by a factor of 10 and the carbon fiber microelectrode used was pretreated as described elsewhere (Gonon et al., 1981). For MSH detection, the potential was scanned from 0 to 1.2 V at 800 V/s. Voltammetric conditions for the other compounds are given in the Experimental section. Each point is the average of 3 trials and the error bars are ±1 standard deviation.

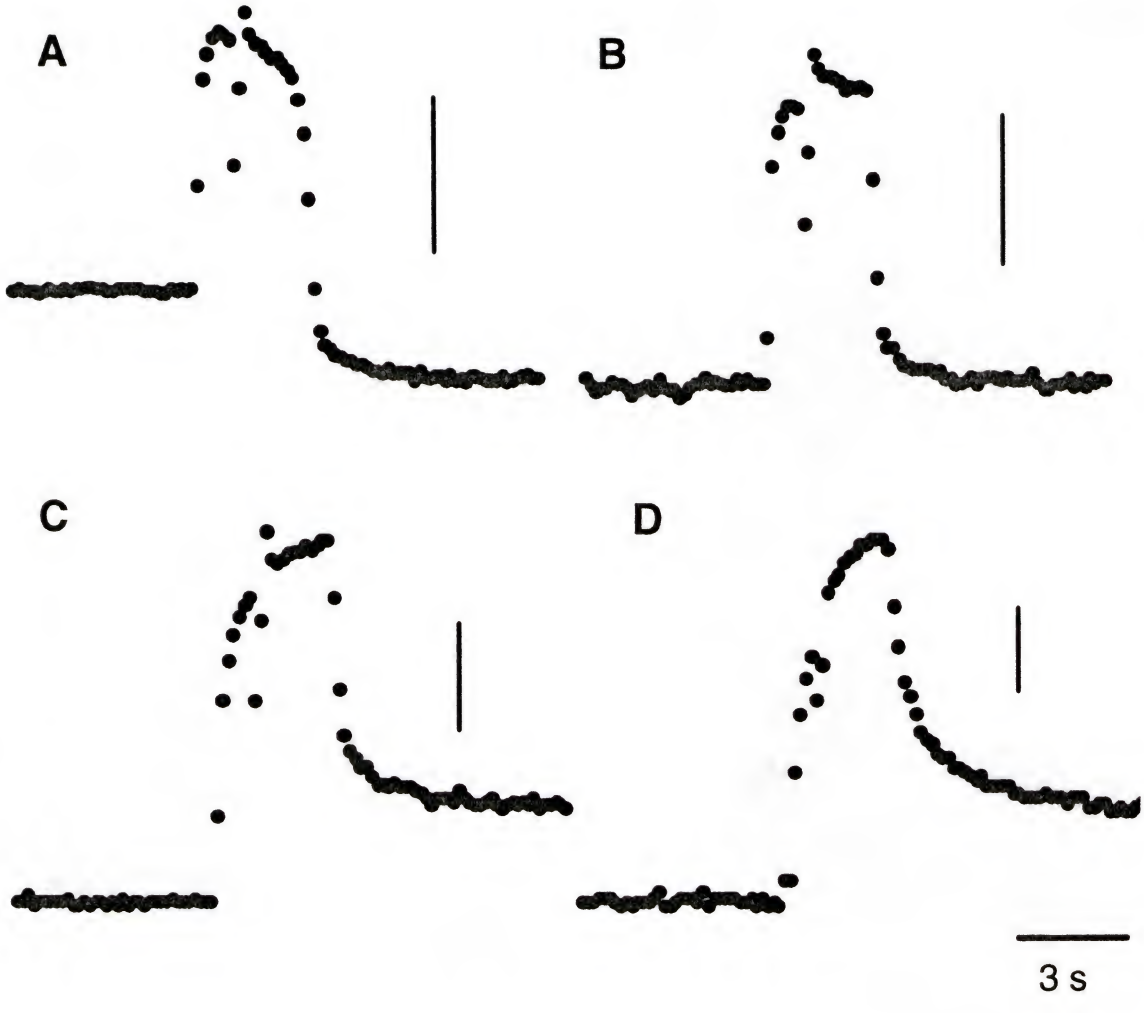

Figure 3-10. Effects of potential window on time response during FIA of 1 μM MSH using CV detection. Each point is the averaged current between 0.9 and 1.0 V for a single cyclic voltammogram. Cyclic voltammograms were recorded at 800 V/s every 100 ms. The potential windows were: (A) 0.5 to 1.2 V; (B) 0 to 1.2 V; (C) -0.4 to 1.2V; and -0.7 to 1.2 V. MSH was injected for 3 s. The current bars correspond to 0.3 nA. Other FIA conditions were similar to Figure 3-6.

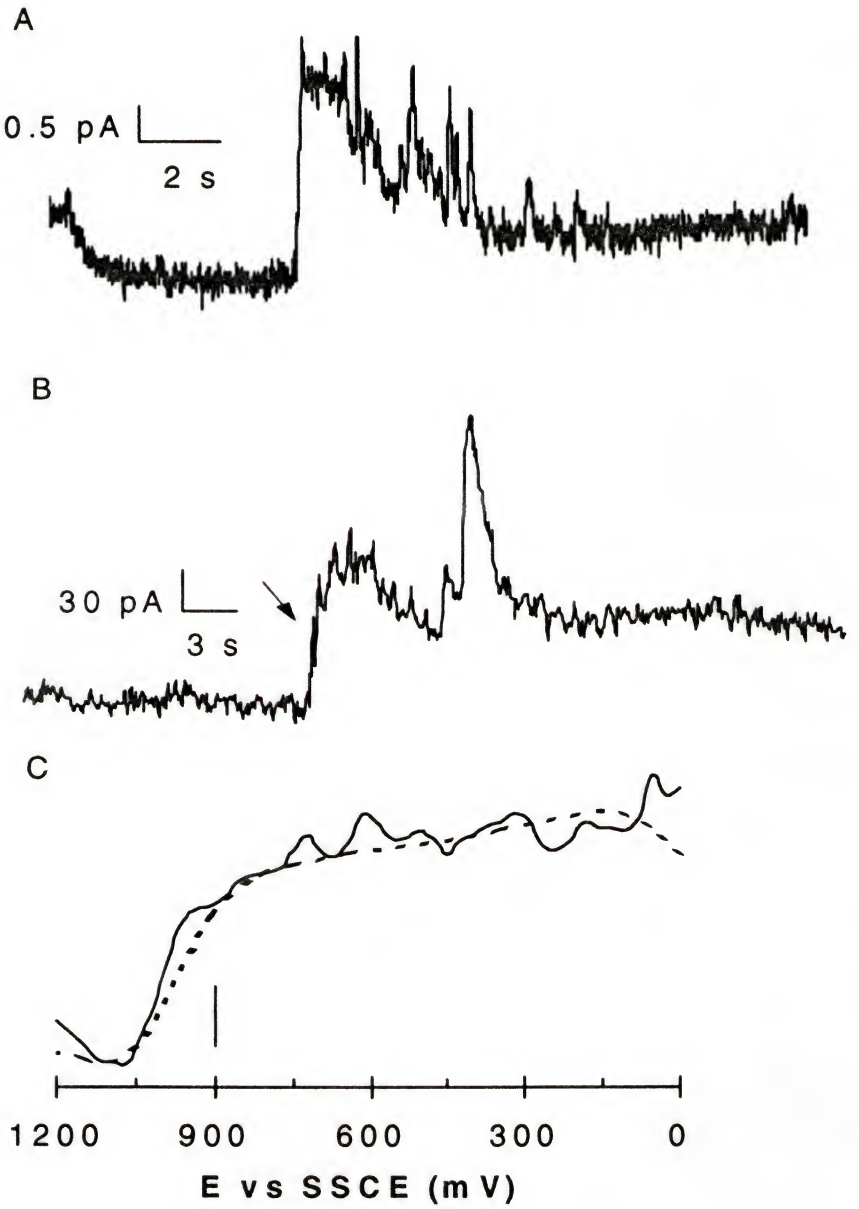

Figure 3-11. Detection of peptide secretion from single melanocytes during digitonin stimulation using (A) amperometry and (B) CV. For the CV recording, the current recorded between 0.95 and 1.15 V was averaged for each voltammogram. To reduce noise, the current measured in the 0.1-0.2 V interval was used to remove the noise at the oxidation peak of MSH (0.95-1.15V) as described elsewhere (Pihel et al., 1995). (C) Comparison of the anodic-going portion of background subtracted cyclic voltammograms obtained at a single spike (shown by an arrow in B) after stimulation of a sigle melanocyte (solid line) and an equimolar mixture (1μM) of MSH, CLIP and β-Endorphin (dashed line). The current bar is 0.02 nA for the cell and 0.24 nA for the standard mixture.

CHAPTER 4
A COMPARISON OF CATECHOLAMINE DEPLETION BY RESERPINE AND TYRAMINE

Introduction

Studies on the mechanisms and regulation of catecholamine synthesis, storage and release are necessary to provide better perspective on the roles of catecholaminergic systems. For instance, an improved understanding of the variety of physiological conditions that affect catecholamine release has direct relevance for the identification and treatment of clinical abnormalities ranging from arterial hypertension to schizophrenia (Nagatsu and Stjarne, 1998). Several mechanisms have been proposed on the release or depletion of catecholamines at the cellular level. Stimulants like high K^+ and nicotine are known to induce catecholamine secretion by Ca^{2+} dependent process exocytosis (Chen et al., 1994; Nagatsu and Stjarne, 1998). During exocytosis, vesicles containing catecholamines fuse with the cell membrane and subsequently, contents are release to the extracellular space. Many drugs such as reserpine, tetrabenazine and chlorpromazine deplete intracellular catecholamines by blocking the uptake of catecholamines into storage granules (Scherman and Henry, 1980). While several studies have been performed on catecholamine secretion, the mechanism of release for certain drugs such as tyramine is remains unclear.

It is well established that reserpine is a powerful inhibitor of the vesicular monoamine transporter (Henry et al., 1998). In fact, early studies have used reserpine as a marker of

monoamine storage vesicles (Elfvin, 1968; Schubert et al., 1980, Wagner, 1985). Electron micrographs obtained after reserpine treatment exhibit a decrease in the number of secretory granules which were assumed to be catecholamine stores (Elfvin, 1968; Schubert, et al., 1980; Schubert and Klier, 1977). Interestingly, depletion of catecholamine stores upon reserpine treatment is not accompanied by release of catecholamines to the extracellular media (Schubert and Klier, 1977; Kittner et al., 1987). In contrast, tyramine, an indirectly acting sympathomimetic amine, has been shown to release catecholamine from adrenergic neurons and PC12 cells (Youdim, 1991). Early reports suggest that tyramine release norepinephrine from readily available storage sites in peripheral adrenergic neurons (Kopin, 1964; Finberg and Youdim, 1985) while, other reports indicated that tyramine causes the release of catecholamines from the cytoplasm (Smith, 1973). Therefore, mechanism of release of tyramine remains unclear.

In this study we further explore the effect of reserpine and tyramine by direct monitoring of catecholamine release using carbon fiber microelectrodes. Some of the results presented in this work were obtained by Ms. Karen Burton as part of her undergraduate research. A clonal cell line derived from a rat adrenal medulla, known as PC12 (pheochromocytoma) line was used as a model for the study of catecholamine depletion (Greene and Tischler, 1976). The PC12 cell line was maintained and cultured in our laboratory.

PC12 cells are known to synthesize and store catecholamine neurotransmitters and extend neuronal-like processes when exposed to nerve growth factor protein (NGF) (Greene and Rein, 1977a). In addition, catecholamines are secreted in response to cholinergic agonists (e.g. nicotine) (Greene and Rein, 1977b) or to elevated extracellular

K^+ (Greene and Rein, 1977a). These findings suggest the similarities of PC12 cells to sympathetic neurons and adrenal chromaffin cells. However, these cells are more similar to sympathetic neurons than adrenal chromaffin cells because they predominantly synthesize dopamine and store norepinephrine to a lesser extent (Takashima, 1994). Moreover, like sympathetic neurons, PC12 cells contain primarily monoamine oxidase A and exhibit tyramine induced catecholamine release (Youdim, 1991).

Experimental

Electrode preparation. Glass encased carbon fiber microelectrodes were prepared as described elsewhere (Kelly and Wightman, 1986). A carbon fiber of 10 μm diameter (P-55S from Amoco Performance Products) was placed to a 1.2 x 0.68 mm glass capillary (A-M Systems). This capillary was then pulled on a Narishige PE-2 pipet puller yielding two electrodes per capillary. The tip of each electrode was cut and dipped in epoxy to seal. The electrodes were left overnight and then cured the following day for 2 hours at 100 °C and then for 2 hours at 150 °C. Before use, the electrode was polished at an angle of 45° on a micropipet beveler (Sutter Instruments), dipped in 2-propanol for 10 minutes and then ultrasonicated in water for 5 minutes.

Cell culture. PC12 cells were purchased from American Type Culture Collection (Rockville, MD) and grown in 100 mm untreated plastic cell culture plates (Falcon) in phenol red free RPMI-1640 culture media supplemented with 10% heat inactivated horse serum, 5% fetal bovine serum, and 1% penicillin/streptomycin (all from GIBCO). Cells were incubated at 37°C and 5% CO_2. All experiments were performed on cells grown to near confluence in mouse collagen IV coated 60 mm Falcon cell culture dishes (Collaborative Biomedical Products).

Single-cell measurements. Single cell measurements were performed in a manner similar to that described elsewhere (Leszczyszyn et al., 1990; Wightman et al., 1991). Culture plates were rinsed 3 times with warm (37°C) unsupplemented culture media (RPMI-1640) and then filled with balanced salt solution containing 150 mM NaCl, 4.2 mM KCl, 2 mM $CaCl_2$, 0.7 mM $MgCl_2$, 1 mM NaH_2PO_4, and 10 mM HEPES at pH 7.4. All experiments were performed on the stage of an inverted microscope (Zeiss axiovert 35) at room temperature (25°C). To perform the measurements, a cell was located with the microscope and the carbon fiber microelectrode was positioned to within 1 μm of the cell using a piezoelectric micropositioner (Burleigh PC-100). Secretion was induced by application of stimulant solution from a micropipette which was also positioned near the cell. The micropipette was connected to a pressure ejection system (General Valve Picospritzer) and stimulant pulse of 10 psi for 5 s were used unless otherwise noted. Stimulants were dissolved in balanced salt solution. For Nicotine/K^+ stimulation, 105 mM K^+ was prepared in balanced salt solution by decreasing the NaCl by an equivalent amount. 1 mM Nicotine was then dissolved in 05 mM K^+ solution. All amperometric measurements were performed at 0.65 V.

Data collection and analysis. Data for single cell measurements were collected using a Stanford Research Systems low-noise current amplifier (model SR570) and voltages were applied to the reference electrode using a battery and a voltage divider circuit. Data were collected at 150 to 220 Hz by an IBM -compatible personal computer (Gateway 2000 486-66 MHz) via a National Instruments (Austin, TX) multifunction board (AT-MIO16-F5) and low pass filtered at 30 Hz. Spike areas were calculated using locally written software from Professor Wightman of the University of North Carolina. Spikes

were used only if their peakheight was at least 8 times greater than the noise level. All mean values are reported ± 1 standard deviation unless otherwise noted. The two-tailed Student's t-test was used for statistical comparison of the means.

Results and Discussion

Effects of reserpine and tyramine on the secretion of catecholamines had been previously investigated on population of cells (Rebois et al., 1980; Scherman and Henry, 1980; Youdim et al., 1986). However, in these reports the transient effects of these drug were concealed by the variability and asynchrony of individual cells (Tatham et al., 1991). Carbon fiber microelectrodes allow measurement of catecholamine release with high temporal resolution and mass sensitivity (Wightman et al., 1991). By applying a constant oxidation potential at carbon fiber microelectrodes (amperometry), individual quantal release of catecholamines can be observed as isolated current spikes. The immediate effect of drugs can be determined from the latency of release (Zerby and Ewing, 1996) and the amount of catecholamine released per vesicle (Wightman et al., 1991; Finnegan et al, 1996, Chen and Ewing, 1995; Bruns and Jahn, 1998) can be obtained from the spike area. Hence, by directly monitoring the release of catecholamines in real time we have obtained new information about the mechanism of release.

Effect of reserpine incubation. Although, morphological evidence shows a decrease in the number of catecholamine containing vesicles after reserpine administration it would be interesting to monitor the effect of reserpine on the amount of catecholamine release from a single vesicle, or cell. Figure 4-1A shows the current trace obtained from a single PC12 cell upon exposure to 1 mM nicotine in 105 mM K^+ balanced salt solution (Nicotine/K^+). Multiple current spikes were obtained within 1 s of exposure to the

stimulant. The same cell was then incubated in 1 μM reserpine for several minutes. Figure 4-1B and Figure 4-1C show the current recordings obtained when the cell was restimulated with Nicotine/K^+ after 19 min and 20 min of reserpine incubation. The average areas of current spikes in Figures 4-1 A, B, and C are 0.0605 ± 0.0468, 0.0306 ± 0.0263 and 0.0259 ± 0.0084 pC, respectively. The effect of reserpine is also noticeable in the delayed response of the cell and decrease in the number of spikes. During reserpine incubation, the current at the electrode was monitored and a typical response is shown in Figure 4-1D. As shown in this figure, reserpine does not induce quantal release of catecholamine from PC12 cells.

In order to determine the effect of reserpine, several other cells were tested before and after reserpine exposure (see Table 4-1). Based on the results, depletion of catecholamine stores is more apparent on the number of spikes observed during stimulation rather than on spike areas. As shown in Figure 4-2, after 15 min of incubation with reserpine, the number of spikes was decreased by 82% (of the control experiment) while the mean spike area was reduced by 59%. Similar results were obtained after 20 to 30 min of incubation. The number of secretory event decrease by 76-82% while the average spike area was reduced by 42-54%. Based on these results, it is apparent that reserpine can cause fast depletion of catecholamine-containing secretory granules. For the remaining catecholamine containing vesicles we cannot rule out the possibility of slow leakage of catecholamines or the presence of reserpine insensitive pool (Schubert et al., 1977). The results are in agreement to a previous investigation on permeabilized PC12 cells (Nakanishi et al., 1995). It was noted in this study that upon reserpine administration for 30 minutes at concentrations higher than 100 nM, serotonin (5HT) uptake was

reduced to 10-15 % of control. These results suggest that during reserpine treatment the number of catecholamine granules is greatly diminished and in effect there is a decrease in the number of secretory events. Thus, the decrease in the catecholamine release from tissues or population of cells upon reserpine pretreatment as shown in previous reports (Kittner et al., 1987) is mainly due to the decrease in the number of vesicles that still contains the catecholamine granules.

Inhibition of the vesicular monoamine transporter. Our results can be explained with previous findings on reserpine. Reserpine inhibits catecholamine uptake by binding to the vesicular monoamine trasporter (VMAT). VMAT has two isoforms, VMAT1 and VMAT 2 (Henry et al., 1998) and VMAT1 was observed to be present in PC12 cells (Finn et al., 1998). Reserpine binds almost irreversibly to VMAT with a K_i in the subnanomolar range (Finn et al., 1998; Henry et al., 1998). The main function of vesicular monoamine transporters (VMAT) is to maintain the high concentration gradient between storage vesicles and cytoplasm (Nagatsu et al, 1998). VMAT compensates for the considerable leakage of transmitter from stores into the cytoplasm (Kittner et al., 1987) and so, when reserpine binds to VMAT1 in PC12 cells, uptake of catecholamines is inhibited and continuous efflux of catecholamines causes fast depletion. As soon as dopamine reaches the cytoplasm, it is metabolized by monoamine oxidase to DOPAC and could be recovered as DOPAC in the extracellular medium (Kittner at al., 1987). Like dopamine, DOPAC is electroactive at carbon fiber microelectrodes, yet we did not observe leakage of DOPAC through the cell membrane. In Figure 4-2D, a steady baseline was observed during the incubation. It is possible that, even though DOPAC was diffusing through the plasma membrane but at concentration was too low to be detected at the electrode.

Secretion due to tyramine. An earlier investigation indicated the existence of a tyramine releasable pool that is distinct from the K^+ releasable pool in PC12 cells (Youdim et al., 1986). In the present study, we further explored the dynamics of the release due to tyramine. It is well established that Nicotine/K^+ causes the release of catecholamines from PC12 cells by exocytosis (Chen et al., 1994). To elucidate the mechanism of secretion of tyramine, we compared the kinetics of secretion induced by K^+/Nicotine application to tyramine stimulation. In addition we studied the effect of Ca^{2+} on secretion due to tyramine. In Figure 4-3A, stimulation with Nicotine/K^+ caused a rapid onset of catecholamine secretion from a single PC12 cell. Current spikes were observed within 2 s of stimulant application. In Figure 4-3B, application of 10 μM tyramine also induced secretion but the onset of the release was delayed and the frequency of spikes was lesser than that of Nicotine/K^+ stimulation. In addition, longer duration of secretion was observed in the presence of tyramine. This effect of tyramine is consistent with a previous study on rat hippocampal slices (Su, et al., 1990). In this study, monoamine efflux was investigated by positioning a Nafion coated graphite electrodes at selected regions of the rat hippocampal slice and drugs were applied from a micropipette positioned near the electrode. Electrochemical responses to local application of tyramine (2mM) show a much slower rise and decay times as compared to high K^+ stimulation (Su, et al., 1990). The effect of tyramine on PC12 cells is summarized in Table 4-2. When the tyramine concentration was increased to 100 μM, there was an increase in the frequency of spikes. Based on this results, the dose dependence of catecholamine release due to tyramine, can be attributed to the increase in frequency of quantal release.

Ca^{2+} dependence of secretion. Previous results described tyramine induced release as Ca^{2+} independent. Population of cells or isolated tissues were labelled with [3H]-norepinephrine and the total radioactivity of [^{3}H]-norepinephrine release in the presence of tyramine was determined (Fozard and Mwaluko, 1976; Wakade et al., 1985; Dumont et al., 1997). For instance, it was observed that the tyramine induced norepinephrine release from rabbit isolated hearts was unaffected when the Ca^{2+} concentration was lowered from 7.2 to 0.4 mM (Fozard and Mwaluko, 1976). Removal of Ca^{2+} from the perfusion medium did not affect the tyramine-induced release of [3H]-NE from isolated rat salivary gland (Wakade, et al., 1985). The release of [3H]-NE from rat cardiac synaptosomal-mitochondrial fractions due to tyramine was also reported as Ca^{2+} -independent (Dumont et al., 1997).

Contrary to earlier investigations, our results from single cell experiments show that removal of Ca^{2+} from the incubation medium eliminate the stimulatory effect of tyramine. In Figure 4-4A, a single PC12 cell in Ca^{2+} free buffer was stimulated with Nicotine/K^+ buffer with 3mM Ca^{2+}. Multiple current transients were observed within 2 s of stimulation. The same cell was incubated with 100 µM tyramine in in Ca^{2+}-free buffer for 11 min. Response of the cell was monitored and the current trace is shown in Figure 4-4B. As illustrated, there was no evident release in the absence of Ca^{2+} and similar results were obtained on 4 other cells under similar conditions. Figure 4C shows the typical response of PC12 cells incubated with 100 µM tyramine for 11 min in the presence of 2.0 mM Ca^{2+} in buffer. This was observed on 4 out of 5 cells. In a recent report it was demonstrated that tyramine can induced Ca^{2+} influx in the sino-auricular fibers of the frog heart (Knoll et al., 1996). As Ca^{2+} ions enter the cell, the increase in in cytosolic Ca^{2+}

triggers fusion of vesicles with the plasma membrane leading to the release of vesicular contents. In our present results, the resulting quantal release induced by tyramine in the presence of Ca^{2+} was detected as current spikes.

The results discussed above strongly suggest that tyramine induces secretion of catecholamines from PC12 cells. To explore the possibility that tyramine releases catecholamine from a different class of vesicles other than that for Nicotine/K^+, the distribution of the cube root of spike areas was plotted. If it is assumed that the total amount of catecholamine in each vesicle is proportional to the volume of the vesicle and that vesicles have a spherical shape, then, the cube root of vesicle content should be proportional to the radius of the vesicle (Finnegan et al.,1996). Since the distribution of vesicular radii in PC12 cells exhibit a Gaussian distribution (Schubert et al, 1980), the distribution of the cube root of the charges or spike areas ($Q^{1/3}$) should also exhibit a Gaussian distribution. Spike areas from Nicotine/K^+ stimulation were plotted as a $Q^{1/3}$ histogram in Figure 4-5A while the tyramine induced spikes were used to construct the $Q^{1/3}$ histogram shown in Figure 4-5B. The $Q^{1/3}$ plot of spikes obtained from five PC12 cells (n=123) after application of Nicotine/K^+ exhibited a Gaussian fit of 0.300 ± 0.080. Spikes obtained after incubating a single PC12 cell with 100 μM tyramine (n=104) were used to form a $Q^{1/3}$ histogram with a Gaussian fit of 0.270 ± 0.080. Interestingly, the SDs of the Gaussian curves for Nicotine/K^+ stimulation (27%) and tyramine stimulation (28%) are almost identical to the reported SD of vesicular radii (25%) (Schubert et al., 1980). This suggests that Nicotine/K^+ and tyramine induce secretion of catecholamines from the same size of vesicles. However, the means are significantly different at the 99.5% confidence level possibly due to the following reasons. First, tyramine may be causing

secretion from the same pool of vesicles as Nicotine/K^+ but at the same time it also depletes the catecholamine amount inside the vesicles. And second, tyramine may be causing catecholamine secretion from a different pool of vesicles.

It is unknown if Nicotine/K^+ and tyramine actually, cause the release of catecholamine from different pools of vesicles. And so to investigate this possibility, cells were incubated overnight (16 hours) in 10 μM tyramine then checked for response to Nicotine/K^+ stimulation. Table 4-3 shows the effect of tyramine incubation on spike occurrences and areas upon Nicotine/K^+ stimulation. After tyramine incubation (16 hours), the frequency of spikes (number of spikes/duration of spike activity) and the mean spike area were still similar to those of control cells. Surprisingly, tyramine did not deplete all the catecholamine stores including those that are released by Nicotine/K^+. This implies that tyramine is depleting catecholamines from a different pool of vesicles. During tyramine incubation, we cannot rule out the possibility of tyramine being transported into storage vesicles. Hence, to eliminate this possibility, the electrochemical activity of tyramine was compared to that of dopamine using flow injection analysis. The amperometric signal (at 0.65 V) obtained for 10 μM dopamine was 8 times larger than that for 10 μM tyramine. If the amperometric signal is due to tyramine we would expect current spikes with lower amplitudes. However, based on our results the mean spike area remained the same. Hence, we can conclude that the current spikes were due primarily to catecholamine detection and not tyramine. Tyramine uptake into catecholamine containing vesicles may be minimal because it is readily metabolized by MAO-A in the cytoplasm (Finberg et al., 1981).

Conclusion

The present results demonstrate the fate of catecholamine storage vesicles following reserpine and tyramine incubation. Our results are compatible with previous reports concerning the effect of reserpine. When reserpine binds to the vesicular monoamine transporter (VMAT), leakage of catecholamines outside the vesicles could not be compensated by inward transport. Depletion of catecholamine stores is not accompanied by secretion of catecholamines because they are easily oxidized by MAO-A in the cytoplasm. Our results show that reserpine causes a massive decline in the number of secretory events induced by Nicotine/K^+. In addition, reserpine alone does not induce secretion. When the PC12 cells were exposed to tyramine, quantal release of catecholamines was observed. The studies on tyramine provide new information on the mechanism of secretion and demonstrate the presence of two pools of vesicles containing catecholamines in PC12 cells which respond differently to tyramine and Nicotine/K^+ stimulation. These may represent exocytoses of vesicles in two independent secretory pathways.

Table 4-1. Effect of Reserpine (1μM) Incubation on Current Spikes Due to Nicotine/K^+ Stimulation.

Cell #	Conditions	Spikes/ Stim	Spike Area (pC)	(n) ‡
1	control	87	0.1230 ± 0.0630	(32)
1	15 min, 1 μM Reserpine	12	0.0503 ± 0.0189 *	(11)
2	control	104	0.1280 ± 0.0750	(41)
2	15 min, 1 μM Reserpine	51	0.0876 ± 0.0456 **	(24)
3	control	26	0.0609 ± 0.0293	(11)
3	15 min, 1 μM Reserpine	3	0.0359 ± 0.0119 **	(3)
4	control	42	0.0946 ± 0.0293	(24)
4	15 min, 1 μM Reserpine	3	0.0336 ± 0.0206 *	(9)
5	control	28	0.0768 ± 0.0361	(15)
5	15 min, 1 μM Reserpine	3	0.0334 ± 0.0145 *	(3)
6	control	69	0.0546 ± 0.0457	(37)
6	18 min, 1 μM Reserpine	26	0.0392 ± 0.0278 **	(35)
7	control	56	0.0605 ± 0.0468	(54)
7	20 min, 1 μM Reserpine	12	0.0259 ± 0.0084 *	(4)
8	control	48	0.0407 ± 0.0269	(45)
8	20 min, 1 μM Reserpine	8	0.0169 ± 0.0180 *	(8)
9	control	63	0.0567 ± 0.0273	(31)
9	25 min, 1 μM Reserpine	11	0.0302 ± 0.0177 **	(22)
10	control	58	0.0614 ± 0.0550	(44)
10	25 min, 1 μM Reserpine	13	0.0182 ± 0.0078 *	(10)
11	control	48	0.0488 ± 0.0394	(32)
11	25 min, 1 μM Reserpine	6	0.0270 ± 0.0090 *	(6)
12	control	53	0.0642 ± 0.0303	(25)
12	30 min, 1 μM Reserpine	13	0.0451 ± 0.0109 *	(7)
13	control	99	0.0696 ± 0.0463	(39)
13	30 min, 1 μM Reserpine	25	0.0323 ± 0.0197 **	(15)

* Different from control at $p < 0.001$

** Different from control at $p < 0.01$

*** Different from control at $p < 0.05$

‡ n is the total number of spikes used to calculate the mean

Table 4-2. Catecholamine Release Due to Tyramine and 1 mM Nicotine in 105 mM K^+.

Cell #	Stimulation condition	Spike Area, pC (n) *	Delay to first spike, s	Duration, s	Frequency s^{-1} **
1	Nicotine/K^+	0.0406 ± 0.0178 (14)	2.32	10.79	1.40
1	10 μM Tyramine	0.0328 ± 0.0162 (13)	17.60	126.44	0.10
1	10 μM Tyramine	0.0320 ± 0.0214 (17)	37.90	74.02	0.23
2	Nicotine/K^+	0.0666 ± 0.0398 (47)	0.60	26.11	3.60
2	10 μM Tyramine	0.0596 ± 0.0298 (11)	42.40	425.05	0.02
3	Nicotine/K^+	0.0666 ± 0.0398 (26)	1.37	23.43	2.60
3	10 μM Tyramine	0.0701 ± 0.0536 (5)	23.70	197.15	0.02
4	Nicotine/K^+	0.0366 ± 0.0242 (40)	0.50	73.2	1.67
4	100 μM Tyramine	0.0271 ± 0.0334 (39)	-	-	0.07
5	Nicotine/K^+	0.0386 ± 0.0135 (36)	1.10	18.4	1.47
5	100 μM Tyramine	0.0224 ± 0.0519 (104)	-	-	0.13
6	Nicotine/K^+	0.0634 ± 0.0388 (53)	1.11	37.2	1.53
6	100 μM Tyramine	0.0544 ± .0403 (61)	-	-	0.17
7	100 μM Tyramine	0.0173 ± .0104 (78)	-	-	0.40

Single PC12 cells were initially stimulated with 1mM nicotine in 105 mM K^+ solution for 5 s and then with 10 (or 100) μM tyramine. 10 μM tyramine was applied by pressure ejection for 10 s while 100 μM tyramine was employed by adding 3 ml of 200 μM tyramine in balanced salt solution into the culture plate with 3 ml balanced salt solution. Only isolated spikes were included in the calculation of mean spike area. For cell #7, overlapping current spikes were obtained upon Nicotine/K^+ stimulation.

* n is the number of isolated spikes considered in the calculation of the mean.

** Frequency of spikes = $\frac{\text{total number of spikes}}{\text{duration of activity}}$

Table 4-3. Effects of Tyramine Incubation on Spike Occurrences and Areas Due to Nicotine/K^+ Stimulation.

Condition	# of cells	# of spikes observed per stimulation	Spike Area (pC)	Duration of secretory activity*
Control*	7	29 $\pm$ 12	0.0432 $\pm$ .0439	13.1 $\pm$ 5.2
Cells incubated with 100 μM Tyramine in culture media for 24 hours*	7	27 $\pm$ 14	0.0407 $\pm$ .0433	14.4 $\pm$ 4.3

* Stimulant solution consists of 1 mM Nicotine in 105 mM K^+ in balanced salt solution.

** Duration of secretory activity refers to the time between the first spike and the last spike as a result of the stimulation. Mean $\pm$ SD is given.

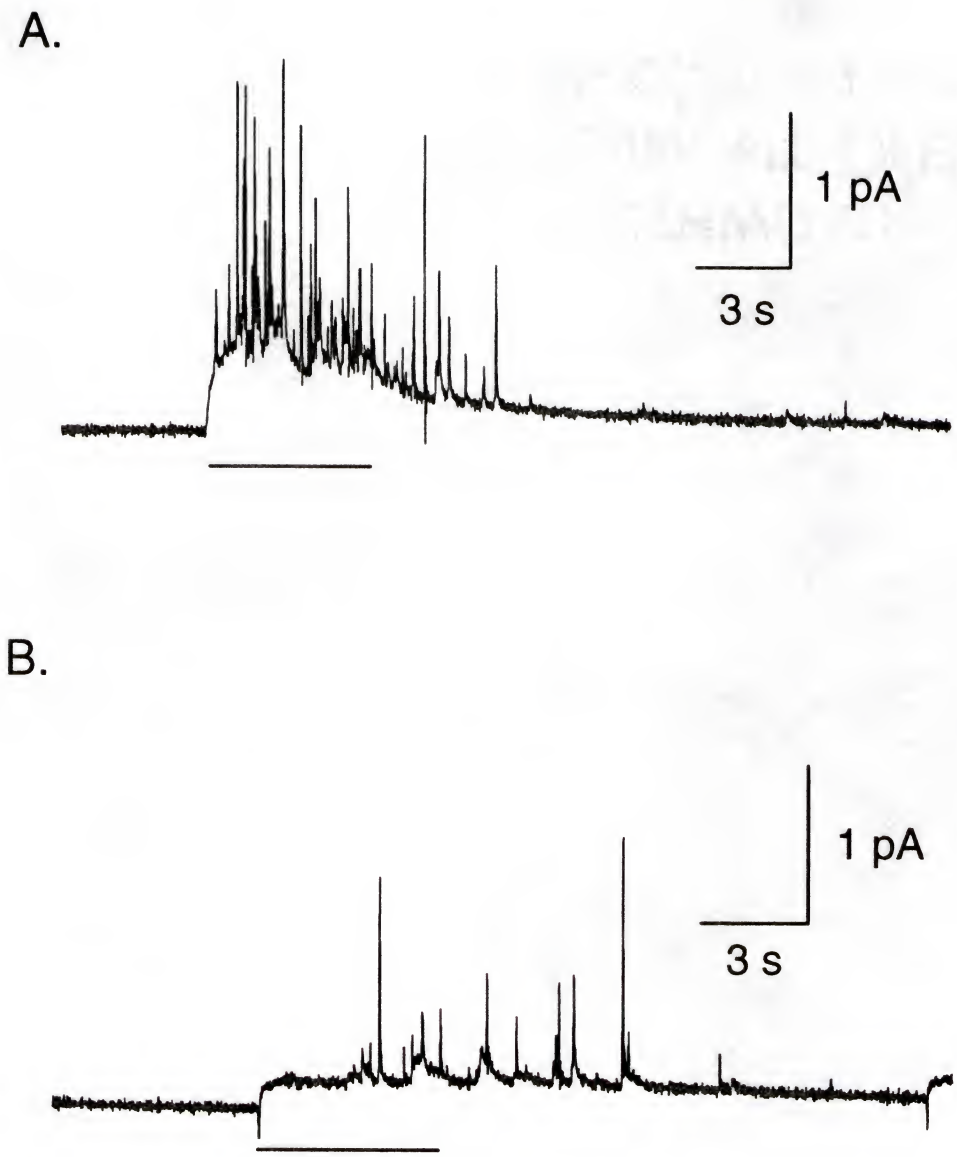

Figure 4-1. Effect of reserpine on catecholamine secretion from PC 12 cells. Current recordings from a single PC12 cell stimulated with 1 mM Nicotine in 105 mM K^+:
A) before exposure to reserpine, B) after 19 min of incubation with reserpine and C) after 20 min of incubation with reserpine. Bars indicate stimulation. D) is a current recording obtained from another PC12 cell while being incubated with reserpine without Nicotine/K^+ stimulation.

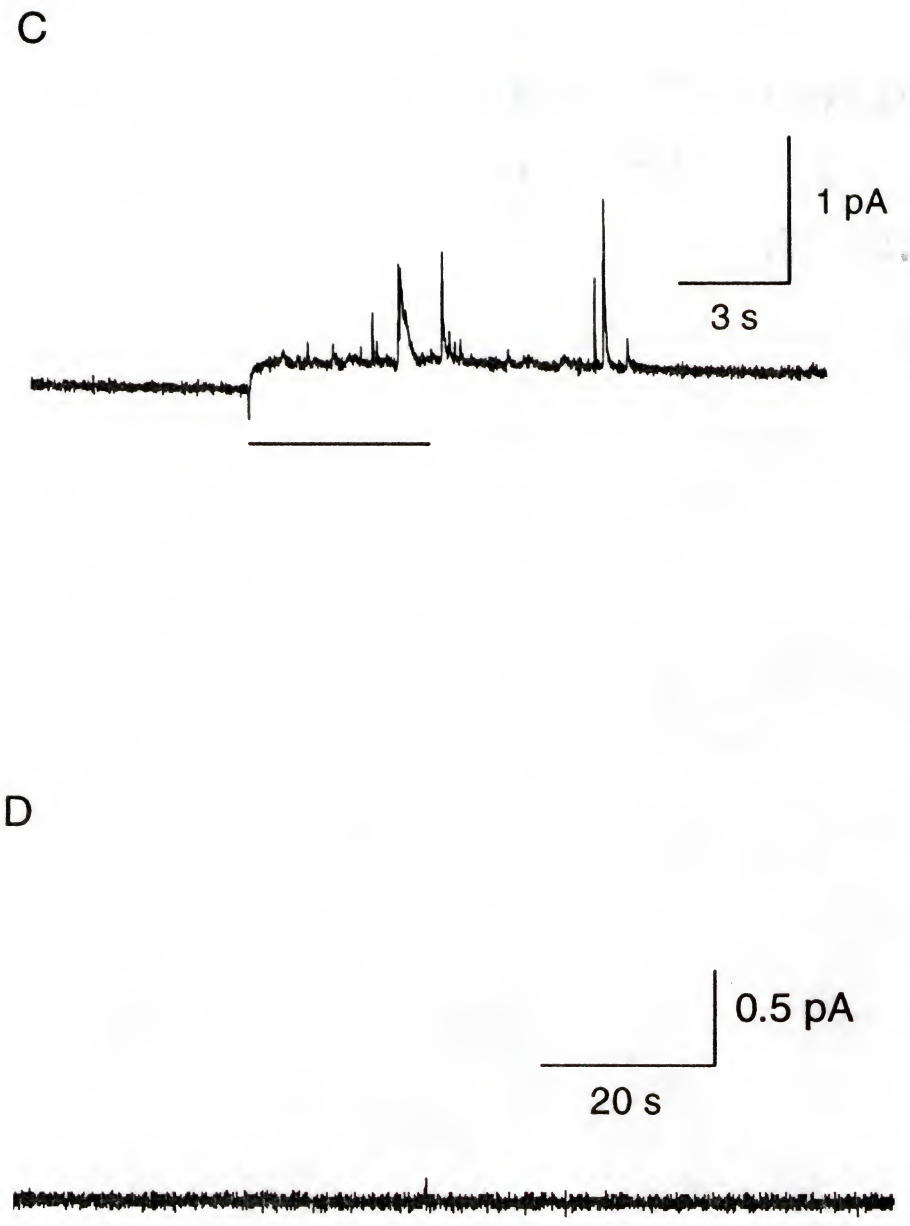

Figure 4-1. Continued.

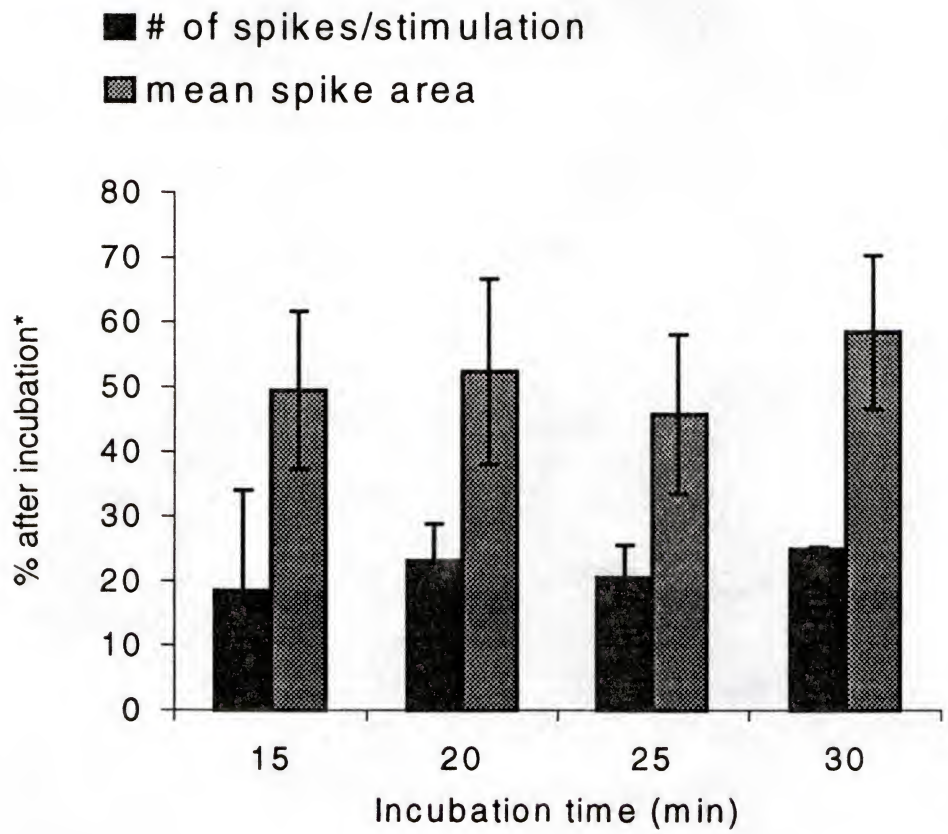

* # of spikes(or mean spike area) before reserpine incubation x 100%
# of spikes(or mean spike area) after reserpine incubation

Figure 4-2. Depletion of cathecolamine stores by reserpine (1 μM). Decrease in the number of spikes per stimulation and spike areas after incubation with reserpine is reported as percentage remaining after incubation. Results in Table 4-1 were used for the calculations. Each value represents the arithmetic mean ± SD.

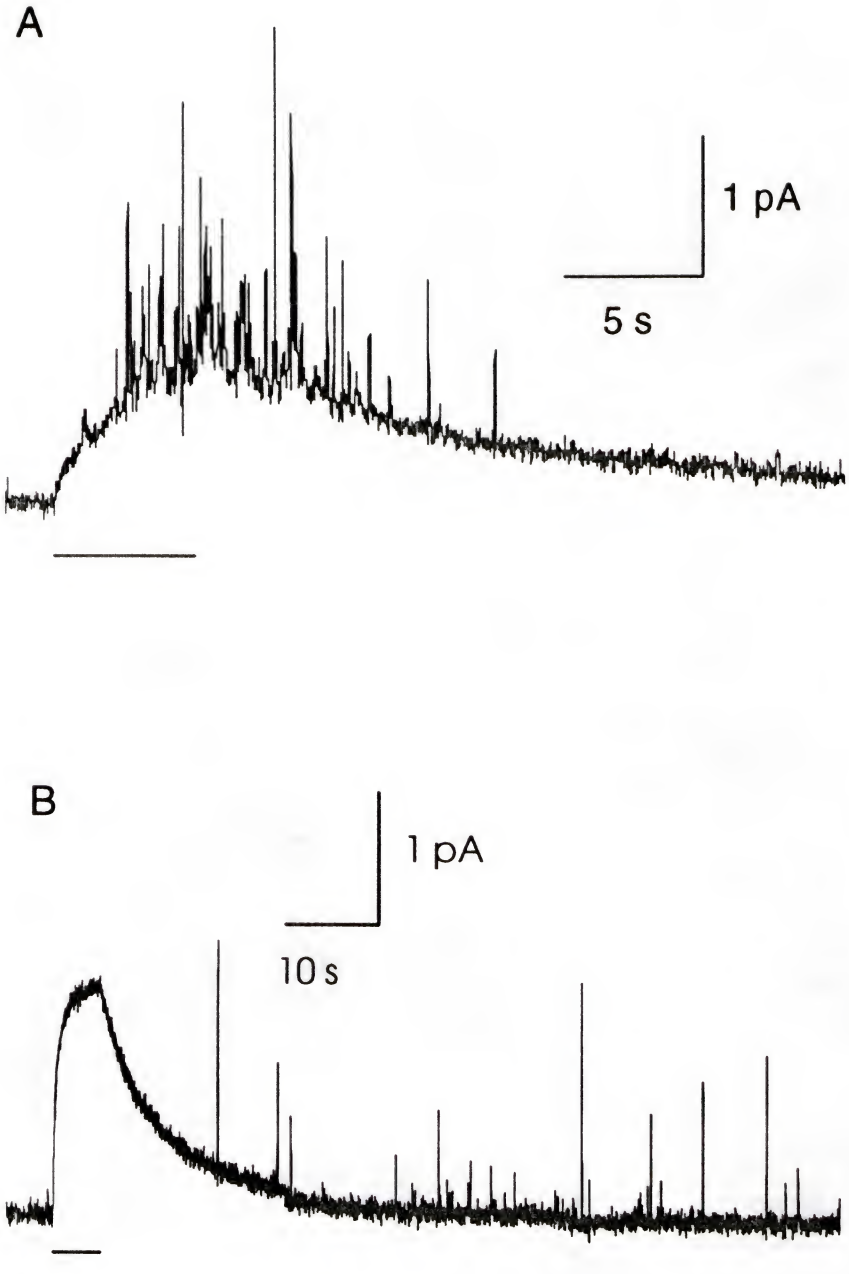

Figure 4-3. Current recordings made at a single PC12 cell after stimulation with: A) 1 mM Nicotine in 105 mM K+, and B) 10 μM Tyramine. Solid line below current trace indicate stimulation.

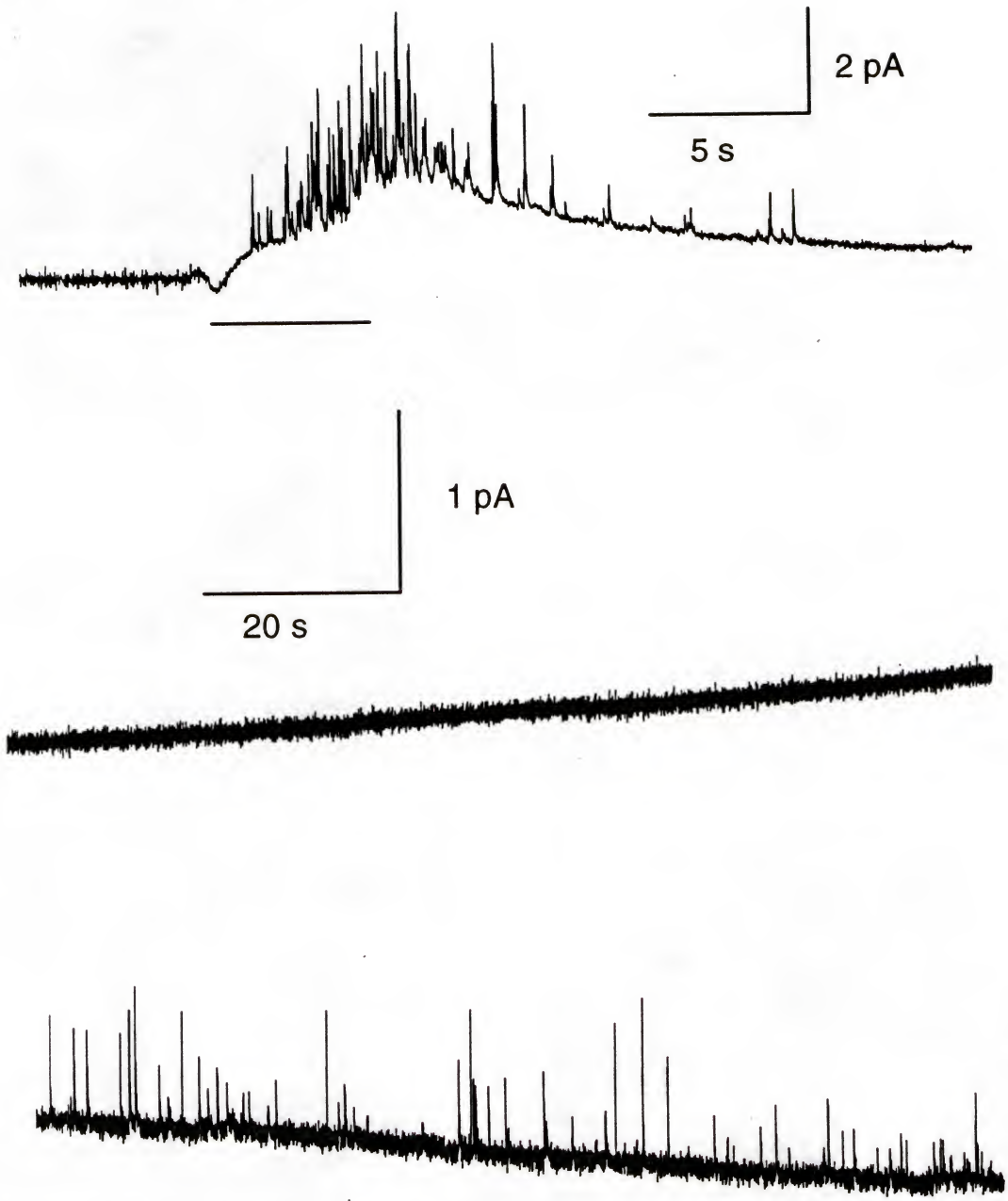

Figure 4-4. Calcium dependence of secretion due to tyramine. (A) and (B) are amperometric current recordings obtained from a single PC12 cell in Ca^{2+}-free media: (A) after stimulation with 1 mM nicotine in 105 mM K^+ with 3 mM Ca^{2+} and (B) after 11 min of incubation with 100 μM tyramine. (C) is a current recording made at another PC12 cell after 11 min of incubation with 100 μM Tyramine in media containing 2 mM Ca^{2+}. Solid line under current trace in (A) indicate stimulation. Scale bars on (B) also apply on (C).

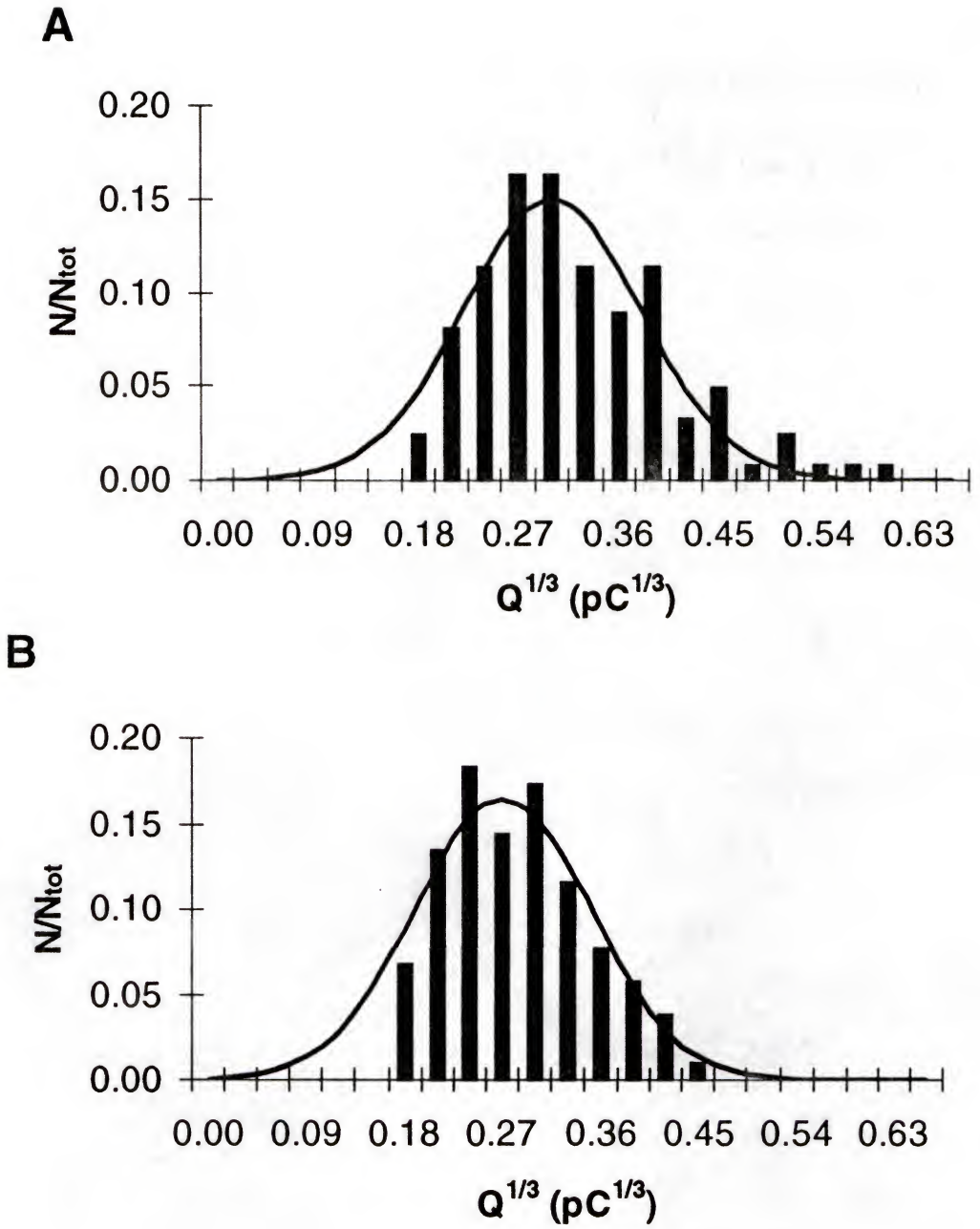

Figure 4-5. Distribution of cube roots of spike areas ($Q^{1/3}$) measured by amperometry at single PC12 cells. (A) Histogram is from 123 spikes obtained after stimulating 5 cells with 1 mM Nicotine in 105 mM K^+. Only isolated spikes with S/N ratio $\geq$ 8 were considered. The fitted Gaussian curve (solid line) has a mean $\pm$ SD of 0.300$\pm$ 0.080 $pC^{1/3}$. (B) Histogram is from 104 spikes obtained from a single cell after incubation in 100 μM Tyramine. The Gaussian fit (solid line) has a mean $\pm$ SD of 0.270 $\pm$ 0.076.

CHAPTER 5
SPATIALLY-RESOLVED AMPEROMETRIC MEASUREMENTS OF 5-HYDROXYTRYPTAMINE SECRETION AT SINGLE PANCREATIC β-CELLS

Introduction

Greater understanding of insulin secretion is of profound medical importance since type II diabetes, the most prevalent form of diabetes mellitus, is associated with insufficient insulin secretion. Insulin secretion has been studied extensively, yet, certain aspects of this complex process remain unknown. Insulin is synthesized and stored in β-cells found in the pancreatic islet of Langerhans (Orci et al., 1988). Like other hormones and neurotransmitters, insulin is stored in intracellular vesicles (357 nm diameter) (Matthews et al., 1982) and then in the presence of an appropriate stimulus secretion occurs through a process called exocytosis.

Recently, microelectrode techniques have been used to explore the dynamics of exocytosis at single β-cells. Kennedy and coworkers have used carbon fiber microelectrodes (r~5 μm) modified with a thin film of ruthenium oxide and cyanoruthenate (Ru-O/CN-Ru) to detect insulin from single pancreatic β-cells (Kennedy et al., 1993). This electrode allows the detection of insulin from a single cell with high temporal resolution; however, the Ru-O/CN-Ru film is not very stable at physiological pH. Another option to monitor insulin secretion is to measure the release of 5-hydroxytryptamine (5-HT), which is co-secreted with insulin when loaded into β-cells (Aspinwall et al., 1997). 5-HT can be easily oxidized at unmodified carbon fiber electrodes and thus, the need for

electrode modification is eliminated.

Previous reports have shown that insulin-containing granules are unevenly distributed in β-cells (Bonner-Weir, 1988; Bokvist et al., 1995) (See Figure 5-1). Interestingly, it was also observed that L-type Ca^{2+} channels are localized near the region of the cell with the highest density of secretory granules (Bokvist et al., 1995). This evidence suggests the presence of specific sites of secretion or hotspots on β-cells. However, until now there is no direct evidence that secretion actually occurs on specific sites on the plasma membrane.

Ultramicroelectrodes with micron or smaller radii can be used to probe different sites of release on single cells with high temporal resolution (Schroeder et al., 1994). In this work, we explored the organization of β-cell secretion sites with the use of flame-etched carbon microelectrodes with ~ 2 μm diameter tips. To accomplish this, 5-HT was loaded into β-cells and was used as a secretion marker. We investigated the possibility of vesicle fusion occurring at predetermined locations (hot spots) or at random locations on the cell surface. As we examined the spikes obtained at these ultramicroelectrodes we observed two different modes of exocytosis that may explain the efficient release of insulin from a small area on the cell membrane. Imaging techniques were used to confirm the results obtained from the use of microelectrodes. We used FM1-43 dye as a marker to indicate membrane changes in single β-cells as a result of vesicle fusion during exocytosis (Betz et al., 1992).

Experimental

Electrode preparation and testing. Carbon fiber disk and cylinder microelectrodes were prepared using previously described techniques (Kelly and Wightman, 1986, Kawagoe et al., 1993). Carbon fibers used were approximately 10 μm in diameter.

Cylinder microelectrodes with protruding 5 mm carbon fibers were used to construct the flame-etched electrodes. The exposed carbon fiber was etched using an air/methane flame, then the electrodes were insulated with a copolymer of 2-allylphenol and phenol as described elsewhere (Strein and Ewing, 1992). The glass capillaries were filled with 3 M NaCl, and a nichrome wire was inserted for electrical connection. The electrodes were polymerized in a solution of 60 mM phenol, 90 mM 2-allylphenol, and 2% 2-butoxyethanol (w/w) in 1:1 (v:v) water methanol (pH = 9.0) by applying 4.0 V for 12-14 minutes. The fibers were cured for 30 minutes at 150 °C. Cyclic voltammograms were collected in phosphate buffer to check the insulating capability of the polymer film. A charging current less than 10 pA (difference between the cathodic and anodic scan) defines a well-insulated electrode (See Figure 5-2A). Before each experiment the tip of the polymerized flame-etched electrodes was polished for 10 s on a polishing wheel at an angle of 45° (Kawagoe et al., 1991). Immediately after polishing, electrodes were dipped in isopropanol for at least 15 minutes and rinsed with water before use. Scanning electron micrographs of the electrodes show the polymer thickness to be 267 $\pm$ 29 nm (n=3). The electroactive surface of the tip was estimated electrochemically. At steady state conditions, the limiting current at a microdisk electrodes of very small dimensions can be described by the equation:

$$i_{lim} = 2\pi rnFDC$$

where r is the radius of the electrode, n is the number of electrons transferred in the electrode reaction, F is the Faraday constant (96,485 Coulombs/equivalent), D is the diffusion coefficient and C is the concentration of the analyte (Strein and Ewing, 1992; Wang, 1994). To estimate the radius of the electrodes, steady state voltammograms were

obtained for the reduction of 1 mM $K_3Fe(CN)_6$ in 0.5 M KCl at pH 3.0 ($D=7.2 \times 10^{-6}$ cm^2s^{-1}, n=1). The potential was linearly scanned from –0.3 to 0.7V then back to –0.3V at 50 mV/s (Kawagoe et al., 1991). A sample voltammogram is presented in Figure 5-2B. For this particular electrode, the radius calculated was 1.48 mm. Nevertheless, in most cases the limiting current was between 0.4 to 0.5 nA corresponding to a radius of 0.9 to 1.1 μm. Radius obtained from scanning electron micrographs of the flame-etched electrodes agreed with the results from electrochemical measurements (n=4). Figure 5-3 shows an electron micrograph of a flame-etched electrode insulated with the allylphenol-phenol copolymer. The electroactive tip is ~ 2 μm in diameter and the polymer is 0.25 μm, thus the overall tip is 2.5. For clarity in succeeding discussion, the size of the tip of the electrode will always refer to the active surface of the electrode (~ 2 μm) unless otherwise noted. The electrodes were tested by puffing 10 μM 5-hydroxytryptamine (5-HT) to the electrodes.

Cell culture. Porcine and canine pancreatic islets were provided by Dr. Jonathan Lakey (University of Alberta, Edmonton, Alberta, Canada). Single pancreatic β-cells were dispersed from islets using a previously described technique (Kennedy et al., 1993; Huang, 1995). Approximately, 3000 islets were placed in 15 ml conical centrifuge tube using transfer pipet. The islets were centrifuged at 1,300 RPM at room temperature for 2 min (IEC Centra MP4R, International Equipment Co.) and washed twice with 1X Ca^{2+}, Mg^{2+}-free Hank's media. Following washing, the media was sucked off by vacuum and islets were resuspended in 7 ml of straight Versene. The islets were incubated in versene for 7 min and resuspended once during the incubation. After incubation, the islets were centrifuged at 1,300 RPM for 2 min. The supernatant was removed and 7 ml of trypsin

solution (1mg/mL in Ca^{2+}, Mg^{2+}-free Hank's media) prewarmed at 37 °C was added. The islets were resuspended in trypsin solution and mixed gently in water bath (37 °C) for 3 min. Islets were triturated 10-20 times using a sterile transfer pipette and shaken gently in water bath for another 30-40 s. After the digestion, 8 ml of culture media was added to the centrifuge tube. Then, the cell suspension was centrifuged at 1,500 RPM for 5 min at 4°C. The supernatant was removed and 2-3 ml of culture media was added depending on the cell density. Cells were plated in 35 mm diameter polystyrene tissue culture dishes (Corning) and incubated at 37°C in 5% CO_2 in G-100 media (CMRL-1066 modified with 1% L-glutamine, 10% fetal bovine serum, 1% penicillin/streptomycin, 25 mM Hepes, 25 mM $NaHCO_3$) at pH 7.4. Cells were used on days 2-6 days of culturing.

Rat islets were isolated in our laboratory with the help of Craig Aspinwall and Liisa Kauri. Rat islets were isolated from 200 to 220 g male Sprague-Dawley rats by collagenase digestion as described elsewhere (Roe et al., 1993; Huang, 1995). Isolated rat islets were digested with 0.8 ml of 0.05% trypsin/EDTA (37°C) for 60 s. 3 ml warmed RPMI 1640 medium was added to inhibit further digestion. The dispersed cells were suspended in 1.5 ml of G100 and plated on 35-mm tissue culture dishes. Cells were incubated as described above.

Unless otherwise stated, all chemicals for islet and cell culture were obtained from Life Technologies, Inc (Gibco).

Loading 5-hydroxytryptamine (5-HT) into β-cells. Dispersed β-cells were incubated in G100 media containing 0.5 mM 5-HT and 1 mM 5-hydroxytryptophan. The plates were placed in an incubator (5% CO_2 at 37°C) for 16 hours (Aspinwall et al., 1997).

Single cell experiments. Single cell experiments were performed as described

elsewhere (Leszczyszyn et al., 1990; Wightman et al., 1991). All experiments were done using 5-HT as a secretion marker for insulin (See Figure 5-4). During experiments, cells were bathed in modified Kreb's Ringer buffer (KRB, 118 mM NaCl, 5.8 mM KCl, 2.4 mM $CaCl_2$, 1.2 mM $MgSO_4$, 1.2 mM KH_2PO_4, 20 mM 2-(N-hydroxyethylpiperazin-N'-yl)ethanesulphonic acid (HEPES) and 3 mM d-glucose). The dish was placed in a microincubator (Medical Systems, Inc.) on the stage of an inverted microscope (Zeiss axiovert 35). The microincubator maintained the temperature at 37 °C. To perform measurements, a cell was located with the inverted stage-microscope and a working microelectrode was slowly brought closely to the cell until the cell membrane just began to deform using a micropositioner (Burleigh PC-1000). For the two electrodes setup two micropositioners were used and the electrodes were positioned at different sites on the cell membrane as shown in Figure 5-5. With the small size of the electrode, ~ 2.5 μm total diameter, we were able to probe several spots on the cell membrane (~ 14 μm diameter). This is evident in Figure 5-6 which shows the size of the flame-etched electrode relative to the size of the cell.

Stimulants were applied to individual cells by pressure ejecting solutions from the tips of micropipettes (~ 10 μm diameter tip) which were positioned approximately 30 μm from the cell. Flow rates through the pipette tips were approximately 1 nL/s. Stimulants (e.g. tolbutamide) were dissolved in modified KRB. For K^+ stimulation, 60 mM K^+ was prepared in modified KRB by decreasing the NaCl with an equivalent amount.

Data collection and analysis. Data were collected using a dual channel potentiostat (EI400, Ensman Instrumentation, Bloomington, IN). The electrodes were poised at 0.65 V versus sodium saturated calomel electrode. Amperometric data were collected at 167

Hz using a software, Axotape (Axon Instruments) and low pass filtered with a cut-off frequency of 30 Hz. The data were collected by an IBM-compatible personal computer (Gateway 2000 486-66 MHz) via a data acquisation board (Digidata 1200A, Axon Instruments). Software provided by Prof. R. Mark Wightman (University of North Carolina) was used to remove residual 60 Hz noise and calculate current spike characteristics including spike area, half rise time and onset time. For data analysis, spikes were used only if the signal to noise ratio was greater than 8. All means are reported $\pm$ 1 standard deviation. Statistical differences between means were evaluated using two-tailed Student's t-test.

Fluorescence microscopy. For quinacrine measurements, cells were plated on coverslips (25 mm, Carolina Biological Supply). Cells were incubated overnight in G-100 culture media with 0.4 μM quinacrine at 37 °C in 5% CO_2. The coverslip was mounted in a tissue culture dish and bathed with modified KRB on the stage of an inverted fluorescence microscope (Olympus XII, 40x objective) connected to a mercury arc lamp (100 watt with neutral density filter). A CCD camera was used to collect images (1 s /image) using an imaging software (Princeton Instruments). Quinacrine was excited at 340 nm and emitted light was collected at 510 nm using a bandpass filter (510-530 nm).

For FM1-43 measurements, cells were plated on coverslips (25 mm, Carolina Biological Supply) and incubated as described above. For single cell experiments, cells were immersed in modified KRB with 1 μM FM-43. FM1-43 was excited at 488 nm and emitted light was collected at 580 using a long pass filter (530 nm). To combine electrochemical measurements with fluorescence measurements, the electrochemical setup described above was incorporated into the fluorescence setup. The modified setup is

described in Figure 5-7.

Results and Discussion

Simultaneous amperometric measurements using two flame-etched electrodes.

Flame-etched electrodes (~ 2 μm diameter) were used to spatially map sites of secretion or hotspots on porcine pancreatic β-cells. In Table 5-1, data from 12 cells are summarized. For these cells, further stimulations were unsuccessful. When two electrodes were positioned 3-4 μm apart, spikes were typically observed at only one electrode. This occurred on 5 out of the 6 cells examined. This was not due to one electrode being less sensitive since post-calibration showed that the two electrodes had comparable sensitivity (See Figure 5-8).

When the two electrodes were ≤ 2 μm apart, spikes were observed simultaneously on both electrodes. This occurred 4 times out of 6 trials with the small spacing. For 4 cells, the mean spike areas obtained at the two electrodes were not statistically different. To evaluate the spatial resolution of the flame-etched electrodes, we determined the occurrence of coincident spikes as described elsewhere (Schroeder et al., 1994). Spikes detected at the two electrodes correspond to the same exocytotic event if the difference in onset times (Δt) is lesser than the time required for the molecules to diffuse to each electrode Δt_o ($\Delta t_o = \Delta l^2/6D$; Δl = distance that molecules travel to each electrode and D = diffusion coefficient of 5-HT molecules). Based on our calculations there were no coincident spikes even when the gap is 2 μm or less. This indicates that the two flame-etched electrodes are detecting distinct exocytotic events.

When the two flame-etched electrodes were positioned as close as possible (gap ~ 0.5 μm due to polymer insulation layer) spikes were only observed at one of the electrodes.

For the 12th cell in Table 5-1, spikes were only observed on electrode 1 even though the two electrodes were positioned as close as possible (gap ~ 0.5 μm due to the insulation layer). In this case, it is possible that electrode 1 was positioned near the edge of a hot spot. Since only part of the electrode was on the hotspot a few vesicular release events were detected. On the other hand, electrode 2 was probably positioned outside the hotspot since there were no spikes detected. The absence of coincident spikes and the occurrence of spikes on just 1 electrode for very small gaps prove that the electrode is detecting secretion directly underneath it.

Exploring inactive and active sites of release. Figure 5-9 shows amperometric current recordings obtained at a single porcine pancreatic β-cell. The cell was stimulated with 60 mM K^+ several times at 5 min intervals. Initially, the two electrodes were positioned on top of the cell. When the cell was stimulated, current spikes were observed at both electrodes. As the electrodes were moved toward the periphery of the cell lesser spikes were obtained during the stimulation. Results demonstrate the presence of a hotspot at the center of the cell that was larger than 2 electrodes. In Figure 5-10, another porcine pancreatic β-cell was investigated. Again, the cell was stimulated with high K^+ buffer and the electrodes were positioned on different areas on the cell surface. This cell exhibited an ovoid active site of release on the top of the cell. When electrode 1 was positioned at the periphery of the cell, there were no current spikes observed, but when it was placed back near the top of the cell, current spikes were obtained. This strengthens our assumption that secretion occurs at specific sites on the cell. Secretion does not always occur on the top (center) of the cells, hotspots near the periphery of the cell were also observed on other single β-cells.

Figure 5-11 shows the current recordings obtained at a single canine β-cell. The cell was stimulated with 200 μM tolbutamide for 10 s. Initially, the electrodes were positioned at the left periphery of the cell. Even though the two electrodes were positioned as close as possible, release from the region monitored by electrode 2 was more robust, while the released spikes detected by electrode A were smaller in amplitude and infrequent. When the two electrodes were moved a little bit upward spikes observed on electrode 2 were lower in amplitude and only a couple of spikes were observed on electrode two. Secretion from other sites on the cell membrane was also monitored, however, active release was not evident. Thus this cell displayed a hotspot of release at the left periphery of the cell. In general, the size and location of hotspot vary from cell to cell and are stationary for 15-30 minutes.

Comparison of spikes obtained at regular carbon fiber disk electrodes and flame-etched electrodes. Table 5-2 compares the mean spike areas obtained at regular carbon fiber disk electrodes (r~ 5 μm) to those of flame-etched carbon fiber electrodes (r~ 1 μm). The mean spike area measured at regular disk electrode is sometimes larger than the mean spike area at flame-etched electrode. The difference in spike areas can be due to three different reasons. First, the regular disk electrodes may be more sensitive than the flame-etched electrodes. To test this possibility we tested the response of these electrodes to 10 μM 5HT at 0.65 V. We can eliminate this possibility since the amperometric signal obtained at the flame-etched electrodes (~ 1 μm radius active surface) is 5x smaller in magnitude than the response that we get at regular disk electrode (~5 μm radius active surface). Second, the larger spike area measured at regular disk electrode may be due to the occurrence of overlapping spikes. In Figure 5-12, spikes obtained at regular carbon

fiber disk electrode (A) are compared to those obtained at flame-etched carbon fiber electrodes (B). Well-resolved current spikes were obtained at flame-etched electrodes whereas at the regular disk electrode, the presence of overlapping spikes was evident. Therefore, the difference between the mean spike areas obtained at regular disk electrode may be attributed to the presence of overlapping spikes. With flame-etched electrodes, it is possible to measure exocytosis from much smaller location on the cell membrane and this minimize overlap due to exocytosis events occurring at different sites on the cell. Finally, the difference in spike area may be due to the fouling of small electrodes. This can be eliminated by considering the fact that when less overlapped spikes are observed at regular disk electrode (See cell #1 in Table 5-2), the mean spike area is not statistically different to that of flame-etched electrode.

Occurrence of very large spikes. Although well-resolved spikes were obtained at flame-etched electrodes, the distribution of spike areas exhibits the presence of large spikes which are 3 to 10 times larger than the average spike area. Figure 5-13 shows a typical distribution of spike areas obtained at a single β-cell. The mean spike area for this histogram is 0.343 ± 0.579. The histogram exhibits a skewed non Gaussian distribution and the presence of abnormally large spikes is evident. It was calculated that 4.6 % of the spikes have spike areas at least 3 times larger than the mean spike area. If all the spikes in this histogram are integrated, these really large spikes contribute 33% to the total spike area.

Analysis of the cube root of spike areas. In a previous work, it was demonstrated that the histogram of the cube root of spike areas exhibits a Gaussian distribution (Finnegan et al., 1996). This was observed for chromaffin cells, mast cells, PC12 cells and

pancreatic β-cells. This observation was attributed to the Gaussian distribution of vesicular radii (or diameter). If it is assumed that each vesicle contains similar concentration, and that vesicles have spherical shape, the amount of neurotransmitter or peptide (N) in millimoles can be defined by: $N = VC$ or $N = {}^4/_3\pi r^3 C$ where C is the vesicular concentration (M); V is the vesicular volume (cm^3 or ml); and r is the radius (cm). According to these assumptions, the histogram of cube root of the charges should exhibit a Gaussian or normal distribution with a SD similar to that of the vesicular radii. In pancreatic β-cells, the diameter of the vesicles have been shown to exhibit a Gaussian distribution (Dean, 1973; Laarson et al., 1976) with a standard deviation of ~ 22 % of the mean radius (Laarson et al., 1976). Figure 5-14 shows the distribution of the cube root of spike areas used for Figure 5-13. The Gaussian equation is defined by:

$$F(x) = \frac{n}{(2\pi\sigma^2)^{1/2}} \exp\left[-(x - u)^2 / 2\sigma^2 \right]$$

where, x is the calculated cube root of spike areas ($Q^{1/3}$), u is the mean value of x, σ is the standard deviation and F is the normalized frequency. In Figure 5-14A the fitted Gaussian curve (solid line) was obtained by considering all the $Q^{1/3}$ values and by using Systat program to determine n, σ and u. The fitted Gaussian curve had a mean ± SD of 0.534 ± 0.104 $pC^{1/3}$. In Figure 5-14B, the Systat program was used to calculate n, σ and u for the same data set but only values of $Q^{1/3} \leq 0.72$ $pC^{1/3}$ were included. The Gaussian curve derived had a mean ± SD of 0.529 ± 0.093 $pC^{1/3}$. For both cases although most of the $Q^{1/3}$ values are distributed within the Gaussian curve, the presence of abnormally large $Q^{1/3}$ values are still evident. Assuming the concentration within the vesicles is maintained this indicates that these large $Q^{1/3}$ values correspond to larger vesicular-like structures or

multifusion of vesicles.

To ascertain if the large spikes are due to overlapping spikes, the probability of obtaining multiple spikes was determined as described elsewhere (Alvarez de Toledo et al., 1990). A probability distribution function ($P(t) = e^{-t/\tau}$) was obtained from the distribution of latency times between successive exocytotic events. The latency times were obtained by calculating the time between the onset of two consecutive spikes. For the spikes shown in Figure 2, the time constant τ was calculated as 0.734 s and the probability of detecting three events within time t (average half rise time) was calculated as 0.0016. This value is very small compared to the occurrence of large spikes which can be calculated as the ratio of large spikes to the total number of spikes (0.046). Table 3 summarizes the results obtained from three cells. Results imply that large spike areas are not due to overlapping spikes. With the inherent high temporal and spatial resolution of flame-etched electrodes, the possibility of detecting simultaneous exocytotic events is very minimal.

Fluorescence measurements. Fluorescence measurements were used to verify the results obtained from electrochemical detection. When quinacrine is loaded into β-cells, it accumulates in insulin-containing granules (Abrahamsson and Gylfe, 1980; Bokvist et al., 1995). Figure 5-15 shows the fluorescence images of cells incubated in quinacrine. For most of the cells the dye is concentrated in a specific region indicating an uneven distribution of insulin-containing granules in the cytoplasm.

FM1-43 (N-(3-triethylammoniopropyl)-4-(p-dibutylamino-styryl) pyridinium dibromide) is a fluorescent dye that has been used to measure membrane area changes during exocytosis (Betz et al., 1992; Stafford et al., 1993; Ryan and Smith, 1995; Smith

and Betz, 1996). This styryl dye does not exhibit fluorescence in aqueous media but becomes highly fluorescent upon incorporation into membranes (Betz et al., 1992). When a cell is stimulated, vesicles fuse with the plasma membrane and the increase in the membrane area induces a corresponding increase in fluorescence (Betz et al., 1992; Stafford et al., 1993). In Figure 5-16, the change in FM1-43 fluorescence is demonstrated after stimulation of a single rat pancreatic β-cell. Initially, the cell exhibited very low fluorescence (left panel) but after stimulation of the cell with 200 μM tolbutamide for 10 s a corresponding increase in fluorescence was observed (center panel) on a specific spot on the cell membrane. When the cell was restimulated, the increase in fluorescence on the same spot was evident. Our results suggest that that secretion is localized in specific regions on the cell membrane. Figure 5-17A (left panel) shows the change in fluorescence when another rat pancreatic β-cell was stimulated with 200 μM tolbutamide. The image was obtained by subtracting the fluorescence of the cell before stimulation from that after stimulation. To check whether secretion actually occurs on the region with higher fluorescence, we probed the cell surface with a 2 μm tip etched electrode. The electrode was positioned on zone I, II and III as shown in on Figure 5-17B (right panel). The current traces (I, II and III) correspond to the current recordings obtained at specific zones on the cell membrane as illustrated in Figure 5-17 B. When the electrode was positioned at zone I, there were no current spikes observed, however, when the electrode was positioned at zone II current spikes were observed in the presence of 200 μm tolbutamide. After zone II, the electrode was moved to zone III and again, we did not detect secretion. The broad spike at the start of the stimulation is an artifact due to the puffing of stimulant solution. This is indeed interesting because if we refer to the

fluorescence image in (A), zone II has a higher change in fluorescence as compared to zone I and III. Based on our results we conclude that FM1-43 can be used as an indicator of secretion in β-cells. From the fluorescence and electrochemical data, the presence of a hotspot is again evident. The size of the region with higher fluorescence is comparable to the size of hotspot we predicted using flame-etched electrodes.

Detection of hotspots. We have demonstrated the advantages of using flame-etched carbon fiber microelectrodes with 2 μm tip in probing different sites of release on β-cells. When positioned as close as possible to the cell membrane, these electrodes only detect secretion directly underneath. Consequently, even with a small gap between two flame-etched electrodes (< 2 μm) no coincident spikes were observed. Because of the small size of these electrodes, detection is confined on a small area on the cell membrane and detection of simultaneous exocytotic events from different areas on the cell is minimized. More resolved spikes were obtained as compared to regular carbon fiber disk electrodes. Since the spikes detected correspond to single exocytotic events, we were able to explore the dynamics of secretion by analyzing the area and the frequency of spikes.

Results clearly show the presence of specific sites of secretion or hotspots in β-cells. Using two flame-etched electrodes with active surface tip of 1 μm radius, we exhibited the existence of a hotspot on the cell membrane that was stationary during the time course of our experiment (15-30 minutes). When these two electrodes were positioned 3-4 μm apart, most of the time secretion was only observed at one of the electrodes. The hotspot could be bigger than two flame-etched carbon fiber electrodes and may vary from cell to cell. Using fluorescence images of FM1-43 dye, we confirmed the size of the hotspot. Fluorescence images also show that the site of release can be bigger than two electrodes.

These two high resolution techniques combined provide dynamic observation with reasonable signal to noise ratio. The fluorescence images provide information about the size of hotspot while demonstrating the fusion of vesicles at the specific site of the cell. The flame-etched electrodes allowed detection of 5-HT release from single β-cells with high sensitivity and temporal resolution at very small areas on the cell membrane. Analysis of current spikes obtained at the electrodes provides new insights into the process of secretion. Although, electron micrographs of degranulated β-cells exhibited the polarization of insulin-containing granules (Bonner-Weir, 1988) and fluorescence measurements using quinacrine showed the uneven distribution of these granules (Bokvist et al., 1995), our results provide the first direct evidence of hotspots on β-cells.

Modes of exocytosis. In Figure 5-18, the different modes of exocytosis are illustrated (Alvarez de Toledo, 1990). In single exocytosis, each vesicle fuses with the cell membrane and, subsequently, releases its contents to the extracellular media. Multigranular exocytosis occurs when vesicles in the cytoplasm fuse together before exocytosis (Kurihara et al., 1986; Alvarez de Toledo et al., 1990). Electron micrographs of anterior pituitary cells (Kurihara et al., 1986; Matsuda et al., 1994), pancreatic acenar cells (Matsuda et al., 1994) and pancreatic β-cells (Kolehmainen, 1995) show multigranular structures fused to the cell membrane. In the third mode of exocytosis known as compound exocytosis, single vesicles also fuse to the cell membrane and as exocytosis proceeds vesicles in the cytoplasm fuse with previously fused vesicles rather than with the plasma membrane. This pattern of exocytosis causes the formation of tubular pathways formed by the membrane of fused granules (Alvarez de Toledo, 1990).

Although sites of multiple granule fusion can be demonstrated using morphological

techniques it is still difficult to determine whether the mass of vesicles fused at the membrane is due to a multigranular structure formed in the cytoplasm or a result of sequential fusion of vesicles (compound). With the use of flame-etched electrodes, the occurrence of these two modes of exocytosis can be distinguished. Multifusion of vesicles prior to membrane fusion increases the amount released in a single exocytotic event. When using microelectrodes to detect exocytosis, this results in larger spike areas. Evidences have been accumulated showing the presence of these really large spikes from different types of cells like adrenal chromaffin cells (Chow et al., 1992; Finnegan et al., 1996) and PC12 cells (Zerby and Ewing, 1996). However, in these previous experiments results were obtained with the use of carbon-fiber electrodes with larger dimensions (r~ 5 μm). With electrodes of large physical dimensions there is a greater possibility of detecting simultaneous exocytosis events that will result in larger spikes. In contrast, with small electrodes (r ~ 1μm) detection of multiple spikes is hindered. The probability of detecting three simultaneous spikes was determined and found to be very low. From the histogram of the cube root of spike areas the presence of extremely large spikes is manifested. This indicates that multigranular exocytosis occurs on the active site or hotspot of the cell. Large capacitance steps during electrophysiological measurements were also attributed to mutifusion events (Alvarez de Toledo and Fernandez, 1990). However, like amperometric recording with regular disk electrodes, there is a great possibility that large capacitance steps are due to simultaneous events occurring at different areas in the cell.

Secretion of insulin via compound exocytosis was initially suggested by Lacy and coworkers (Lacy et al., 1968). Following this report, single and chain release of insulin from pancreatic β-cells in the presence of 16 mM glucose was described using

ultrastructural techniques (See Figure 5-19) (Gabbay et al., 1975; Orci et al., 1980). Prior studies on aesonophils have shown how to detect compound exocytosis with the use of patch-clamp capacitance measurements. However, capacitance measurements can be distorted by changes in cell membrane area (Zorec and Tester, 1993) and changes in the electrical circuit of the cell (e.g. changes in dielectric constant caused by membrane proteins) that are unrelated to secretion (Fernandez et al., 1982; Horrigan and Bookman, 1994; Andres et al., 1996). Moreover, for neuroendocrine cells with smaller vesicle size the technique is not applicable. In the present study we propose a direct approach in examining the presence of compound exocytosis in cells using flame-etched electrodes. The average radius of insulin-containing vesicles was assumed to be ~ 178 nm (Matthews et al., 1982). Figure 5-20 shows the total number of vesicles that can be detected with the use of a flame-etched electrode with an average radius of 1 μm. By considering the angle (45°) at which the electrodes were polished, the major and minor radii were calculated as 1.17 and 0.83 μm. Approximately, 29 vesicles can be fitted under this size of electrode which would imply that only 29 exocytotic events should be observed at this electrode. However, in some cases we detected more than 29 spikes when the cells were stimulated with high K^+. For instance, in Figure 2 we observed 55 spikes at electrode 1 and 86 spikes at electrode 2. These observations can be only explained by the occurrence of chain release or compound exocytosis. By compound exocytosis several vesicles could release their contents on one fusion pore thus allowing more vesicular release within a limited area on the cell membrane. This is not the first evidence that compound exocytosis occurs in β-cells, however, this is the first direct evidence of compound exocytosis.

Related investigations on pancreatic β-cells support the occurrence of multigranular

and compound exocytosis. It has been suggested that limiting membranes of numerous secretory granules are easily fused with one another when they are stimulated by calcium influx (Douglas, 1974). Certainly, Dahl and Gratzl (1976) showed that calcium induces the fusion of isolated secretory vesicles from the islet of Langerhans. The entry of Ca^{2+} that precedes exocytosis is unevenly distributed over the cell and is concentrated to the region with highest density of secretory granules (Bokvist et al., 1995). This arrangement which is obviously reminiscent of the active zones in nerve terminals, is indeed favourable to the β-cell as it ensures that the Ca^{2+} transient is maximal and restricted to the part of the cell (Bokvist et al., 1995). The high concentration of Ca^{2+} in a certain region of the cell induces both compound and multigranular exocytosis and focuses the release of insulin at a specific spot on the cell membrane. Morphological studies on islet organization demonstrate that 8-10 β-cells form a tubelike structure around a central capillary designated as a secretory capillary. Secretory granules were also observed to accumulate towards this central capillary. In relation to our results, hotspots may be situated on the region facing this secretory capillary that have been previously described.

Conclusion

This study provides direct evidence of the presence of hotspots in β-cells. The occurrence of compound and multigranular exocytosis allow maximal release from the active site. Our findings support previous morphological evidence on the organization of β-cells within the pancreatic islet.

Table 5-1. Summary of Simultaneous Measurements Using Two Electrodes.

Cell #	Electrode #	Distance between electrodes (μm)	# of Spikes	Spike area (pC)	Stimulation conditions
1	1 2	4	16 0	0.374 ± 0.339 –	60 mM K^+
2	1 2	3	14 0	0.160 ± 0.121 –	200 μM Tolbutamide
3	1 2	3	6 0	0.241 ± 0.303 –	200 μM Tolbutamide
4	1 2	3	8 11	0.253 ± 0.142 0.311 ± 0.136*	200 μM Tolbutamide
5	1 2	3	12 0	0.590 ± 0.430 –	60 mM K^+
6	1 2	3	14 0	0.295 ± 0.269 –	60 mM K^+
7	1 2	2	14 0	0.320 ± 0.185 –	200 μM Tolbutamide
8	1 2	2	3 8	0.081 ± 0.035 0.377 ± 0.340*	200 μM Tolbutamide
9	1 2	1	24 6	0.201 ± 0.124 0.317 ± 0.413*	200 μM Tolbutamide
10	1 2	1	20 15	0.199 ± 0.219 0.215 ± 0.211*	200 μM Tolbutamide
11	1 2	1	21 11	0.164 ± 0.172 0.127 ± 0.102*	60 mM K^+
12	1 2	0.5	6 0	0.159 ± 0.128 –	60 mM K^+

* Not statistically different, $t_{calculated} < t_{table}$ (α=.05).

Table 5-2. Carbon Fiber Disk Electrode (regular disk) vs Flame-etched Carbon Fiber Electrode (flame-etched).

Cell #	Type of electrode	# of spikes	Spike Area, pC
1	regular disk	32	0.510 ± .494
1	flame-etched	21	0.462 ± .402
2	regular disk	17	0.825 ± .709
2	flame-etched	14	0.295 ± .269 **
3	regular disk	10	1.592 ± 1.202
3	flame-etched	31	0.385 ± .383 *
4	regular disk	40	1.059 ± 1.443
4	flame-etched	31	0.385 ± .383 *
5	regular disk	39	0.469 ± .535
5	flame-etched	367	0.343 ± .501 ***
6	regular disk	22	0.998 ± .997
6	flame-etched	20	0.365 ± .501 **

* Statistically significant difference from spike area obtained at carbon fiber disk electrode ($p < 0.001$).

** Statistically significant difference from spike area obtained at carbon fiber disk electrode ($p < 0.01$).

*** Statistically significant difference from spike area obtained at carbon fiber disk electrode ($p < 0.07$)

Table 5-3. Analysis of Spikes with Large Areas.

Cell #	Total # of spikes	Mean area, *M* (pC)	*$[1 - P(t)]^2$ x 100	% of spikes with area ≥ 3 *M*	% Contribution of large spikes to total spike area
1	365	0.343 ± .579	0.16	4.6	33.0
2	175	0.365 ± .501	0.45	6.3	29.3
3	77	0.249 ± .025	0.20	5.2	20.0

* Probability that 3 insulin-containing granules fuse with the cell membrane within time t (t = average half rise time of the spikes)

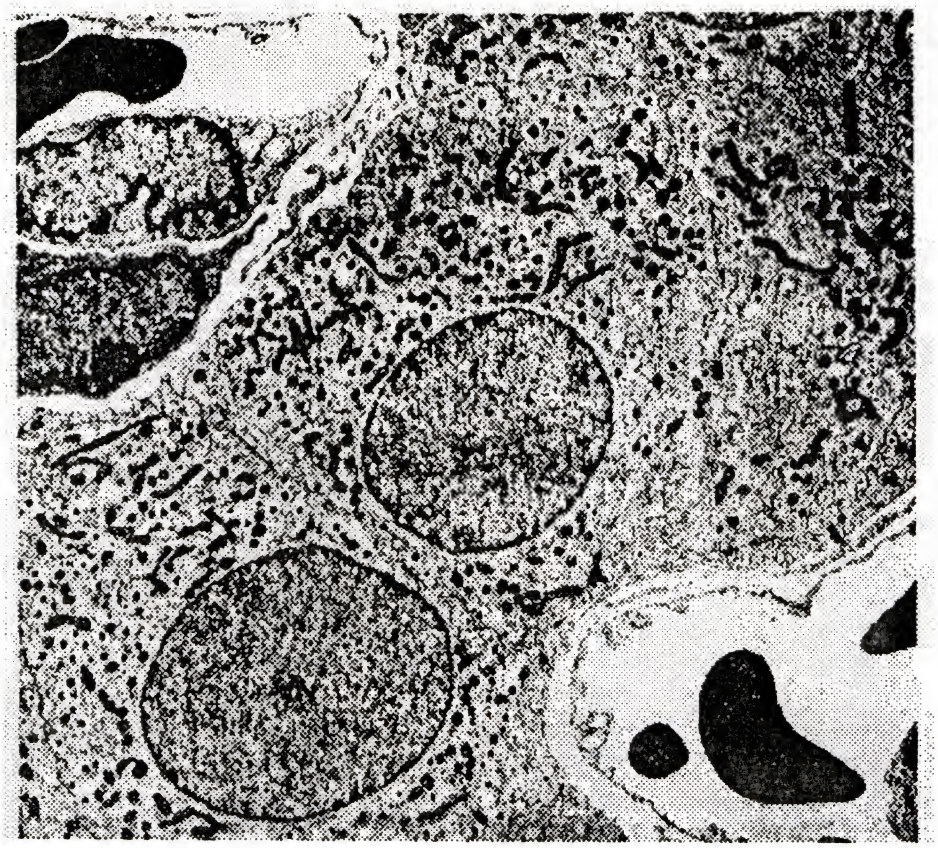

Figure 5-1. Polarity of insulin-containing granules. Micrograph of a section of an islet showing the polarity of granules accumulated at the apical end of two β-cells. After treatment with glyburide, granules tend to accumulate towards a capillary pathway (Bonner-Weir, 1988).

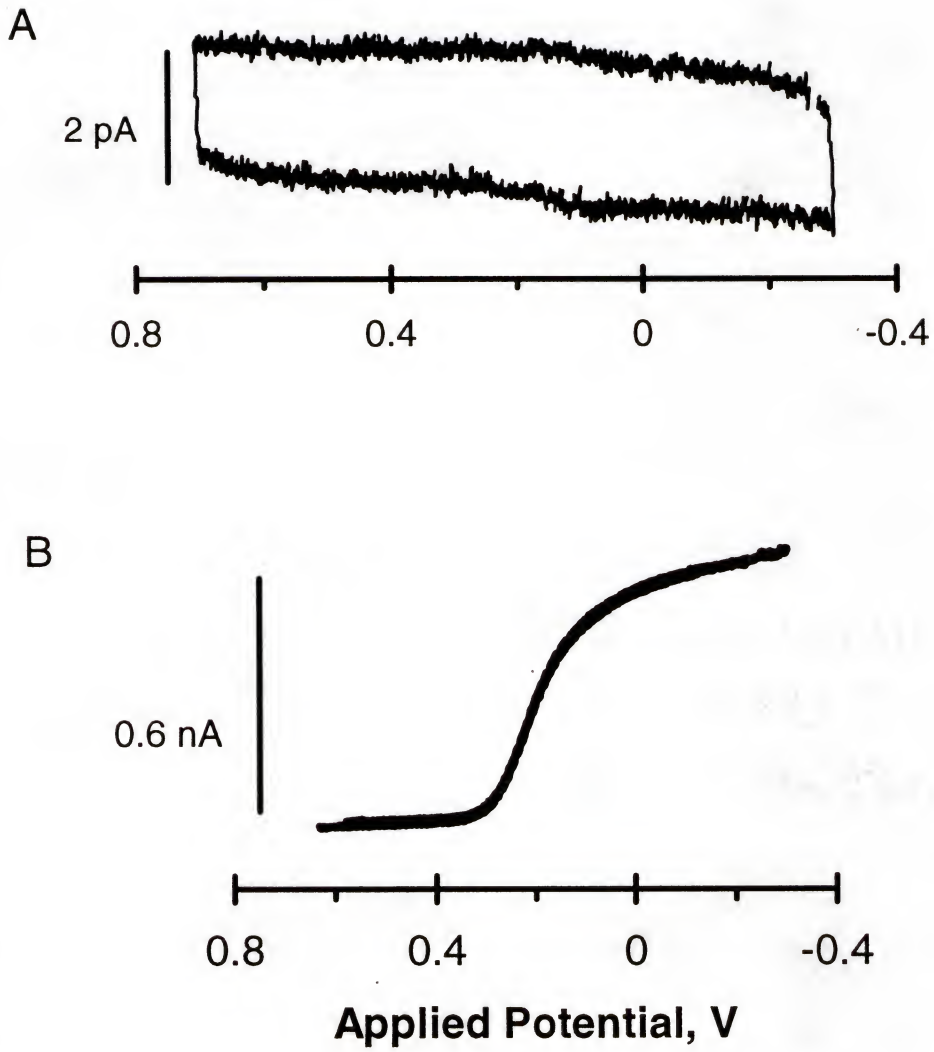

Figure 5-2. (A) Cyclic voltammogram of a well insulated electrode in phosphate buffer. To check the insulation layer the potential applied was linearly scanned from –0.3 to 0.7V and then back to –0.3 V at 50 mV/s. A good insulation layer will only allow a charging current of 10 pA or less. (B) Determination of electrode radius. Cyclic voltammograms were collected in 1 mM $K_4Fe(CN)_6$ in O.5 mM KCl (-0.3 to 0.7V to –0.3V, 50 mV/s). The radius of this particular electrode was calculated as 1.48 μm.

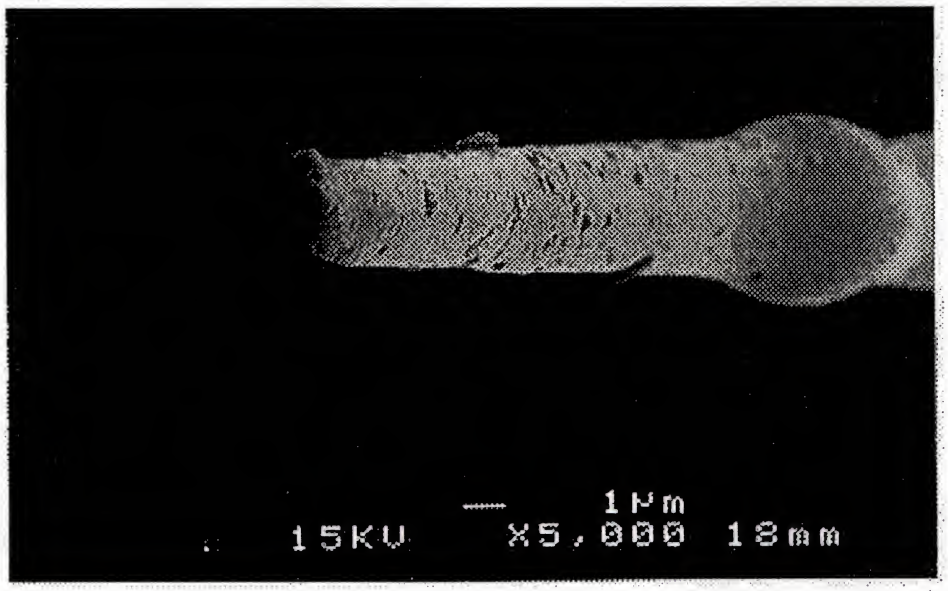

Figure 5-3. Scanning electron micrograph of a flame-etched carbon fiber microelectrode. The outer layer of the electrode was insulated with a phenol-allylphenol copolymer. The thickness of the insulating film was 0.27 µm and the tip radius was ~ 1 µm. The thickness of the insulation layer was measured using separate electron migrographs with higher magnification. The bar indicates 1 µm.

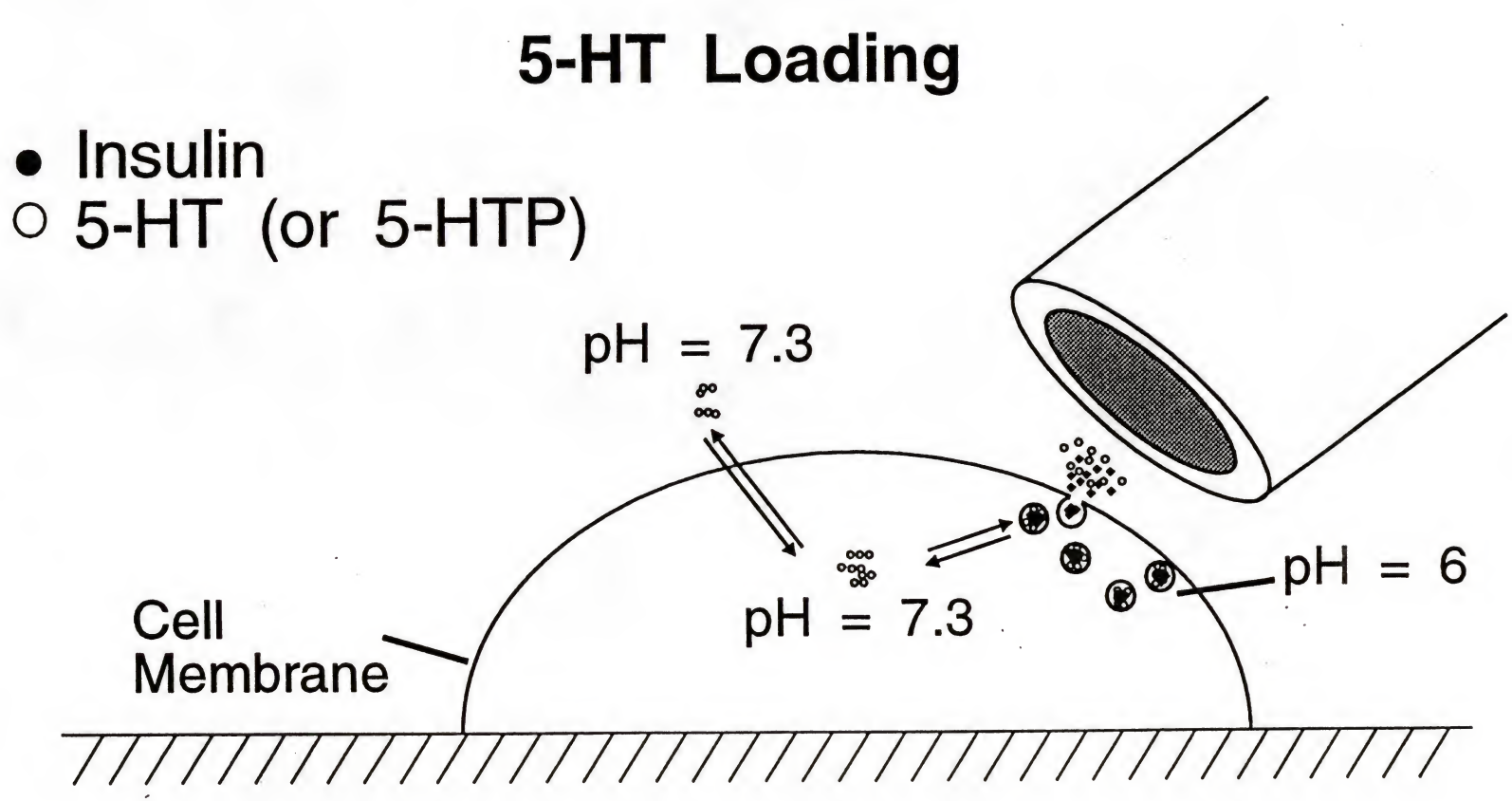

Figure 5-4. 5-hydroxytryptamine (5-HT) as a secretion marker. Cells were incubated with 5-HT for about 16 hours before experiment. 5-HT is accumulated in insulin-containing granules and upon stimulation of a single cell, 5-HT is cosecreted with insulin and can be detected using a bare carbon microelectrode. An applied potential of 0.65V was sufficient to oxidize 5-HT at a bare carbon microelectrode.

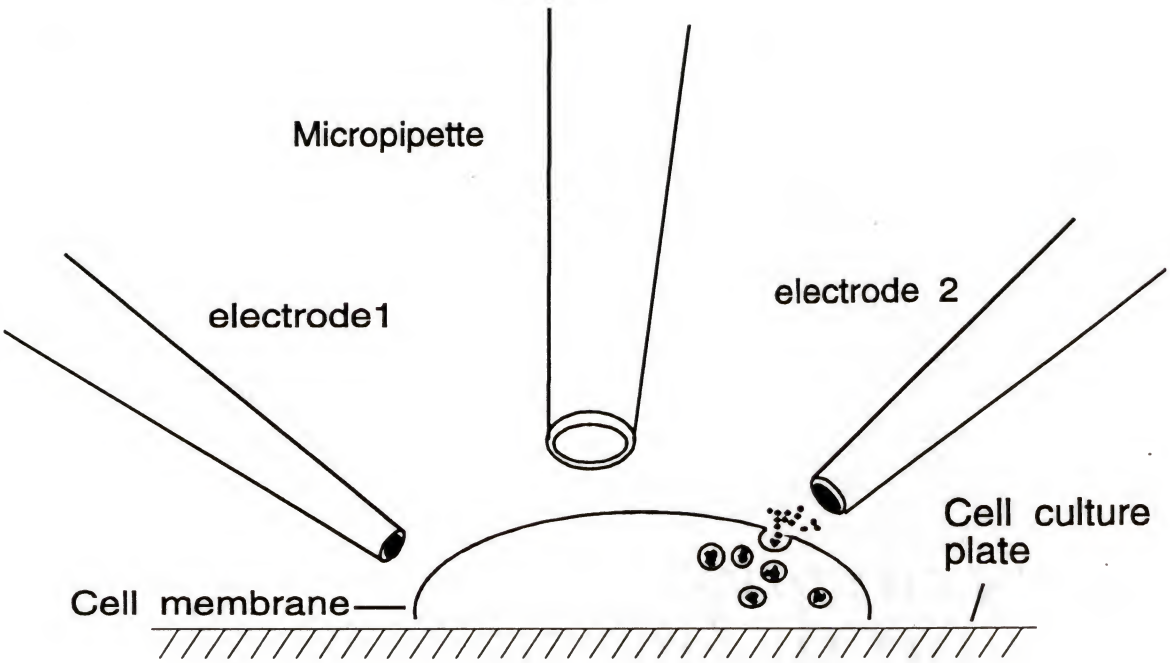

Figure 5-5. Simultaneous measurements of secretion. Microelectrodes were positioned at different locations on the cell surface using piezoelectric micropositioners to determine if hotspots of release exist. Cells were stimulated by application of high K^+ or tolbutamide buffer from a glass micropipette. Release of serotonin from vesicles was detected at the electrode.

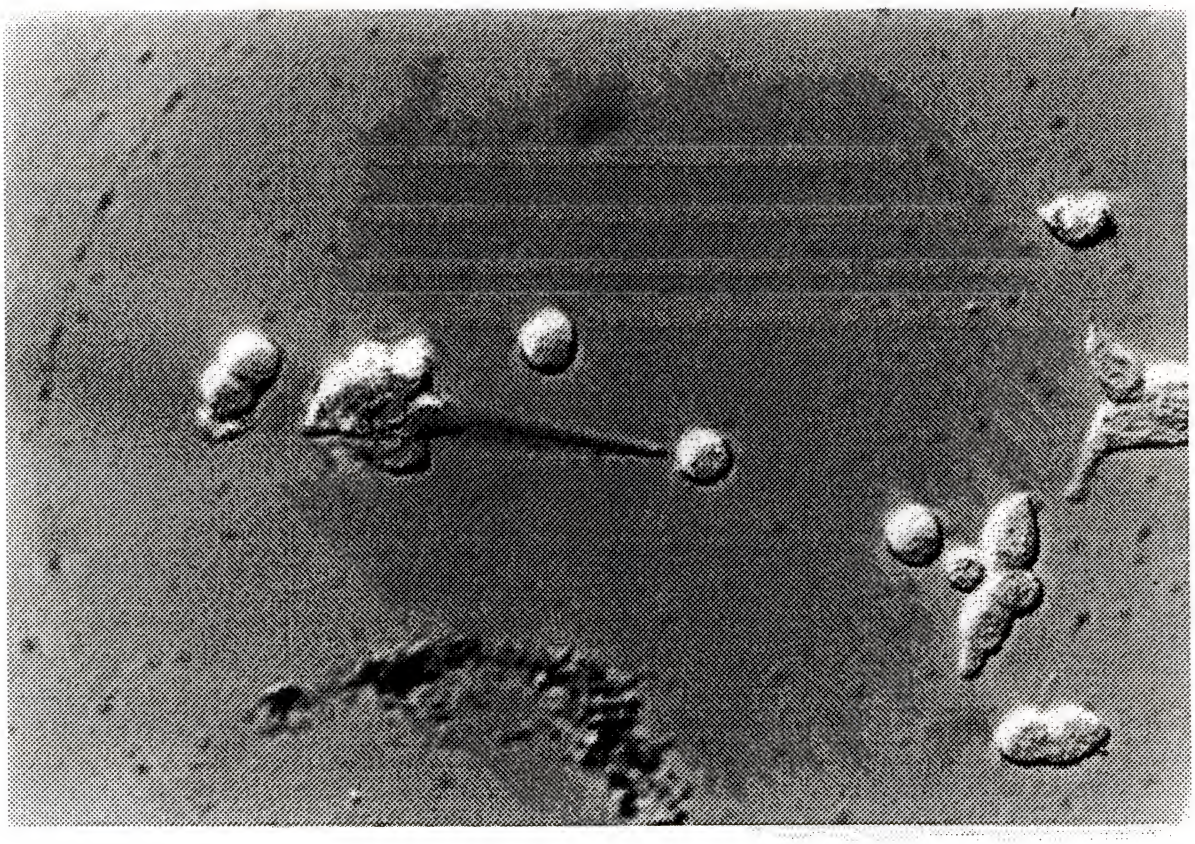

Figure 5-6. Size of the electrode compared with the cell. Image shows the size of the tip of the electrode (~ 2 μm) relative to the size of a single cell (~12 μm). During experiments, the electrode is positioned on top of the cell.

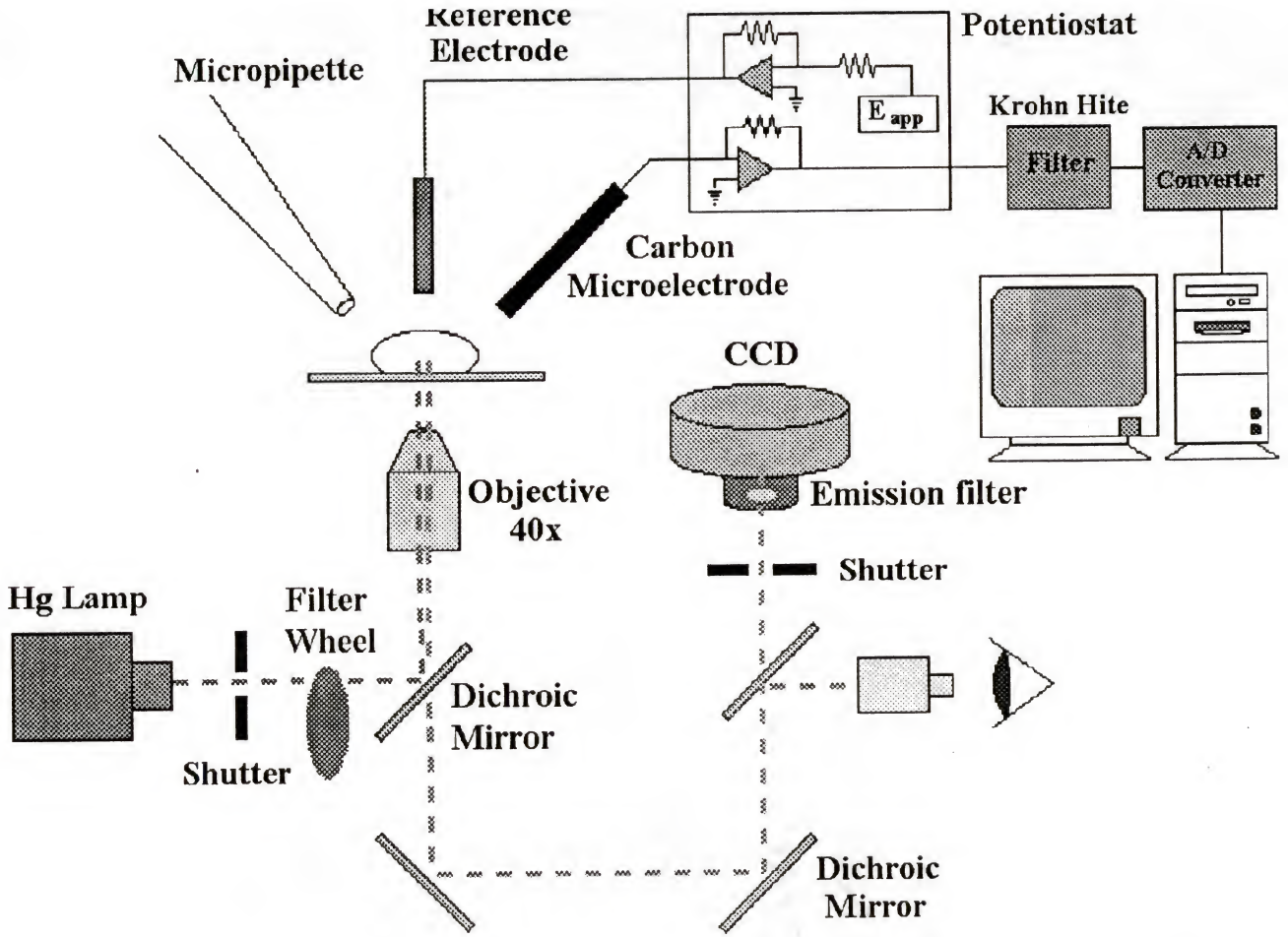

Figure 5-7. Schematic diagram of instrumentation for combining electrochemical techniques with fluorescent measurements. Fluorescence measurements use a Hg arc lamp, various filters, shutters, a 40x oil-immersion objective and a CCD camera. Electrochemical equipment includes a flame-etched carbon fiber microclectrode, a saturated calomel electrode (SCE) reference electrode and a potentiostat. A glass micropipette is positioned to the left of the cell to apply the secretagogue.

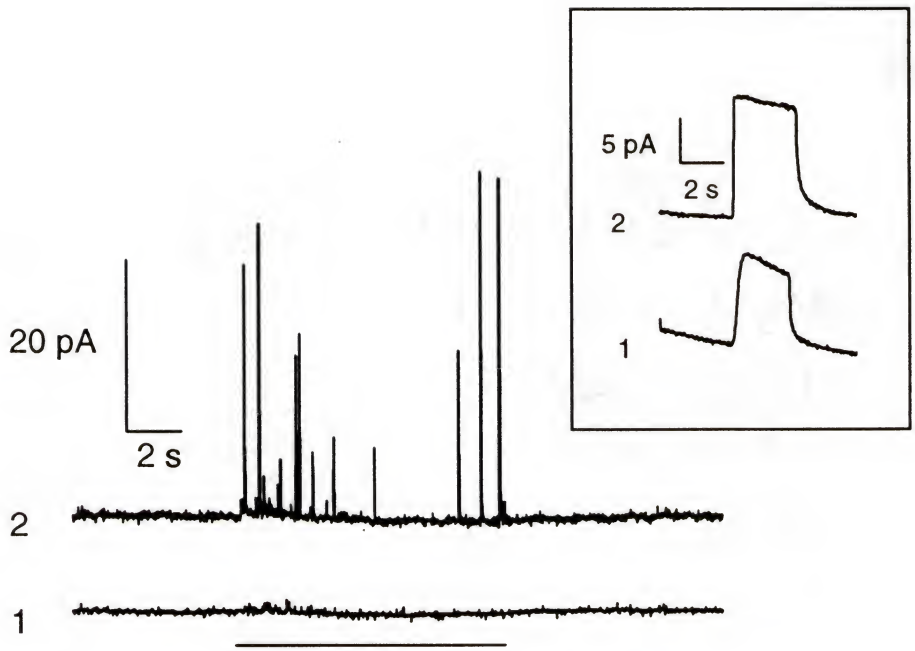

Figure 5-8. Simultaneous current recordings obtained at a single porcine pancreatic β-cell. The two microelectrodes (at 0.65 V) were positioned 3 μm apart. The cell was stimulated with 60 mM K^+ for 10 s as indicated by the bar. Inset shows the response of the two electrodes to 10 μM 5-HT.

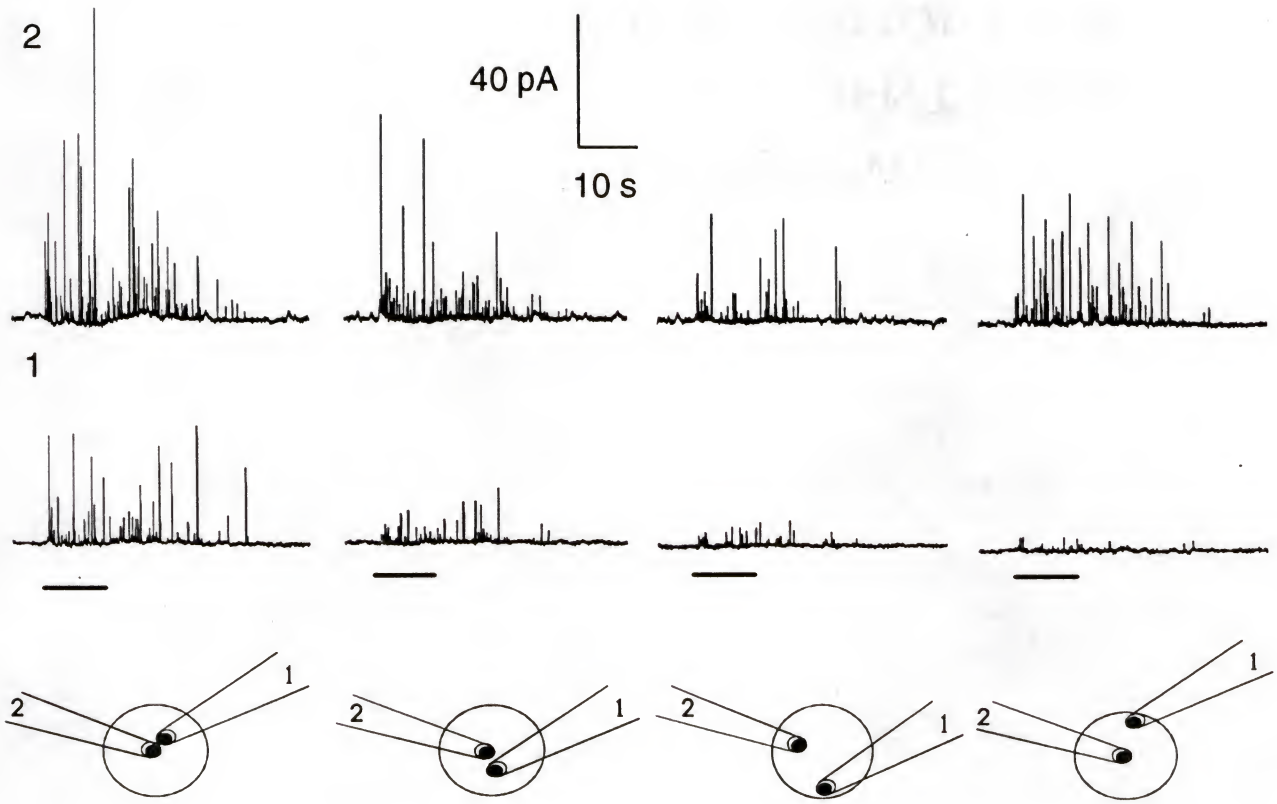

Figure 5-9. Simultaneous amperometric measurements with flame-etched electrodes (0.65 V) at a single porcine pancreatic β-cell. Traces 1 and 2 correspond to the currents from the respective electrodes shown in the lower diagrams after stimulation with 60 mM K^+ buffer. The diagrams show a top view of the positioning of the electrodes at the cell surface. This cell displayed a hotspot for release near the top of the cell. Bar indicates stimulation.

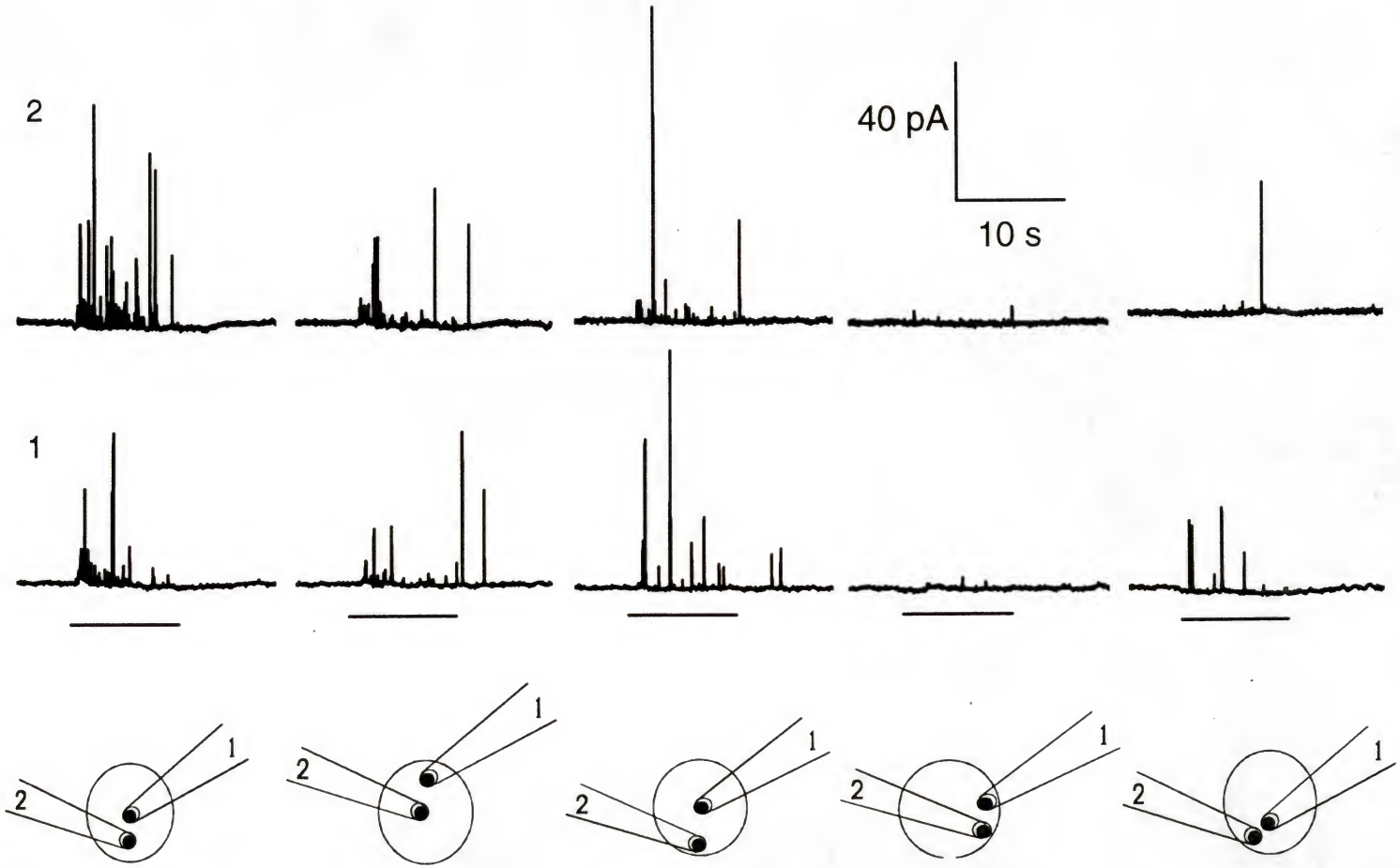

Figure 5-10. Simultaneous amperometric recordings made at a single porcine pancreatic β-cell. Two flame-etched electrodes were used to monitor secretion at different areas on the cell. Measurements were made as in Figure 5-9. This cell exhibited an ovoid shape hotspot at the center of the cell. Bar indicates time of stimulation with 60 mM K^+ buffer.

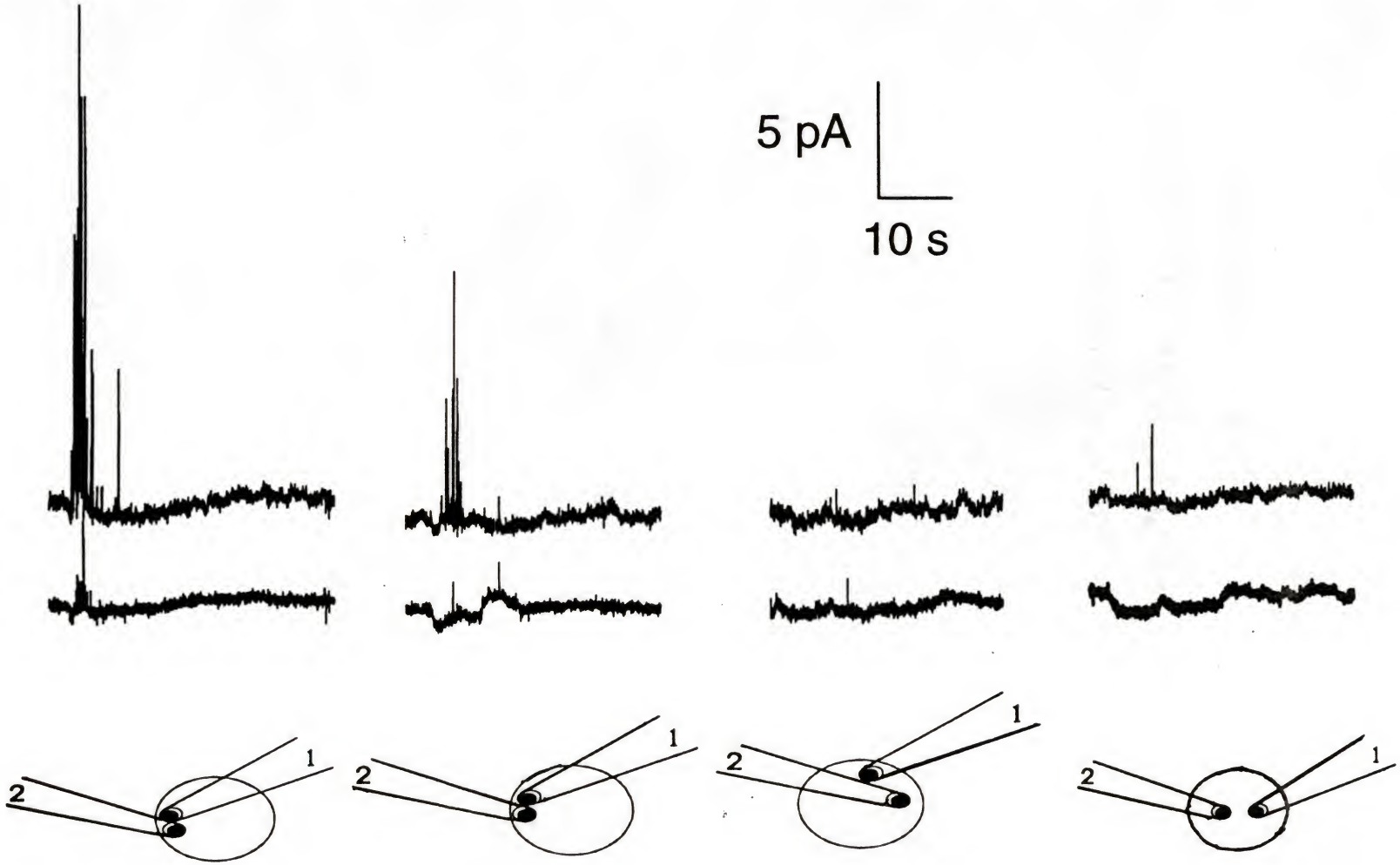

Figure 5-11. Simultaneous current recordings at a single canine pancreatic β-cell. Two flame-etched carbon fiber microelectrodes (0.65V) were used to probe secretion on different sites on the cell membrane. Traces 1 and 2 correspond to the currents from the respective electrodes shown in the lower diagrams after stimulation with 200 μM Tolbutamide. The diagrams below the current traces show a top view of the positioning of the electrodes at the cell surface. This cell displayed a hotspot for release near the left periphery of the cell.

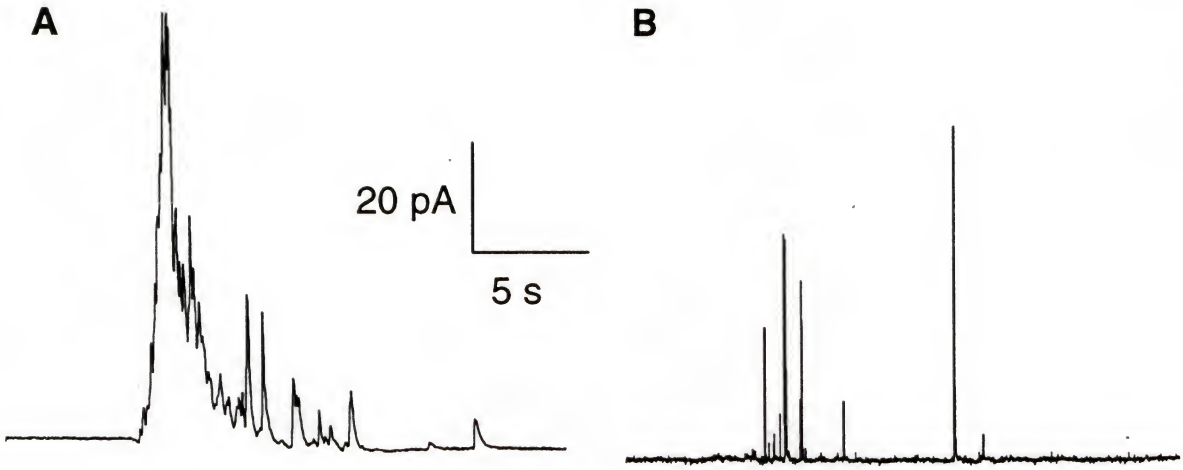

Figure 5-12. Comparison of current spikes obtained at a beveled carbon fiber microelectrode (r~5 μm) and flame-etched carbon fiber microelectrode (r~1 μm). Current recordings were obtained from a single porcine pancreatic β-cell after stimulation with 60 mM K^+ for 10 s. The use of flame-etched electrodes minimized overlap of current spikes.

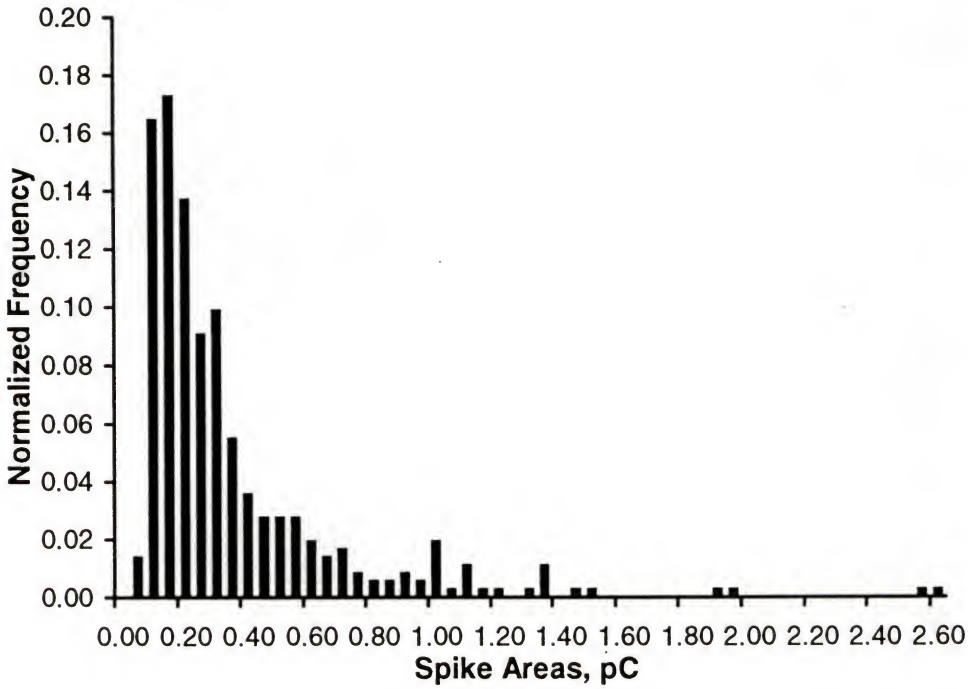

Figure 5-13. Histogram of spike areas obtained using flame-etched electrodes at a single cell. The cell was stimulated with 60 mM K^+ for 10 s. Spikes were obtained at two flame-etched electrodes at 0.65 V. Spikes were used only if the signal to noise ratio was greater than 8. The average spike area for 365 exocytotic events is 0.343 ± 0.579 pC (n=365).

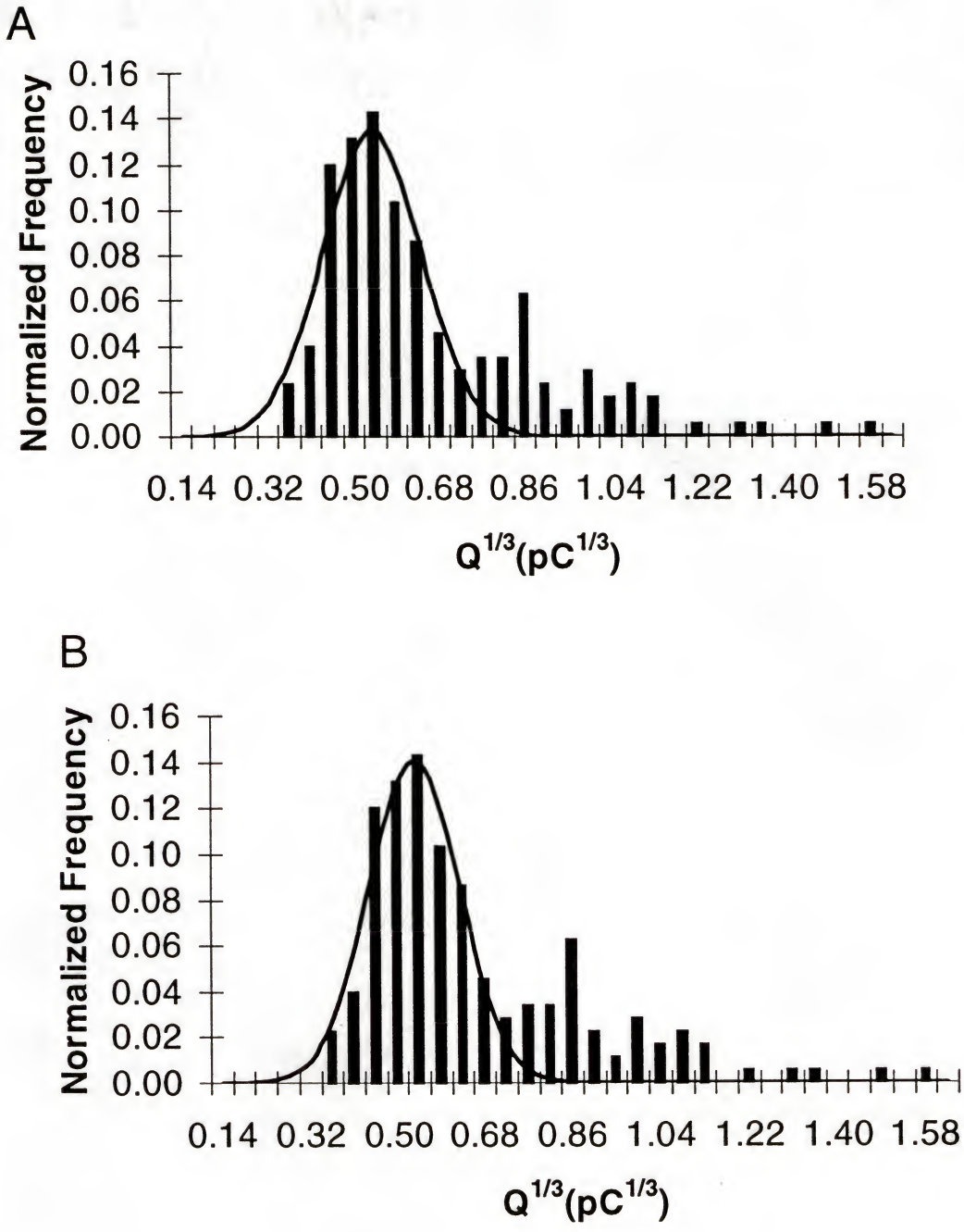

Figure 5-14. Distribution of cube roots of spike areas ($Q^{1/3}$) for the same data set used in Figure 5-13. In (A) all the values of $Q^{1/3}$ were used to obtain a Gaussian fit (solid line) with a mean $\pm$ SD of 0.56 ± 0.12 $pC^{1/3}$. The Gaussian fit in (B) was detemined by eliminating $Q^{1/3}$ values due to large spikes ($Q^{1/3} \leq 0.72$ $pC^{1/3}$). The mean $\pm$ SD for (B) is 0.53 ± 0.09 $pC^{1/3}$.

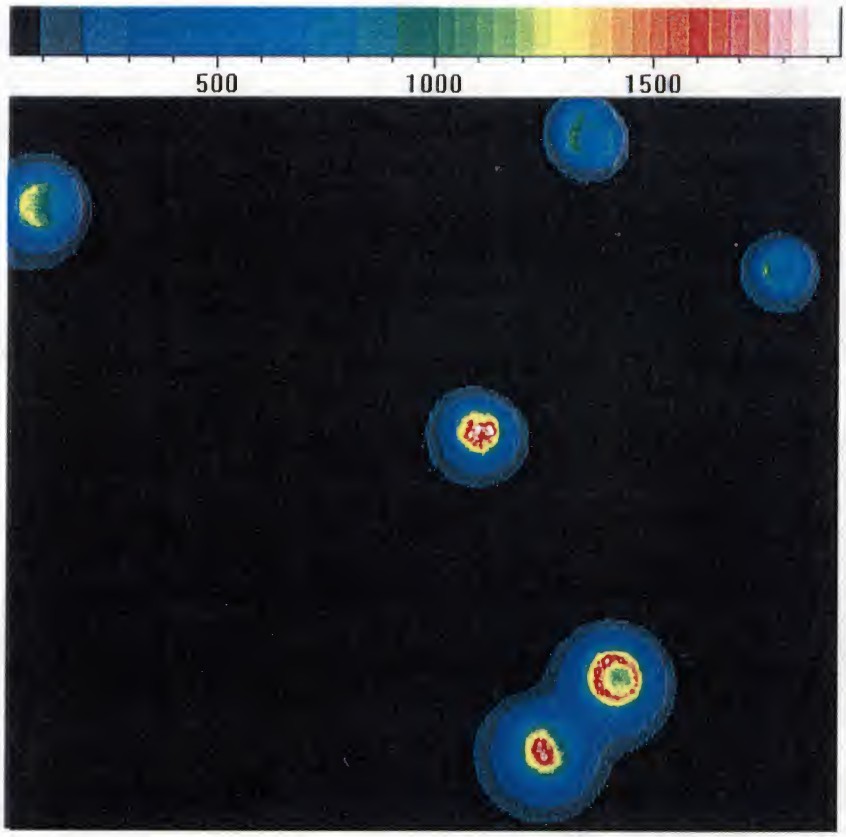

Figure 5-15. Fluorescence image using quinacrine dye. Quinacrine accumulates in insulin-containing granules. Presence of a region with higher fluorescence exhibits the localization of insulin-containing granules.

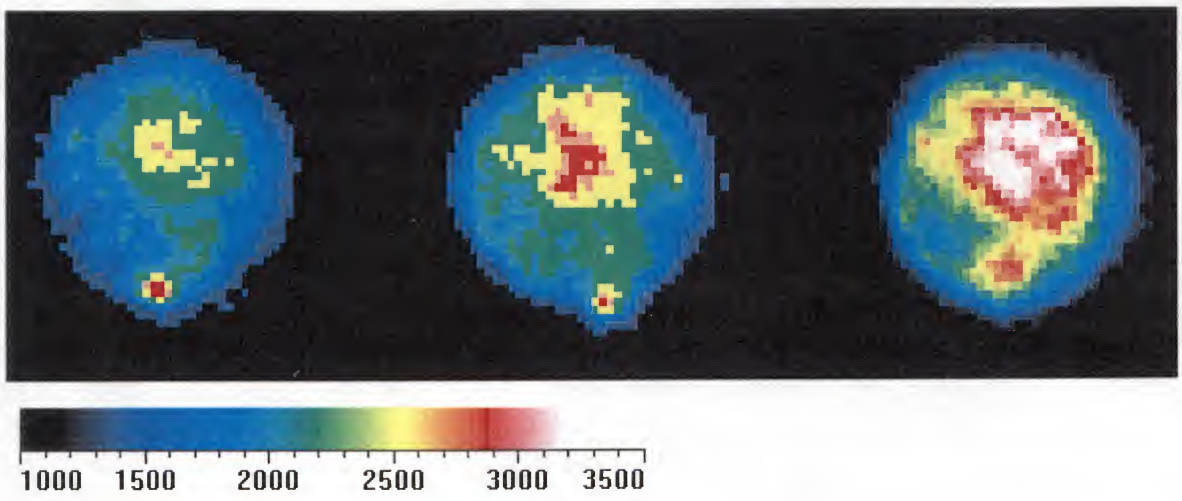

Figure 5-16. Fluorescence images of a single rat pancreatic β-cells cells using FM1-43 dye before (left), and after (center) stimulation with 200 μM tolbutamide for 10 s. On the third panel (right) the cell was restimulated with 200 μM tolbutamide, 5 minutes after the second (center) image was taken. The increase of fluorescence on a specific area on the cell membrane confirms the presence of an active site of release.

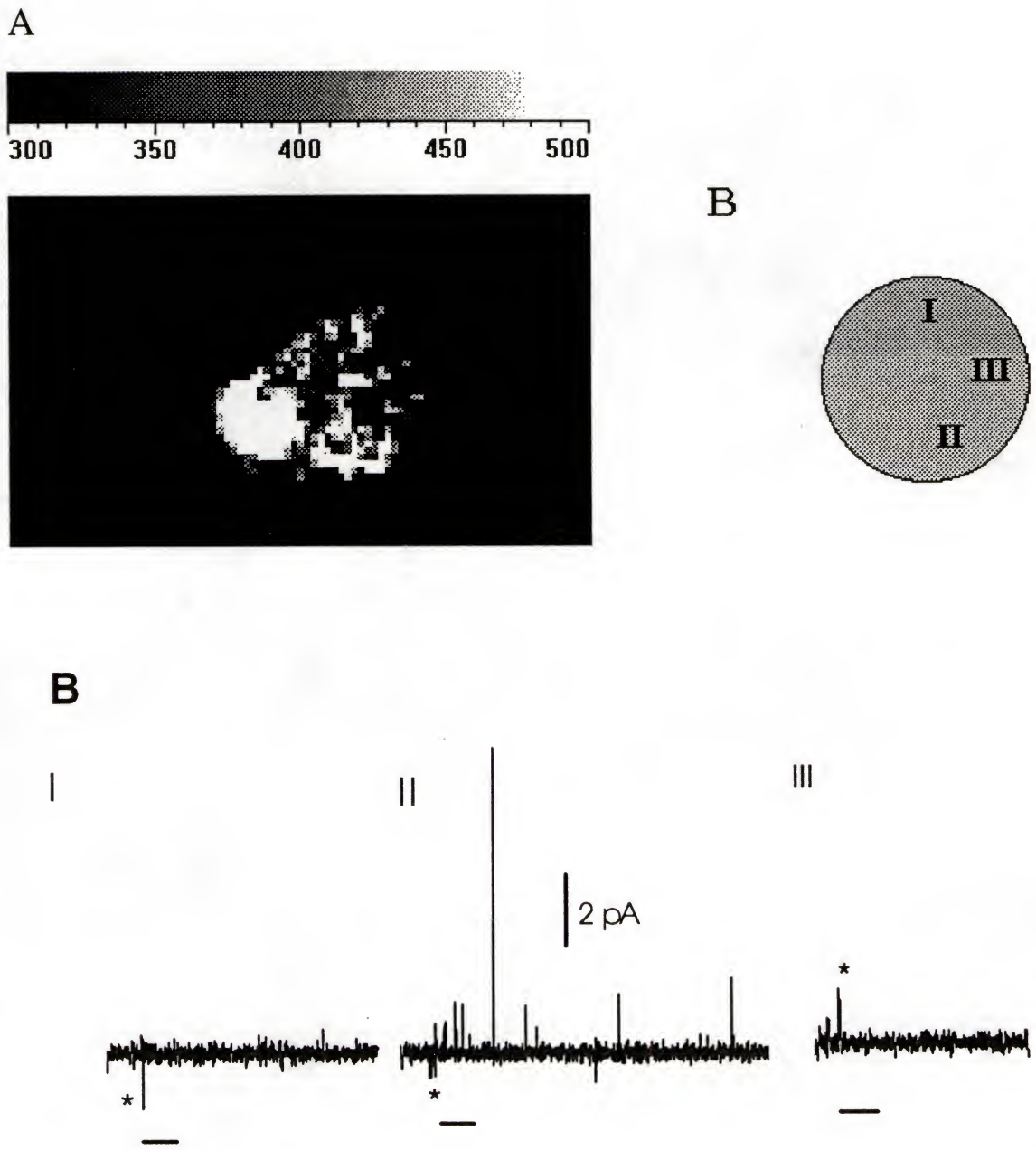

Figure 5-17. (A) illustrates the increase in FM1-43 fluorescence obtained at a single rat pancreatic β-cell upon stimulation with 200 μM tolbutamide. Image was obtained by subtracting the fluorescence image before stimulation to that after stimulation. Notice the increase in fluorescence at the lower periphery of the cell. (C) A flame-etched electrode was used to probe secretion at different zones (I, II, and III) on the cell membrane as shown in (B). Current spikes are observed at zone II but not on I and III. * artifacts due to puffing of stimulant. Bar indicates 10 s stimulation.

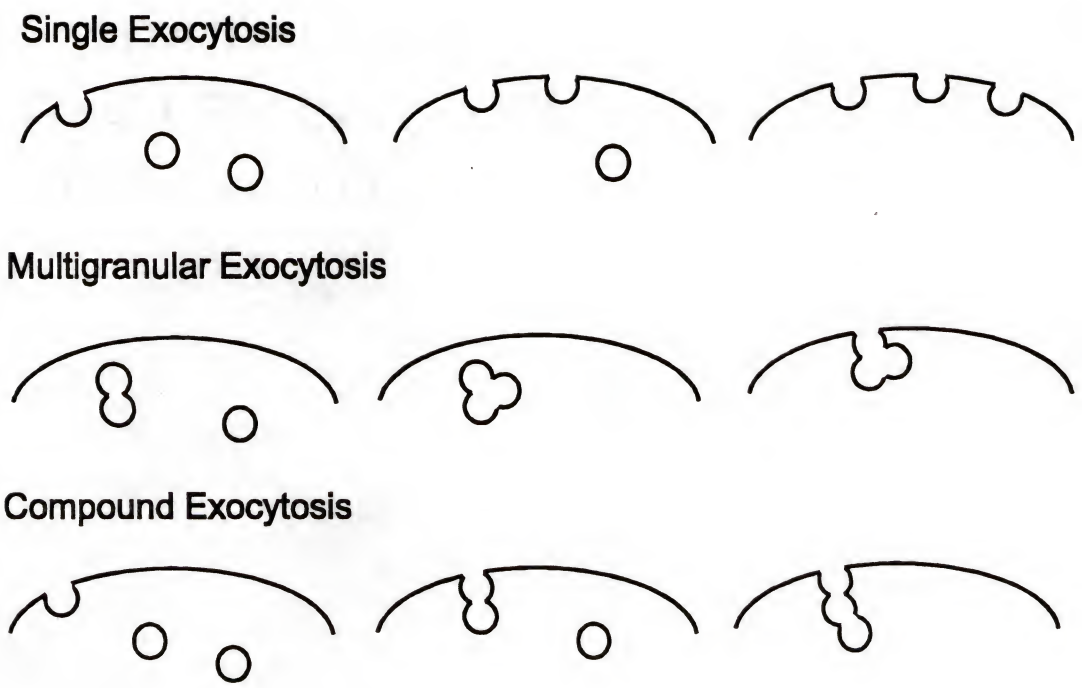

Figure 5-18. Different modes of exocytosis. See text for descriptions.

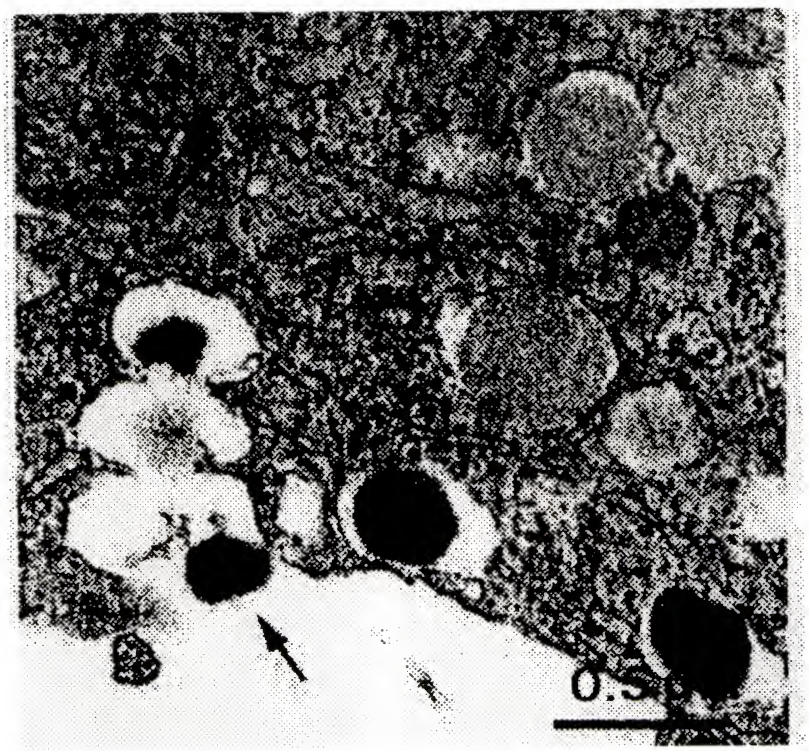

Figure 5-19. Electron micrograph of a rat pancreatic β-cell stimulated with 16.7 mM glucose. The arrow points to a fusion pore through which 3 secretory granules are being discharged. The image results from the fusion of vesicles, one with another. (Orci and Mallaise, 1980)

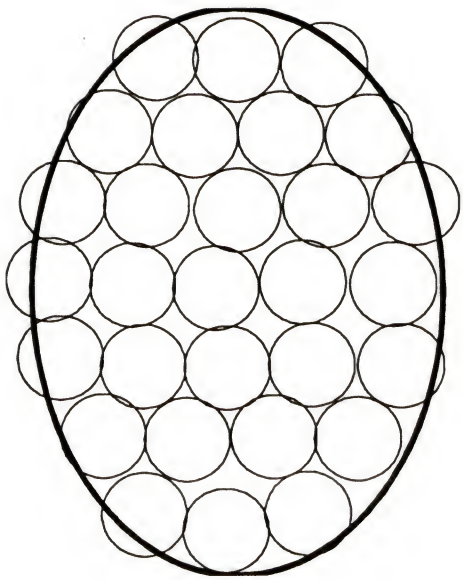

Figure 5-20. Evidence for compound exocytosis. The number of vesicles (small circles) that can be detected on a 1 μm radius electrode (solid line) is ~ 29. In this figure the radius of vesicles was assumed as 178 nm. Results obtained exhibit more than 29 spikes during stimulation. Formation of tubular pathway during compound exocytosis can explain the larger number of spikes (each spike correspond to one vesicular release) detected.

CHAPTER 6
SUMMARY AND FUTURE WORK

Recent devolopments in microelectrode techniques have been very useful in studying the dynamics of secretion from single cells. In this research, these techniques were used to monitor α-melanocyte stimulating hormone (α-MSH), corticotropin-like intermediate lobe peptide (CLIP) and β-endorphin from melanotrophs, norepinephrine and dopamine from PC12 cells and 5-hydroxytryptamine (secretion marker for insulin) from β-cells.

Amperometry at carbon fiber microelectrode was used to monitor secretion of peptides from single melanotrophs of the intermediate lobe of the rat pituitary. The method was based on electrochemical oxidation of tryptophan and tyrosine residues of small pro-opiocortin (POC) derived peptides secreted from these cells. When cells were stimulated by application of high K^+ buffer, a series of randomly occurring spikes was observed. The current spikes were strongly dependent on the presence of Ca^{2+}. Current spikes of nearly identical area and shape were also elicited by mechanical stimulation. Cyclic voltammetry confirmed that the detected substances are small tryptophan or tyrosine containing peptides. Based on amperometric tests of the most abundant peptides in melanotrophs, it was concluded that the current spikes were due to detection of primarily α-melanocyte stimulating hormone. The spike area corresponds to 0.32 amol of α-melanocyte stimulating hormone. It was concluded that the current spikes represent detection of concentration pulses that are expected following exocytosis events.

The amperometric and cyclic voltammetric detection of α-MSH, CLIP and β-endorphin was further explored. For amperometry, fouling of electrodes reduced the response of the electrode after successive application of the peptides in flow injection experiments. The fouling was apparently due to oxidation of tyrosine in the peptides as similar results were found for tyrosine but not for tryptophan. The effect of fouling could be reversed if the electrode was electrochemically treated by scanning from –1.0 V to +1.0V at 300 V/s for 2 min between application of the peptides. Using cyclic voltammetry at 800 V/s, it was possible to distinguish α-MSH, which had a peak shaped voltammogram, from other POC peptides, which had relatively flat voltammetric waves at this scan rate. The selectivity was based on the presence of tryptophan in this peptide. The scan rate dependence of the peak current for α-MSH revealed that the voltammetry was adsorption controlled. As a result, of the adsorptive character of α-MSH, decreasing scan interval increases the temporal response but decreases the sensitivity to α-MSH. By using the improved voltammetric conditions (0 to 1.2V potential window; 800 V/s scan rate; and 67 ms scan interval), it was possible to monitor α-MSH secretion from single melanotrophs during exocytosis.

Amperometric detection at carbon fiber microelectrodes was used to study the mechanisms of catecholamine depletion of reserpine and tyramine. The effect of these two drugs on nicotine and high K^+ stimulation was determined. Catecholamine depletion by reserpine resulted in a decreased in number of current spikes and spike area. The decline in the total amount of catecholamine release was primarily due to the depletion of a large number of catecholamine-containing granules. In the presence of tyramine, secretion was observed at single PC12 cells. By increasing the concentration of

tyramine, larger amount of catecholamine was released due to the increase in secretion events. Studies revealed the presence of two pools of catecholamine containing vesicles in PC12 cells;a tyramine-releasable pool and a nicotine or K^+ releasable pool.

Flame-etched carbon fiber microelectrodes with ~ 2.5 μm tips were used to probe exocytosis release sites on the surface of single β-cells. To measure secretory activity from β-cells, 5-hydroxytryptamine (5-HT) was used as a secretion marker. Simultaneous amperometric recordings at two flame-etched electrodes, demonstrated the presence of hotspots or active sites of release on β-cells. Distribution of spike areas indicated the presence of very large spikes that may be due to multigranular exocytosis. The high frequency of spikes detected at the electrode was attributed to the occurrence of compound exocytosis. Imaging techniques confirmed the results obtained by electrochemical methods. Uneven distribution of insulin-containing granules in β-cells was observed on fluorescent images using quinacrine. Fluorescence measurements of FM1-43 agree with results from electrochemical measurements. The presence of hotspots was evident and secretory activity was detected at the spot with higher fluorescence.

Results from FM1-43 fluorescence measurements are very promising. For future work, a confocal laser-scanning microscope should be used to improve the spatial resolution of FM1-43 fluorescence measurements. We have demonstrated in this work how FM1-43 can be used as a secretion marker in β-cells. Another application of FM1-43 that can be explored is its use as an endocytotic marker. When a cell is stimulated, an increase in fluorescence in the presence of FM1-43 indicates incorporation of the dye into secretory vesicles during exocytosis. During membrane uptake, known as endocytosis,

FM1-43 is incorporated into the endocytotic vesicle and is carried into the cytoplasm (Betz et al., 1992; Stafford et al., 1993). By removing FM1-43 from the extracellular media, the location of recycled vesicles inside the cell can be obtained. Fluorescence measurements will indicate the location of recycled vesicles inside the cell. In addition, it would be also interesting to couple FM1-43 with a Ca^{2+} dye. There is a wide range of Ca^{2+} dyes available commercially but for this particular application, Fluo-3 would be the best choice. FM1-43 and Fluo-3 are both excited at 488 nm. Moreover, FM1-43's emission maximum (~580 nm upon incorporation on membranes) is sufficiently separated from that of Fluo-3 (~ 526 nm) to allow simultaneous fluorescence detection of these two dyes. By monitoring Fluo-3 and FM1-43 simultaneously, the role of Ca^{2+} during exocytosis and endocytosis can be studied.

Flame-etched carbon fiber microelectrodes can be further utilized in investigating the effect of drugs (e.g., A23187) that allow influx of Ca^{2+} throughout the cell. It was previously reported that L-type Ca^{2+} channels in β-cells are co-localized with insulin containing granules (Bokvist et al., 1995). It was implied that the occurrence of Ca^{2+} transients at specific regions of the cell could be related to the presence of hotspots. In order to investigate this assumption A23187, a Ca^{2+} ionophore can be used to induce secretion. A23187 will allow influx of Ca^{2+} throughout the cell. With flame-etched electrodes, the cell membrane can be probe to determine if hotspots still exist upon application of A23187 to the β-cell.

Another interesting application of flame-etched electrodes is to determine the effects of naturally occurring peptides that induce multigranular or compound exocytosis (e.g., myelin basic proteins) according to ultrastructural experiments on β-cells (Kolehmainen,

1995). This will provide us a better understanding of the effect of these peptides on insulin secretion.

REFERENCES

Abe, T., Lau, Y.Y. and Ewing, A.G. (1992) *Anal. Chem.* **64**, 2160.

Abrahamsson, H. and Gylfe, E. (1980) *Acta Physiol. Scand.*, **109**, 113.

Adams, N.R. (1976) *Anal. Chem.* **48**(14), 1129A.

Alvarez de Toledo, G.A. and Fernandez, J.M. (1990) *J. Gen. Physiol.* **95**, 397.

Alvarez de Toledo, G., Fernadez-Chacon R. and Fernandez, J.M. (1993) *Nature* **363**, 554.

Aspinwall, C.A., Brooks, S.A., Kennedy, R.T. and Lakey, J.R.T. (1997) *J. Biol. Chem.* **272**(50), 31308.

Bard, A.J. and Faukner, L.R. (1980) in *Electrochemical Methods*, John Wiley and Sons Inc, New York, pp 222,525.

Bauer, J.E., Kristensen, E.W., May, L.M., Wiedemann, D.J., and Wightman, R.M. (1991) *Anal. Chem.* **60**, 1268.

Bennet, G.W., Brazell, M.P. and Marsden, C.A. (1981) *Life Sci.* **29**, 1001.

Betz, W.J., Mao, F. and Bewick, G.S. (1992) *J. Neuroscience*, **12**:363-375.

Bokvist, K., Eliasson, L., Ammala, C., Renstrom, E., and Rorsman, P. (1995) *EMBO J.* **14**(1), 50.

Bond, A.M.(1994) *Analyst* **119**, R1.

Bonner-Weir, S. (1988) *Diabetes* **37**, 616.

Brabec, V. and Mornstein, V. (1980a) *Biochim. Biophys. Acta* **625**, 43.

Brabec, V. and Mornstein, V. (1980b) *Biophys. Chem.* **12**, 159.

Bruns, D. and Jahn, R. (1998) *Advances in Pharmacology* **42**, 87.

Cabassi, A., Bergamaschi, E., Mutti, A., Franchini, I. and Borghetti, A. (1995) *Clinical*

and Experimental Pharmacology and Physiology, **Suppl. 1**, S83.

Chen, T.K., Luo, G. and Ewing, A.G. (1994) *Anal. Chem.* **66**, 3031.

Chen, G. and Ewing, A.G. (1995) *Brain Res.* **701**, 167.

Chen, G. and Ewing, A.G. (1997) *Critical Reviews in Neurobiology* **11**, 59.

Chien, J.B., Wallingford, R.A.and Ewing, A.G., (1990) *J. Neurochem.* **54**, 633.

Chow, R.H., Von Ruden, L. and Neher, E. (1992) *Nature* **356**, 60.

Chronwall, B.M., Bishop, J.F. and Gehlert, D.R. (1988) *Peptides* **9** (Suppl.1), 169.

Ciolkowski, E.L., Cooper, B.R., Jankowski, J.A., Jorgensen, J.W. and Wightman, R.M. (1992*) J. Am. Chem. Soc.*, **114**, 2815.

Cooper, P.E. and Martin, J.B. (1980) *Annals of Neurology* **8**, 551.

Cox, J.A. and Kulesza, P.J. (1984) *Anal. Chem.* **56**, 1021.

Dahl, G and Gratzl, M. (1976) *Cytobiologie* **12**, 344.

Dean, P.M. (1973) *Diabetologia* **9**, 115.

De Toledo, G.A., Fernandez-Chacon and Fernandez, J.M. (1993) *Nature* **363**, 554.

Douglas, W.W. (1974) *Biochim. Soc. Symp.* **39**, 1.

Drumheller, A.L., Bachelard, H., St-Pierre, S. and Jolicoeur, F.B. (1985) *J. Liq. Chromatogr.* **8**, 1829.

Dumont, M., Roy, D. and Lemaire, S. (1997) *Journal of Cardiovascular Pharmacology* **30**, 302.

Edmonds, T.E. and Guoliang (1983) *Anal. Chim. Acta* **151**, 109.

Elfvin, L.G. (1968) *Ultrastructure Research* **21**, 459.

Feng, J.X., Brazell, M., Renner, K., Kasser, R. and Adans, R.N. (1987) *Anal.Chem.* **59**, 1863.

Fernandez, J.M., Bezanilla, F. and Taylor, R.E. (1982) *Nature* **297**, 150.

Finberg, J.P.M., Tenne, M. and Youdim, M.B.H. (1981) *Br. J. Pharmacol.* **73**, 65.

Finn, J.P., Merickel, A., Peter, D. and Edwards, R.H. (1998) *Advances in Pharmacology* **42**, 233.

Finnegan, J.M. and Wightman, R.M. (1995) *J. Biol. Chem.* **270**. 5353.

Finnegan, J.M., Pihel, K., Cahill, P.S., Huang, L., Zerby, S., Ewing, A.G., Kennedy, R.T. and Wightman, R.M. (1996) *J. Neurochem.* **66**(5), 1914.

Fozard, J.R. and Mwaluko, G.M.P. (1976) *Br. J. Pharmac.* **57**, 115.

Gabbay, K.H., Korff, J., and Schneeberger, E.E. (1975) *Science* **187**, 177.

Glembotski, C.C. (1981) *J. of Biol. Chem.* **260**, 7433.

Golay, M. (1959) in *Gas Chromatography 1958* (Desty, D.H. Ed.) Butterworths, London, p.36.

Goldman, M.E., Beaulieu, M., Kebabian, J.W. and Eskay, R.L. (1983) *Endocrinology* **112**, 435.

Gonon, F.G., Fombarlet, C.M., Buda, M.J. and Pujol, J.F. (1981) *Anal. Chem.* **53**, 1386.

Greene, L.A. and Tischler, A.S. (1976) *Proc. Natl. Acad. Sci. USA* **73**, 2424.

Greene, L.A. and Rein, G. (1977a) *Brain Research* **129**, 247.

Greene, L.A. and Rein, G. (1977b) *Brain Research* **138**, 521.

Harrison, D.J., Turner, R.F.B. and Balter, H.P. (1988) *Anal. Chem.* **60**, 2002.

Heinze, J. Angew (1993) *Chem. Intl. Ed. Engl.* **32**, 1268.

Henry, J.P., Sagne, C., Botton, D., Isambert, M.F. and Gasnier, B. (1998) *Advances in Pharmacology* **42**, 237.

Horrigan, F.T. and Bookman, R.J. (1994) *Neuron.* **13**, 1119.

Huang, L. (1995) *Time Resolved Measurement of Insulin Secretion from Single Pancreatic Beta-Cells*, Ph.D. Dissertation, University of Florida.

Huang, L., Shen, H., Atkinson, M.A. and Kennedy, R.T. (1995) *Proc. Natl. Acad. Sci. USA* **92**, 9608.

Jackson, S. and Lowry, P.J. (1983) *Neuroendocrinology* **37**, 248.

Jankowski, J.A., Finnegan, J.M. and Wightman, R.M. (1994) *J. Neurochem.* **63**(5), 1739.

Kawagoe, K.T., Jankowski, J.A. and Wightman, R.M. (1991) *Anal. Chem.* **63**(15), 1589.

Kawagoe, K.T., Zimmerman, J.B. and Wightman, R.M. (1993) *J. Neurosci. Meth.* **48**, 225.

Kelly, R.S. and Wightman, R.M. (1986) *Anal. Chim. Acta* **187**, 79.

Kennedy, R.T., Huang, L., Atkinson, M.A. and Dush, P. (1993) *Anal. Chem.* **65**, 1882.

Kennedy, R.T., Huang, L. and Aspinwall, C.A. (1996) *J. Am. Chem. Soc.* **118**, 1795.

Kissinger, P.T. and Bruntlett, R.E. (1981) *Life Sci.* **28**(5), 455.

Kissinger, P.T., Preddy, C.R., Shoup, R.E. and Heineman, W.R. (1996) in *Laboratory Techniques in Electroanalytical Chemistry*, Marcel Dekker, Inc., New York, p 118.

Kittner, B., Brautigam, M. and Herken, H. (1987) *Arch. Int. Pharmacodyn.* **286**, 181.

Knoll, J., Miklya, I., Knoll, B., Marko, R. and Raez, D. (1996) *Life Science* **58**, 2101.

Kolehmainen, E. (1995*) Neurochem. Int.* **26**, 503.

Kongsamut, S., Shibuya, I., Uehura, M. and Douglas, W.W. (1993) *Endocrinology* **133**, 336.

Kopin, I.J. (1964) *Pharmac. Rev.* **16**, 179.

Kurihara, H, Kitajima K., Senda, T., Fujita, H. and Nakajima, T. (1986) *Cell Tiss. Res.* **243**, 311.

Lau, Y.Y., Abe, T. and Ewing, A.G. (1992) *Anal. Chem.* **64**, 1702.

Leszczyszyn, D.J., Jankowski, J.A., Viveros, O.H., Diliberto, E.J., Near, J.A. and Wightman, R.M. (1990) *J. Biol. Chem.* **265,** 14736.

Mains, R.E. and Eipper, B.A. (1979), *J. Biol. Chem.* **254**, 7885.

Matsuda, M., Okabe, T., Sugimoto, N., Senda, T. and Fujita, H. (1994*) Ann N.Y. Acad. Sci.* **710**, 94.

Matthews, E.K., McKay, D.B., O'Connor, M.D.L. and Borowitz, J.L. (1982) *Biochim. Biophys. Acta* **715**, 80.

Munemura, M., Eskay, R.L.and Kebabian, J.W. (1980) *Endocrinology* **106**, 1795.

Nagatsu, T. and Stjarne, L. (1998) *Advances in Pharmacology* **42**, 1.

Nakanishi N., Onozawa, S., Matsumoto, R., Hasegawa, H., and Minami, N. (1995) *J. Biochem.* **118**, 291.

Neher, E. and Marty, A. (1982) *Proc. Natl. Acad. Sci. USA* **79**, 6712.

Oberhauser. A.F., Robinson, I.M. and Fernandez, J.M. (1996) *Biophys. J.* **71**, 1131.

Orci, L. and Malaisse, W (1980) *Diabetes* **29**, 943.

Orci, L., Vassali, J.D. and Perrelet, A. (1988) *Scientific American* **260,** 85.

Paras, C.D. and Kennedy, R.T. (1995) *Anal. Chem.* **67**, 3633.

Paras, C.D. and Kennedy, R.T. (1997) *Electroanalysis* **9**(3), 203.

Pihel, K., Hsieh, S., Jorgensen, J.W. and Wightman, R.M. (1995) *Anal. Chem.* **67**, 4514.

Ponchon, J.L., Cespuglio, R., Gonon, F., Jouvet, M. and Pujol, J.F. (1979) *Anal. Chem.* **51**(9), 1483.

Pothos, E.N. and Sulzer, D. (1998) *Advances in Pharmacology* **42**, 199.

Raymond, V., Lepine, J., Giguere, V., Lissitzky, J.C., Cote, J., and Labrie, F. (1981) *Mol. Cell. Endocrinol.* **22**, 295.

Rebois, R.V., Reynolds, E.E., Toll, L. and Howard, B.D. (1980) *Biochemistry* **19**, 1240.

Roe, M.W., Lancaster, M.E., Mertz, R.J., Worley, J.F., III, and Dukes, I.D. (1993) *J. Biol. Chem.* **268**, 9953.

Ryan, T.A. and Smith, S.J. (1995) *Neuron* **14**, 983.

Sasso, S.V., Pierce, R.J., Walla, R. and Yacynych, A.M. (1990) *Anal. Chem.* **62**, 1111.

Sauter, A. and Frick, W. (1984) *J. of Chromatogr.* **297**, 215.

Scherman, D. and Henry, J.P. (1980) *Biochem. Pharmacol.* **29**, 1883.

Schroeder, T.J., Jankowski, J.A., Senyshyn, J., Holz, R.W. and Wightman, R.M. (1994)

J. Biol. Chem. **269**(25), 17215.

Schubert, D. Heinemann, S. and Kidokoro, Y. (1977) *Proc. Natl. Acad. Sci. USA* **74**(6), 2579.

Schubert, D. and Klier, F.G. (1977) *Proc. Natl. Acad. Sci. USA* **74**(11), 5184.

Schubert, D., LaCorbiere, M., Klier, F.G. and Steinbach, J.H. (1980) *Brain Research* **190**, 67.

Schweizer, F.E., Betz, H. and Augustine G.J. (1995) *Neuron* **14**, 689.

Smelik, P.G., Berkenbosch, F., Vermes, I. and Tilders, F.J.H. (1983) in *The Anterior Pituitary Gland* (Bhatnagar A.J., Ed.) Raven Press, New York, p 113.

Smith, A.D. (1973) *Br. Med. Bull.* **29**(2), 123.

Smith, C.B. and Betz, W.J. (1996) *Nature* **380**, 531.

Somers, G., Blondel, B., Orci L., and Mallaisse, W.J. (1979) *Endocrinology* **104**(1), 255.

Spatola, A.F. and Benovitz, D.E. (1985) *J. Chromatogr.* **327**, 165.

Stafford, S.J.V., Shorte, S.L. and Schofield, J.G. (1993) *Bioscience Reports*, **13**, 9.

St. Claire III, R.L. (1986) Ph.D. Dissertation, University of North Carolina at Chapel Hill.

Strein, T.G. and Ewing, A.G. (1992) *Anal. Chem.* **64**, 1368.

Suaud-Chagny, M.F., Cespuglio, R., Rivot, J.P., Buda, M.and Gonon, F (1993) *J. Neurosci. Meth.* **48**, 241.

Su, M.T., Dunwiddie, T.V. and Gerhardt, G.A. (1990) *Brain Research* **518**, 149.

Tatham, P.E.R., Duchen, M.R. and Millar, J. (1991) *Pflugers. Arch.* **419**, 409.

Thomas, P., Surprenant, A. and Almers, W. (1990) *Neuron* **5**, 723.

Tsuruta, K., Grewe, C.W., Cote, T.E., Eskay, R.L. and Kebabian, J.W. (1982) *Endocrinology* **110**, 1133.

Tucker, T.J., Bond, A.M., Qing, Z., and Rivett, D.E. (1989) *J. Electroanal. Chem.* **261**,127.

Wagner, J.A. (1985) *J. of Neurochemistry* **45**, 1244.

Wakade, A.R., Malhotra, R.K. and Wakade, T.D. (1985) *Naunyn-Schmiedeberg's Arch. Pharmacol.* **331**, 122.

Wang, J. (1994) *Analytical Electrochemistry*, VCH Publishers Inc., New York, pp 96,97.

Wightman, R.M., May, L.J. and Michael, A.C. (1988) *Anal. Chem.*, **60**(13), 769A.

Wightman, R.M. , Jankowski, J.A., Kennedy, R.T., Kawagoe, K.T., Schroeder, T.J., Leszczyszyn, D.J., Near, J.A., Diliberto, E.J. and Viveros, O. (1991) *Proc. Natl. Acad. Sci. U.S.A.* **88**, 10754.

Wightman, R.M., Schroeder, T.J., Finnegan, J.M., Ciolkowski, E.L. and Pihel, K. (1995) *Biophys. J.* **68**, 383.

Youdim, M.B.H., Heldman, E., Pollard, H.B., Fleming, P. and Mchughs, E. (1986). *Neuroscience* **19**(4), 1311.

Youdim, M.B.H. (1991) *J. Neural Transm.* **34**(Suppl.), 61.

Zerby, S.E. and Ewing, A.G. (1996*) J. Neurochem.* **66**(2), 651.

Zhou, Z. and Misler, S. (1995) *J. Biol Chem.* **270**(8), 3498.

Zorec, R. and Tester, M. (1993) *FEBS. Lett.* **333**, 283.

BIOGRAPHICAL SKETCH

Charina Dizon Paras was born on March 4, 1969, in Angeles City, Philippines. She stayed in Angeles City with her family for 13 years. In June 1986, she moved to Manila to enter a science oriented high school known as Philippine Science High School. She received her Bachelor of Science degree in chemistry (cum laude) from University of the Philippines in April 1990. For three years she worked as a laboratory instructor in the Institute of Chemistry at the University of the Philippines. While teaching she took several graduate courses in the same department and started research concerning speciation analysis of sediments from Paracale Bay, Philippines. In July, 1993 she left for the United States and entered the Ph.D. program of the Department of Chemistry at University of Florida. With an interest in bioanalytical techniques she decided to join the research group of Dr. Robert T. Kennedy. She completed her research and obtained her Doctor of Philosophy degree in May of 1998.

I certify that I have read this study and that in my opinion it conforms to acceptable standards of scholarly presentation and is fully adequate, in scope and quality, as a dissertation for the degree of Doctor of Philosophy.

Robert T. Kennedy, Chairman
Associate Professor of Chemistry

I certify that I have read this study and that in my opinion it conforms to acceptable standards of scholarly presentation and is fully adequate, in scope and quality, as a dissertation for the degree of Doctor of Philosophy.

James D. Winefordner
Graduate Research Professor of Chemistry

I certify that I have read this study and that in my opinion it conforms to acceptable standards of scholarly presentation and is fully adequate, in scope and quality, as a dissertation for the degree of Doctor of Philosophy.

Anna F. Brajter-Toth
Associate Professor of Chemistry

I certify that I have read this study and that in my opinion it conforms to acceptable standards of scholarly presentation and is fully adequate, in scope and quality, as a dissertation for the degree of Doctor of Philosophy.

Benjamin A. Horenstein
Assistant Professor of Chemistry

I certify that I have read this study and that in my opinion it conforms to acceptable standards of scholarly presentation and is fully adequate, in scope and quality, as a dissertation for the degree of Doctor of Philosophy.

Mohan K. Raizada
Professor of Physiology

This dissertation was submitted to the Graduate Faculty of the Department of Chemistry in the College of Liberal Arts and Sciences and to the Graduate School and was accepted as partial fulfillment of the requirements for the degree of Doctor of Philosophy.

May 1998

Dean, Graduate School